ASSESSING THE UTILITY OF DRONE TECHNOLOGY IN MONITORING WATER AVAILABILITY AND QUALITY IN SMALL RESERVOIRS

Report to the

WATER RESEARCH COMMISSION

by

T Bangira[1], M Sibanda[3], O Mutanga[2], A Clulow[2], S K Gurmessa[2] and T Mabhaudhi[1]

[1]Centre for Transformative Agricultural and Food Systems

[2]School of Agricultural, Earth and Environmental Sciences, University of KwaZulu-Natal

[3]Faculty of Arts, University of the Western Cape

Report No. 3224/1/25

ISBN 978-0-6392-0731-5

August 2025

Obtainable from:

Water Research Commission
Private Bag X03
Gezina, 0031
South Africa

hendrickm@wrc.org.za or download from www.wrc.org.za

This is the final report of WRC project no. C2022/2023-00912.

EXECUTIVE SUMMARY

Background

Global water demand has sharply increased over the last century. Water is a fundamental input in agricultural production and plays a principal role in maintaining food security. Small water bodies such as dams, ponds and lakes can capture rainwater runoff and provide water for irrigation during dry periods. In addition, small water bodies are home to a large amount of biodiversity, including endangered species. Anthropogenic activities and climate change can affect their nutrient retention and the quality and quantity of water stored in these reservoirs. However, little is known about the spatial-temporal variations of water quality and quantity in small water bodies at a local scale and in South Africa at large.

South Africa's semi-arid climate (mean annual precipitation of 500 mm) highlights how erratic and unpredictable precipitation is, a significant obstacle for the country's rain-fed agriculture. To boost agricultural production and promote food security during dry seasons, farmers in semi-arid regions (including most rain-fed areas in South Africa) must irrigate the crops using water stored in small water bodies. The Department of Water and Sanitation in South Africa reported that irrigation and stock watering account for about 52–55% of all water used in South Africa, with small water bodies supplying about 80%. However, the quality and quantity of water stored in small water bodies are threatened.

To protect the water resources, the government of South Africa initiated the National Water Resource Strategy 2 (NWRS2) in 2013 – the strategy aimed at strengthening the regulation of water resources and water quality regardless of the reservoir size. Although the document listed the major concerns of eutrophication and sedimentation of reservoirs, it did not provide a holistic strategy to quantify and monitor them.

The prevalent challenges of stressed water resources, timely information on water quality and quantity, with known uncertainty, are critical for farmers to suit irrigation management based on in-field spatial variability and seasonal changes in water quantity and availability. Therefore, evidence-based solutions and effective technologies are needed to improve water use efficiency while increasing agricultural

productivity. To achieve this, improved spatially explicit assessments of the current water resources are imperative.

Previous work on water quality and quantity in South Africa has typically focused on selected large individual reservoirs, which makes it difficult to extrapolate to small water bodies. Additional research is warranted in light of emerging trends in estimating water level and water quality changes in small waterbodies using satellite remotely sensed data. However, satellite-borne data sets are excessively susceptible to cloud cover, and most of their applications have been for ‘snapshot’ detecting and predicting optical water quality elements rather than generating seamless monitoring of water quality parameters in large lakes. However, the derivation of high-resolution images using unmanned aerial systems (UAS) has become an alternative form of novel earth observation technologies that could offer accurate, seamless field measurements of surface water level fluctuations and their quality at local scales.

METHODOLOGY

The project's general aim was to assess the utility of drone technology to monitor water availability and quality in irrigation canals and dams. In this study, four systematic reviews were undertaken to review the literature on methods and algorithms available for utilising UAVs in monitoring water quality and quantity in small reservoirs. The second aim assessed the feasibility of using drones in detecting and mapping flooding or leaks along irrigation canals and dams. It is worth mentioning that this aim was challenging to achieve since the irrigation canals were not easy to access. Nevertheless, the study has monitored the changes in water bodies by using change detection. The assumption is that flooding occurs when a usually dry pixel becomes wet. Conversely, drought occurs when a usually wet pixel becomes dry. Notably, this assumption aligns with the recommended practices advocated by many researchers. The third aim was to assess drones' spatial and temporal resolution capabilities in detecting and mapping water levels and quality in irrigation canals and dams. The results from the reviews paved the way for the choice of suitable algorithms for monitoring water quality and quantity in small reservoirs using remotely sensed data collected by multispectral and LiDAR sensors on board the UAVs. Several spectral

indices and machine learning algorithms were used to monitor the spatiotemporal variability of water quality and quantity at a local scale in near-real-time.

Findings

With the development of Unmanned Aerial Vehicles (UAVs) and artificial intelligence, there has been a significant advancement in remotely sensed water quality retrieval of small water bodies, which provides water for crop irrigation. The results show modest progress in the utility of UAVs, especially in the global south. This could be attributed, in part, to high costs, a lack of relevant skills, and the regulations associated with drone procurement and operational costs. The progress is further compounded by a general lack of research focusing on UAV application in water resources monitoring and assessment. More importantly, the lack of robust and reliable water quantity and quality data to parameterise models remains challenging. However, there are opportunities to advance scientific inquiry for water quality and quantity accounting by integrating UAV data and machine learning.

The application of remotely sensed data from UAVs to retrieve key water quality parameters such as surface water temperature, total suspended solids (TSS), cyanobacteria, temperature, nutrients, and Chromophoric Dissolved Organic Matter (CDOM) in inland water bodies is still in rudimentary stages in the Global South. Multispectral sensors, especially those on DJI platforms, dominate the literature for water quality monitoring in small water bodies due to their cost-efficiency, portability, and ability to capture key spectral bands (green, red, red-edge, and near-infrared) sensitive to chl-a. Machine learning models like Random Forest and Support Vector Machines are widely used for chl-a retrieval. However, a significant gap exists in Africa due to financial, regulatory, and technical barriers. Standardised algorithms and validation protocols also remain a key research priority. The empirical study integrates UAV-based multispectral data from April, June, and July 2024 with in-situ measurements of chl-a, total nitrogen (TN), total phosphorus (TP), and dissolved oxygen (DO). Among machine learning models tested, Artificial Neural Networks (ANN), Random Forest (RF), Support Vector Machine (SVM), and Extreme Gradient Boost (XGBoost), K-Nearest Neighbours (KNN), ANN outperformed others, achieving R^2 values of 0.949, 0.991, and 0.734. The green, red, and red-edge bands were the

most sensitive for chl-a estimation. Seasonal patterns emerged, with high chl-a concentrations in April and June, followed by a decline in July due to reduced water levels. In July, strong correlations were found between chl-a and nutrient parameters, particularly TP (R^2 = 0.87) and TN (R^2 = 0.71). This study highlights the potential of UAV-based remote sensing for high-resolution chl-a monitoring in small water bodies. The findings underscore the importance of continuous water quality monitoring to adapt to rapidly changing environmental conditions, offering a scalable solution for water resource management in smallholder agricultural systems worldwide.

Spectral indices such as the Specific Near-Infrared Index (SNIR) and Shortwave Band Reflectance Edge (SBRE) were used to characterise TSS. In contrast, the Normalized Difference Vegetation Index (NDVI), Green Normalized Difference Vegetation Index (GNDVI) and Green Chlorophyll Index (GCI) were used to characterise CDOM. These indices were instrumental in estimating and predicting TSS and CDOM concentrations using machine learning algorithms, individual models and model ensembles. The model ensembles for TSS and CDOM produced the highest predictive accuracies, respectively (RMSE=30.50 mg/l and R^2=0.62) and (RMSE=0.17 mg/L and R^2=0.61), respectively. Although the model performance metrics were moderate, many limitations did arise during this study, which are further elaborated on in future research recommendations.

New Knowledge and Capacity Development

This work made a substantial contribution to the body of knowledge. In particular, it is novel to map water quality and quantity in small water bodies of the Umgeni catchment in almost real-time using remotely sensed data collected by cameras aboard UAVs. To our knowledge, the estimation of chlorophyll-a, total suspended solids (TSS) and nutrients in small water bodies using drone imagery in Umgeni Catchment has not been previously conducted. Furthermore, using machine learning algorithms to estimate TSS and chlorophyll-a from high-resolution (5ccm) drone images is innovative. Three MSc students were funded in this project, and they have managed to use their results to publish manuscripts in peer-reviewed journals.

Recommendations

This study's findings may be valuable for the ongoing discussions on managing water resources during the climate change era. The spatio-temporal variations in water quality and quantity in small water bodies highlighted in this study should also be considered in other catchments, especially in areas with arid environments. This study showed that a water body can contain many water quality parameters, which require hyperspectral sensors to characterise the spatio-temporal variability of these parameters. For instance, sensors with coarse spectral resolution can miss different species of cyanobacteria. The impacts of land use and water pollution sources should also be considered during similar studies. Ideally, the increase in TSS in water bodies originates from poor farming practices. Using fertilisers to boost agricultural production contributes a lot to the eutrophication of water bodies. The use of organic manure in crop farming must be encouraged.

For evaluating optically active water quality parameters in small water bodies, it is advised to evaluate other machine learning techniques that were not examined in this study. Collaborative research efforts involving government bodies, academic institutions and local communities can provide interdisciplinary applications and ensure that UAV-based technologies are accessible and beneficial to a broader audience. Expanding the scope of research to include underrepresented regions and parameters is also essential. Most studies have focused on large lakes, rivers and coastal areas, leaving smaller inland water bodies like farm reservoirs underexplored. Given their socio-economic importance, particularly for agriculture and rural development, these water bodies should be a primary focus of future research. Finally, future efforts should emphasize the socio-economic benefits of UAV-based monitoring. By demonstrating its value in improving water resource management, agricultural productivity, and environmental sustainability, researchers can build a stronger case for investment and adoption.

ACKNOWLEDGMENTS

The research presented here was a component of an unsolicited project initiated, funded, and overseen by the Water Research Commission (WRC) in the Key Strategic Area 4 (Water Utilisation in Agriculture). The project team sincerely thanks the WRC for funding and managing the project. The project team also wishes to sincerely thank the following members of the Reference Group for their valuable contributions and guidance:

Prof S Mpandeli	Water Research Commission (Chairman)
Dr L Nhamo	Water Research Commission
Dr S Hlophe-Ginindza	Water Research Commission
Prof A van Niekerk	Stellenbosch University
Dr ZE Mashimbye	Stellenbosch University
Terry Newby	Consultancy
Mike Wallace	Western Cape Department of Agriculture

In addition, the project team would also like to thank the following individuals:

- The Water Research Commission for funding this research.
- Mr T Mnguni, manager at UKZN Umgenipoort Research Facility, for supplying the boat and facilitating access to High Flight Farm.
- Dr C Dlamini, Dr T Matongera and Dr S Gokool of the University of KwaZulu-Natal for drone flying.
- Postgraduate students Ms Pillay, Ms Ngwenya, and Mr Mawodzeke of the University of KwaZulu-Natal, thank you for contributing to this research project.
- Administration personnel at the Center of Transformative Agriculture and Food Systems (CTAFS) for all the administrative work.
- Many stakeholders whose contributions laid the groundwork for the data used in the report.

TABLE OF CONTENTS

LIST OF TABLES

LIST OF FIGURES

LIST OF ACRONYMS AND ABBREVIATIONS

ANN	Artificial Neural Networks
BOD	Biological Oxygen Demand
CDOM	Chromophoric Dissolved Organic Matter
CHL-a	Chlorophyll a
COD	Chemical Oxygen Demand
DO	Dissolved Oxygen
DP	Dissolved Phosphorus
EO	Earth Observation
ETM+	Thematic Mapper Plus
GBDT	Gradient Boost Decision Trees
GRRI	Green Red Ratio Index
LiDAR	Light detecting and ranging
LST	Land surface temperature
LULC	Land use and land cover
ML	Machine learning
MNDWI	Modified Normalised Difference Wetness Index
MSI	Multispectral instrument
NDVI	Normalised Difference Vegetation Index
NDWI	Normalised Difference Wetness Index
NIR	Near Infrared
NN	Neural networks
OA	Overall accuracy
RF	Random forest
RMSE	Root mean square error

SVM	Support Vector Machines
SWI(s)	Spectral Water Index (Indices)
SWIR	Shortwave Infrared
TN	Total Nitrogen
TSS	Total Suspended Solids
UAVs	Unmanned Aerial Vehicles
VARIGREEN	Visible Atmospherically Resistant Index

LIST OF SYMBOLS

m^3	Cubic metre
NH3-N	Ammonia Nitrogen
NO3-N	Nitrate Nitrogen
GDP	Gross domestic product
kg	Kilogramme
kg/ha	Kilogrammes per hectare
ha	Hectare
mm	Millimetre
km^3	Cubic kilometres
km^2	Square kilometres
°C	Degrees Celsius

REPOSITORY OF DATA

For details related to the project's data, please contact:

Dr Tsitsi Bangira (Project Leader and Principal Researcher)
Centre of Transformative Agriculture and Food Systems
School of Agricultural, Earth and Environmental Sciences
University of KwaZulu-Natal
P Bag X 01 Scottsville 3209
Pietermaritzburg, South Africa
Email: bangirat@ukzn.ac.za

1. INTRODUCTION AND PROJECT OVERVIEW

1.1. Background and Rationale

Growing populations in developing countries rely on freshwater stored in small waterbodies for agricultural, domestic, mining and industrial use (Bangira et al. 2019; Sibanda et al. 2021). The global water demand has sharply increased over the last century. Water is a fundamental input in agricultural production and plays a principal role in maintaining food security. Agriculture primarily uses irrigation to consume about 70% of freshwater globally (Riches 2018). These water resources, especially those in Africa, are highly susceptible to climate variations and pollution. Subsequently, the available resources are generally insufficient to withstand these perturbations.

Meanwhile, climate change is already affecting the water cycle processes (e.g. precipitation, evaporation, runoff, etc.) and water demand. Specifically, an increase in temperature increases the rate of evaporation of water into the atmosphere, which in turn increases the atmosphere's capacity to "hold" water. Increased evaporation may dry out some areas and fall as excess precipitation in other areas (Kundzewicz et al. 2018). Heavy downpours are increasing the runoff into rivers and lakes, washing sediment, nutrients, pollutants, trash, animal waste, and other materials into water supplies, making them unusable and unsafe for consumption (Tebbs et al. 2020).

Furthermore, the increasing impacts of anthropogenic activities on water resources negatively affect the quality and quantity of water stored in reservoirs. The effects of climate change on water availability and quality affect many sectors, including energy production, infrastructure, human health, agriculture, and ecosystems. Irrigation is approximately twice as productive per unit of land concerning rain-fed agriculture. Above all, irrigation facilitates production intensification and high crop diversification and fosters food security (FAO 2022; Cao et al. 2023). However, competition for water resources is increasing alarmingly due to climate change, high population growth rates, and urbanisation, with a magnified effect on agriculture. Currently, crop irrigation focuses on reducing water use while increasing productivity. Given the prevalent challenges of stressed water resources, timely information on water quality and quantity, with known uncertainty, is critical for farmers to suit irrigation management based on in-field spatial variability and seasonal changes in water quantity and

availability (Dong et al. 2022). Therefore, evidence-based solutions and effective technologies are needed to improve water use efficiency while increasing agricultural productivity (Dube et al. 2022). To achieve this, improved spatially explicit assessments of the current water resources are imperative. Specifically, there is an urgent need to monitor water levels across all carriageways and sources to reduce water losses directly through leakages and degradation.

Monitoring water levels will help formulate robust and effective frameworks for sustainable utilisation and management from local farm scales to national and regional scales. Hence, there is a growing need to establish integrated, cheap, robust and spatially explicit water quality monitoring approaches as a yardstick for achieving food and water security under climate change (Bangira et al. 2019; Congalton & Green 2019; Cao, Yu & Qiao 2023).

Water quantity and quality in natural and artificial reservoirs are evaluated using conventional in-situ field sampling and laboratory measurements (Banna et al. 2014; Fisher et al. 2016). These point-based sampling strategies with laboratory processing are discrete, costly, labour-intensive, time-consuming, and cannot adequately assess the entire water body (Bangira et al. 2024). The accuracy and precision attained when using in-situ collected data can be questionable because of the potential field sampling and laboratory-generated errors. Furthermore, these conventional methods lack an optimal revisit frequency required to capture the water quality and quantity dynamics across the growing season, which is essential to facilitate sound irrigation planning and improve water use efficiency. To overcome the limitations of in situ water quality monitoring methods, which are continuously and rapidly changing, there is a need for regular near-real-time, inexpensive, automated and non-invasive approaches with adequate spatial-temporal coverage (Gholizadeh et al. 2016). Over the previous decade, near real-time remote monitoring of basins and water bodies using remotely sensed data has emerged as an alternative and promising technique for increasing our knowledge of the characteristics of irrigation water from local farms to global scales (Carpenter & Carpenter 1983; Seyhan & Dekker 1986).

Remote sensing data acquired by sensors onboard satellites provides invaluable, unbiased, rapid and cheap spatially explicit information about the quality and quantity

of surface water bodies required to improve water use efficiency while increasing agricultural productivity (Carpenter & Carpenter 1983). Specifically, numerous studies have demonstrated the utility of remotely sensed data in monitoring water quality by generating empirical algorithms based on the optical biochemical elements that define the upwelling radiance above the water surface and in the water surface about its equivalent surface reflectance (Matthews et al. 2010; Chebud et al. 2012; Choo 2018; Chen 2021). For instance, a growing body of literature illustrates that Landsat remotely sensed data can be used to optimally estimate water quality parameters such as total suspended matter, chlorophyll-a, turbidity, Secchi disk depth, total phosphorus, dissolved oxygen, chemical oxygen demand (COD) and biochemical oxygen demand (BOD) due to their relatively low cost, temporal coverage and spatial resolution (Torbick et al. 2013; Malahlela et al. 2018; Lai et al. 2021). Torbick et al. (2013) in testing the utility of Landsat 8 OLI data in estimating turbidity, total suspended solids (TSS), chemical oxygen demand (COD), biological oxygen demand (BOD), and dissolved oxygen (DO) attained optimal accuracies (R^2 values were 0.991, 0.933, 0.937, 0.930, and 0.934 for turbidity, TSS, COD, BOD, and DO, respectively). However, numerous other water quality parameters are often omitted by existing literature. Yet, they are critical in crop irrigation, such as pH, total nitrogen (TN), ammonia nitrogen (NH3-N), nitrate nitrogen (NO3-N), and dissolved phosphorus (DP). To benefit from the potential advantages of remote sensing in evaluating water resources, it is necessary to assess the utility of remotely sensed data in detecting, mapping, and seamlessly monitoring all critical water quality parameters.

Although satellite-borne earth observation (EO) technologies such as Landsat have played a critical role in accurately characterising water quality and quantity of basins and water bodies for irrigation seamlessly, these data sets are excessively susceptible to cloud cover. Most of their applications have been for ‘snap-shot’ detecting and predicting optical water quality elements rather than generating seamless monitoring of water quality parameters (Yang et al. 2022). However, the derivation of high-resolution images using unmanned aerial systems (UAS) has become an alternative form of novel EO technologies that could offer accurate seamless field measurements of surface water level fluctuations and their quality at local scales. Compared to other remote sensing facilities, UAVs offer an advanced, reliable, automatic, durable,

practical and near real-time method of objectively and seamlessly assessing and monitoring the quantity and quality of available irrigation water sources at local scales, which was previously impossible using satellite-derived data (De Keukelaere et al. 2023). Furthermore, drones provide high spatial resolution data for detecting and mapping water quality and quantity parameters compared to cheap and readily available satellite-derived data from sensors such as MODIS, Landsat and Sentinel 2. While hyperspectral satellite-borne sensors, such as QuickBird, RapidEye, World View, and IKONOS, can offer high-resolution data sets, their acquisition costs are significantly higher than those of UAVs (Brando & Dekker 2003; Kim et al. 2020).

In South Africa's context, this transdisciplinary research project sought transformation and redress, sustainable development, informing policy and decision-making, supporting food systems, and generating new products and services for economic development. Over the three years, six deliverables have been due to the WRC, which addressed four specific project objectives.

1.2. Objectives

The contractually specified objectives of the project were to:

1.2.1 General objective

To assess the utility of drone technology to monitor water availability and quality in irrigation canals and dams.

1.2.2 Specific objectives

Specific objective 1: To review the literature on the available models for remote sensing water quantity and quality using UAVS.

Specific objective 2: Assessing the feasibility of using drones in detecting and mapping flooding or leaks along irrigation canals and dams.

Specific aim 3: Assessing the spatial and temporal resolution capabilities of drones in detecting and mapping the levels and quality of water in irrigation canals and dams.

All the contractually stated objectives were achieved and form the basis of this research report.

1.3. Scope and the overview of the report

This document is the final WRC CON2022/2023-00912 project report. The document is divided into independent chapters, each authored by multiple authors. Based on the recommendations and suggestions from the WRC project managers, technical reference group members, and the crucial international peer review system for chapters published in peer-reviewed journals. It is worth mentioning that each of these chapters fully or partially addresses at least one of the project's contractual objectives. However, in this report, the general methodology chapter is excluded because each chapter has its specific methodology. There will undoubtedly be similarities or duplicates, specifically in the methods and materials sections, considering the paper technique used in presenting this report because the stand-alone chapter addresses the same overall project goal. This was considered trivial because the methods and principles presented in each of these chapters flow together seamlessly to meet the same overall goal of the project. In addition, certain chapters are modified from previous publications in international peer-reviewed journals. The report is set up to address each project's contractual goals logically.

Specifically, the chapters in this report are as follows;

Chapter 1: Outlines a thorough overview, background information, and project conceptualisation. It explains the purpose of the general study as outlined in the terms of reference, and it lays out the specific goals and objectives of the project as specified in the project contract.

Chapter 2: Presents a comprehensive and state-of-the-art systematic review of the literature on the potential use of remote sensing-based models for monitoring chlorophyll-a and nutrients in small water bodies using remotely sensed data acquired by sensors onboard UAVs. The first contractual aim is directly addressed in this chapter.

Chapter 3: Provides systematic reviews of the literature on the utility of remotely sensed data from sensors onboard UAVs for assessing water quality in irrigation canals and dams for improving crop water productivity and enhancing precision agriculture in smallholder farms. The reviews focus on the temporal and spatial scale of studies and the techniques and sensors used in the global south in water quality monitoring. The specific water parameters, techniques or algorithms, and accuracy achieved using remotely sensed data acquired by sensors onboard UAVs were revealed. The major water quality parameters, including cyanobacteria, chlorophyll a, total suspended solids (TSS), temperature, turbidity, coloured dissolved organic matter (CDOM), dissolved oxygen (DO) and clarity, were revealed. The findings from these reviews influenced the choice of the methods used in **Chapters 4** to **8**. Contractual objective number 3 was addressed in this chapter.

Chapters 4 to **8** addressed contractual objectives number 2 & 3.

Chapter 4: Gives a detailed analysis of the potential and advancements of using drone technology for monitoring chlorophyll a, total nitrogen, total phosphorous, water surface temperature, TSS and CDOM in small water bodies in the Umgeni catchment. This chapter addresses contractual objective 3.

Chapter 5: Applied machine learning algorithms on remotely sensed data acquired by sensors onboard UAVs to estimate the concentration of Chlorophyll-a, dissolved oxygen and nutrients in a small reservoir. The limitations, strengths and challenges of the suggested techniques are also discussed in this chapter. This chapter also partially addresses contractual objective number 3.

Chapter 6: Presented an assessment of the feasibility of using drones in mapping changes in water levels as a proxy for detecting and mapping flooding or leaks along irrigation canals and dams in the Umgeni catchment. This chapter partially addresses contractual objectives number 2 and 3.

Chapter 7: Provides a comprehensive discussion of the entire project, connecting all individual studies to fulfil the project objectives. The chapter also delivers conclusions and recommendations for future research.

2. APPLICATION OF DRONE TECHNOLOGIES IN MONITORING CHLOROPHYLL-A IN SMALL WATERBODIES: SYSTEMATIC REVIEW OF PROGRESS, CHALLENGES, AND OPPORTUNITIES IN THE GLOBAL SOUTH.

2.1. The significance of small waterbodies in the global South

Freshwater accounts for only 2.5% of the total water on the earth's surface, and about 1.5% is accessible for biophysical processes (Stephens et al. 2020). Meanwhile, fresh water is a fundamental input in agricultural production and numerous manufacturing industries, and it is a basic need for domestic use. Specifically, agriculture accounts for about 70% of the total freshwater usage globally, mainly through irrigation (Finley & Seiber 2014; FAO 2022). The world's population is expected to rise from the current 7.8 billion to around 9.7 billion people by 2050, resulting in increased competition for water resources across various industries. Consequently, global agricultural production is expected to increase by 60% to 70% (Fischer 2009), substantially increasing water demand.

In the global south, particularly Southern Africa, water resources are unevenly distributed, compounded by climate variability (i.e., an unpredictable seasonality of precipitation). The quality and quantity of available water affect all water users, including crop irrigation. Based on the recent findings presented by Bronkhorst et al. (2017), irrigation agriculture contributes to 25 – 30% of South Africa's agricultural production and is responsible for up to 90% of high-value crop production and 25 to 49% of industrial crop production; however, it uses 60% of freshwater resources (Von Bormann & Gulati 2014; Bronkhorst, Pengelly & Seyler 2017). Meanwhile, urban and rural water use (including domestic use) consumes 30% of the available water resources. In this regard, there is an urgent need to identify accurate and efficient methods for assessing the quality and quantity of available surface water resources. The quantity and quality of available water resources are conventionally determined from in situ measurements, which can sometimes be time-consuming and costly (Gholizadeh, Melesse & Reddi 2016). In situ measurements do not always provide adequate spatial representativeness, and information may not be readily available to users such as farmers. In situ measurements may not always provide information

about the temporal variability of available water, which is necessary for managing crop irrigation (Gholizadeh, Melesse & Reddi 2016).

2.2. Eutrophication in Upper Umgeni Catchment

Literature notes that the excessive use of pesticides and fertilisers contributes to nutrient loading, specifically phosphorus and nitrogen, in water bodies, a phenomenon known as eutrophication (Serediak et al. 2014; Gao et al. 2015; Dlamini et al. 2016). Farmers aiming to enhance production frequently utilise nitrogen and phosphorus-based fertilisers and pesticides (Baiphethi & Jacobs 2009; Davis et al. 2017). Some studies have recorded the highest loads of 4 602 kg/year of ammonia (NH_3), 7 998 kg/year of nitrate, and 800 kg/year of total phosphorus entering Midmar Dam (Van Deventer et al. 2022). Additionally, eutrophication in the catchment is exacerbated by inadequate sanitation maintenance systems impacting water quality within the Midmar sub-catchment, as Ramnath (2010) noted.

The combination of high nutrient concentrations, elevated temperatures due to climate change, and light energy creates favourable conditions for algae proliferation in water bodies (Rankinen et al. 2019; Paerl & Barnard 2020). However, the flourishing algal blooms contribute to fluctuations in dissolved oxygen (DO) (Koparan et al. 2018). Consequently, the alteration in DO emerges as a noteworthy outcome of eutrophication in water bodies (Omer 2019; Zhao et al. 2021). As a result of eutrophication in aquatic environments, there is a significant change in the levels of DO, which has been identified as a crucial indicator of biological activity and eutrophication (Chung & Yoo 2015; Omer 2019; Zhao, Fan & Zhao 2021). It is crucial to emphasise that maintaining healthy water quality entails DO levels above the critical threshold of 4.5 mg/L (Banerjee et al. 2019).

South Africa has witnessed a rapid increase in eutrophication, jeopardising its water bodies' functionality in the last decade (Van Ginkel 2011). According to Harding (2015), 76% of South African dams are affected by eutrophication. In addition, Matthews and Bernard's (2015) study in South Africa on the 50 largest water bodies revealed alarming statistics, with 62% of the dams showing high levels of nutrient enrichment and 52% experiencing cyanobacterial blooms. The South African government has thus been implementing measures to address eutrophication, such

as the National Eutrophication Monitoring Programme (NEMP). This programme is currently operational in over 80 impoundments in the country (DWS 2022). The NEMP programme has produced valuable data sets, such as the Cyanolakes website, focused on chlorophyll-a (chl-a) and cyanobacterial analyses. Despite the initial plans of the government to expand the network from 50 to 100 reservoirs by 2012 (DWAF 2004), challenges, including funding constraints, have limited its reach. Though commendable, the government's efforts indicate that more extensive research and proactive measures are required to combat eutrophication in South African water bodies.

2.3. Cyanobacteria (blue-green algae)

NEMP (2002) defines cyanobacteria, previously called blue-green algae, as a diverse group of prokaryotic bacteria that exhibit single-celled or multicellular structures that undergo photosynthesis as part of their metabolism process. These organisms thrive in environments with water, light, carbon dioxide, and inorganic substances, with optimal growth occurring at temperatures above 25ºC (Falconer et al. 1999). Thus, climate change emerges as one of the significant drivers of cyanobacterial blooms, fueled by rising global temperatures and erratic rainfall patterns (Joehnk et al. 2008; Paerl & Barnard 2020). Cyanobacteria blooms indicate increased eutrophication rates (Van Ginkel 2011) and pose adverse effects, forming toxic scum that can clog irrigation systems, such as pumps and filters (DWAF 2004).

To assess cyanobacteria algal levels, two common algal pigments, chl-a and phycocyanin, are frequently employed (Kutser et al. 2006; Urquhart et al. 2017; Shi et al. 2019). However, estimating phycocyanin in eutrophic water bodies is challenging because it is less sensitive to commercially available equipment (Stumpf et al. 2016; Fernandez-Figueroa et al. 2022). Thus, chl-a serves as a widely used indicator parameter for eutrophication (Harvey et al. 2015; Lins et al. 2017; Rankinen et al. 2019; McEliece et al. 2020; Cao, Yu & Qiao 2023) and functions as a proxy for algae (Schaeffer et al. 2013; Kim & Ahn 2022). Table 2-1 summarises the target water quality range meanings of algae in a water body. Remote sensing is one approach used to estimate chl-a as a proxy for water quality, leveraging the optically active constituents of chl-a to measure and monitor its presence.

Table 2-1 Target water quality range for algae (Odume et al. 2024)

Range	Interpretations
$0 - 15$µg/L	No health effects
$15 - 30$µg/L	Algal scum is likely to occur; water may take a green colour resulting in reduced light penetration.
> 30µg/L	Water appears to have significant levels of algal scum and may present a considerable nuisance.

2.4. Remote sensing of small water bodies

Earth observation and geospatial technologies have been widely proven to provide synoptic, timely, and spatially explicit data on various aspects of the Earth's surface, including the spatiotemporal variability of the quality and quantity of available water (Gholizadeh, Melesse & Reddi 2016). The literature shows that clean water generally absorbs electromagnetic energy from the visible section (green) to the longer wavelengths in the infrared sections [8,9]. Subsequently, water has been detected and discriminated from other land cover types. Furthermore, this attribute of clean water has facilitated the determination of water quantity (surface volumes, spatial extent) and quality of surface water resources based on earth observation data and geospatial approaches. Earth observation facilities have been proven helpful in accurately and efficiently characterising various attributes of surface water resources. These include the moderate-resolution imaging spectroradiometer (MODIS) (Ovakoglou et al. 2016), Landsat (Dube et al. 2016), SPOT (Sallam et al. 2018), and Worldview (Ismail 2012), Medium Resolution Imaging Spectrometer (MERIS) (Campbell et al. 2011), to mention a few. Reddi (2016) provide detailed parameters widely used to estimate water quality using remote sensing techniques. However, Gholizadeh, Melesse and Reddi (2016) extensively illustrate the application of remote sensing techniques at regional and landscape scales. Additionally, freely available satellite-borne earth observation facilities such as the Landsat and Sentinel 2 multispectral instruments remain inapplicable for local to farm-scale water resources monitoring and management.

Unmanned aerial vehicle systems (UAVs), also known as drones, have emerged as a potential alternative for mapping and monitoring the quality and quantity of water resources at local scales. This is because drones are flexible, relatively cheaper in comparison to in situ measurements and space-borne remote sensing, and can be

flown at low altitudes, offering very high spatial resolution data with high prospects of timely and accurately characterising water quality and quantity for smallholder irrigation farms (Xiang et al. 2019). Unlike satellite and other air-borne sensors, UAVs could monitor hazards (i.e., after landslides, floods, and fires) (Xiang, Xia & Zhang 2019) because they generate near-real-time, fine-resolution, spatially explicit information. Despite the usefulness of UAVs, their application in agriculture, rural development, and, more importantly, water resources management remains limited. Although some studies have sought to assess the literature on the utility of drones for a water resources assessment (Lally et al. 2019; Yao et al. 2019), the studies do not provide a systematic review that focuses on characterising water quality and quantity in the context of smallholder farming in the global south.

2.5. Remote Sensing of Chlorophyll-a (Chl-a) and Spectral Properties

Lillesand et al. (2015) define remote sensing as collecting information about an object, land region, or ecosystem process via a non-contact device. Remote sensing is a cost-effective method that complements in-situ data (Li & Li 2004). Remote sensing platforms, equipped with sensors, obtain data from a distance. There are three types of platforms: airborne platforms (manned aircraft, unmanned aerial vehicles (UAVs)), groundborne platforms (ground-based laser scanning (LiDAR), terrestrial photogrammetry), and space-borne platforms (low-earth orbit platforms, geostationary orbit platforms). In remote-sensed water quality, it is fundamental to understand the spectral properties of a parameter of interest.

Chl-a exhibits distinctive spectral properties crucial for its remote sensing and quantification. Chl-a is associated with four key bands: near-infrared (NIR), red (R), blue (B), and green (G) (Kabbara et al. 2008; Chebud et al. 2012). Research by Gitelson 1992 revealed that chl-a primarily absorbs and reflects light within 400 and 500 nm wavelength ranges. It has a high absorption rate in the blue and red regions, particularly around 443 and 675 nm, and reflects strongly in the green and red-edge spectra, around 550-555 nm and 685-710 nm, respectively (Gitelson 1992; Kirk 1994; Mobley 1994). High chl-a concentrations are observed by an increase in reflectance at bands G and R and a decrease at band B (Pulliainen et al. 2001). The maximum reflectance associated with chl-a is observed at 580 nm (Lichtenthaler & Babani 2000)

and peak reflection at 700 nm (Gitelson 1992). Therefore, monitoring changes in reflectance within these bands, particularly increases in G and R and decreases in B, is instrumental in identifying high chl-a concentrations. Figure 2-1 shows the spectral absorbance graph of chl-a.

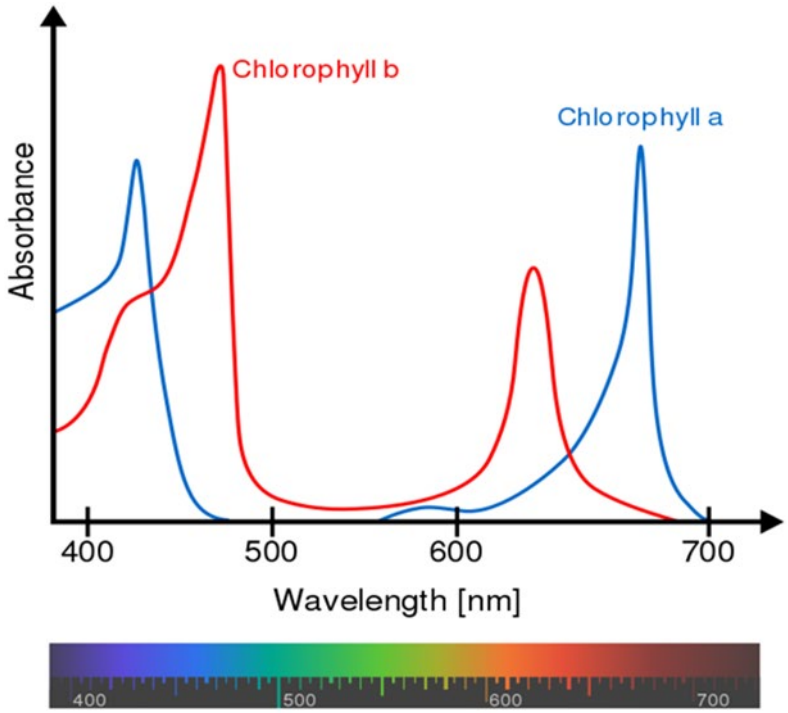

Figure 2-1 Spectral absorbance of chlorophyll-a (Pugliesi 2012)

2.6. Remote Sensing of Chl-a using Satellites Borne Remotely Sensed Data

When combined with conventional monitoring techniques, satellite technology is useful for measuring chl-a levels in aquatic systems. Globally, numerous studies have demonstrated the potential of satellite-based remote sensing for monitoring water quality, particularly chl-a concentrations. For instance, satellites like the Sentinel-2, Medium Resolution Imaging Spectrometer (MERIS), Landsat 8 OLI, and MODIS/AQUA have been widely used to derive spectral data linked to chl-a concentrations. These platforms offer significant advantages, including broad spatial coverage, consistent temporal monitoring, and cost-effectiveness, as they provide free access to historical and near real-time data (Torbick et al. 2013; Matthews & Bernard 2015; Lai et al. 2021; Tian et al. 2023). Applications extend to detecting harmful algal blooms (HABs) and monitoring biomass in large water bodies (Kutser et al. 2006;

Anderson 2009). Studies, such as Harvey, Kratzer and Philipson (2015), have shown a strong correlation between satellite-derived chl-a measurements and in situ observations collected within a 0–3 day time frame, achieving an RMSE of 64% and a mean normalised bias (MNB) of 17%. Similarly, Gohin et al. (2020) demonstrated using MODIS/AQUA, VIIRS/NPP, and OLCI-A/Sentinel-3 in detecting chl-a, revealing consistent trends between satellite retrievals and in situ measurements.

Despite their global utility, satellite platforms face inherent challenges. These include limited spatial resolution, particularly problematic for smaller water bodies like rivers and ponds (Anderson & Gaston 2013; Palmer et al. 2015; Adjovu et al. 2023), and data inconsistencies caused by the time lag between satellite overpasses and field sampling (Su & Chou 2015; Lai et al. 2021). Cloud cover further complicates data acquisition by obscuring optical signals, which impacts accuracy (Sagan et al. 2020b). In addition, satellite platforms have image signal-to-noise ratio (SNR), data storage, and transmission problems (Cao et al. 2021; Yang et al. 2022). To address these limitations, recent advancements in remote sensing have shifted focus toward higher-resolution platforms, such as unmanned aerial vehicles (UAVs).

In South Africa, satellite-based remote sensing has been applied to monitor chl-a concentrations in various water systems, including dams, reservoirs, and wetlands. Studies have utilised platforms like Sentinel-2, MERIS, and Landsat 8 OLI to assess water quality parameters, with some success in identifying patterns of eutrophication and cyanobacteria blooms (Matthews 2014; Malahlela et al. 2018; Sakuno et al. 2018; Ali et al. 2022; Dzurume et al. 2022). These studies highlight the cost-effectiveness and practicality of satellite imagery for large-scale monitoring. However, research on smaller water bodies remains scarce, as the coarse spatial resolution of satellites limits their applicability in such contexts. Additionally, many South African studies were conducted on larger lakes, often overlooking the importance of monitoring smaller water bodies critical for agricultural irrigation and domestic use.

This gap in research underscores the need for innovative approaches like UAV technology, which can provide higher spatial resolution, greater flexibility in data acquisition, and enhanced accuracy for monitoring smaller inland water bodies. By complementing satellite-based observations, UAVs can bridge the gap in monitoring

water quality across various scales, particularly in resource-constrained regions like South Africa.

2.7. Remote Sensing of Chl-a in small lakes using UAVs: a systematic review

2.7.1 Literature Search Strategy

A literature search was conducted to find studies until December 2023 that estimated chlorophyll-a in small water bodies using remotely sensed data acquired by sensors onboard UAVs. The following key terms were used in the search string: “Unmanned aerial vehicle” OR Drone OR “unmanned aerial systems” AND “remote sensing” AND “chlorophyll-a” OR “algae" OR "phytoplankton" OR cyanobacteria blooms" AND "inland waters" OR "lakes" OR "reservoir" in Science Direct, Scopus, Web of Science (WOS), IEEE Xplore, and Google Scholar research databases. All articles with a published status were considered, regardless of their geographical location. Due to the variations in the configuration settings in Scopus and Web of Science, the key search strings were slightly different Table 2-2.

Table 2-2 Number of articles retained using five search engines

Search Engine	Search Criterion	Number of articles retained
Web of Science	All fields (“Unmanned aerial vehicle” OR “Drone”) AND (“remote sensing”) AND (“chlorophyll-a”) AND (“algae") AND ("phytoplankton") AND ("cyanobacteria”) AND (“inland waters”) AND ("lakes") AND (“small water bodies”) AND ("multispectral")	2262
Google Scholar	(“Unmanned aerial vehicle” OR Drone OR “unmanned aerial systems”) AND (“remote sensing”) AND (“chlorophyll-a” OR “algae" OR "phytoplankton" OR "cyanobacteria”) AND (“inland waters”)	900
Science Direct	TITLE-ABS-KEY (“Unmanned aerial vehicle” OR Drone OR “unmanned aerial systems”) AND (“remote sensing”) AND (“chlorophyll-a” OR “algae" OR "phytoplankton" OR "cyanobacteria”) AND (“inland waters”)	84
Scopus	TITLE-ABS-KEY ("Unmanned aerial vehicles" OR "drone") AND ("remote sensing") AND ("chlorophyll-a" OR "algae" OR "phytoplankton" OR "cyanobacteria blooms") AND ("inland waters" OR "lakes" OR "reservoir")	44
IEEE Xplore	ALL METADATA (“Unmanned aerial vehicle” OR Drone AND “remote sensing” AND chlorophyll-a OR algae OR phytoplankton OR “cyanobacteria blooms” AND “inland waters” OR lakes OR reservoir)	5

A total of 3295 studies were retrieved, and 55 studies were retained after the screening process. The Preferred Reporting Items for Systematic Reviews and Meta-Analysis (PRISMA) reporting checklist (https://www.prisma-statement.org/, accessed 20 February 2024) was used as a guide to eliminate bias reporting and structure the review. The articles that qualified for the meta-analysis were those that met the following criteria:

i. The scope of the study focused on the estimation of chl-a or assessment of cyanobacteria in a small water body.
ii. The study utilised data from UAV-based remotely sensed data.
iii. The results of the study and the accuracy assessment are clearly stated.

iv. The study is from an accredited journal and is peer-reviewed.
v. The study paper is written in English.
vi. The first exclusion step was to remove duplicates.

The following sections give an overview of both quantitative and qualitative analyses conducted on the extracted data.

2.7.2 Evolution and Analysis of Keywords in UAV-Derived Chl-a Literature

In assessing the evolution and topical concepts of monitoring chl-a in small water bodies using UAV-derived data, the results showed that “unmanned aerial vehicle”, “chlorophyll”, “algae”, “reservoir”, and “multispectral imagery” were the most utilised keywords around 2019 (Figure 2-2). The period between 2020 and 2021 reveals the wide application of remote sensing in monitoring chl-a in rivers. This period also represents the introduction of deep learning algorithms in water quality monitoring. The 2021 to 2022 period was marked by keywords such as “hyperspectral imaging”, “machine learning, “multispectral image”, “UAV remote sensing”, “water quality monitoring”, “linear regression”, “cyanobacteria”, and “inland waters”. This highlights the growing trend of using UAVs for water quality monitoring, adopting robust methods such as machine learning, and investing in high-resolution sensors such as hyperspectral cameras.

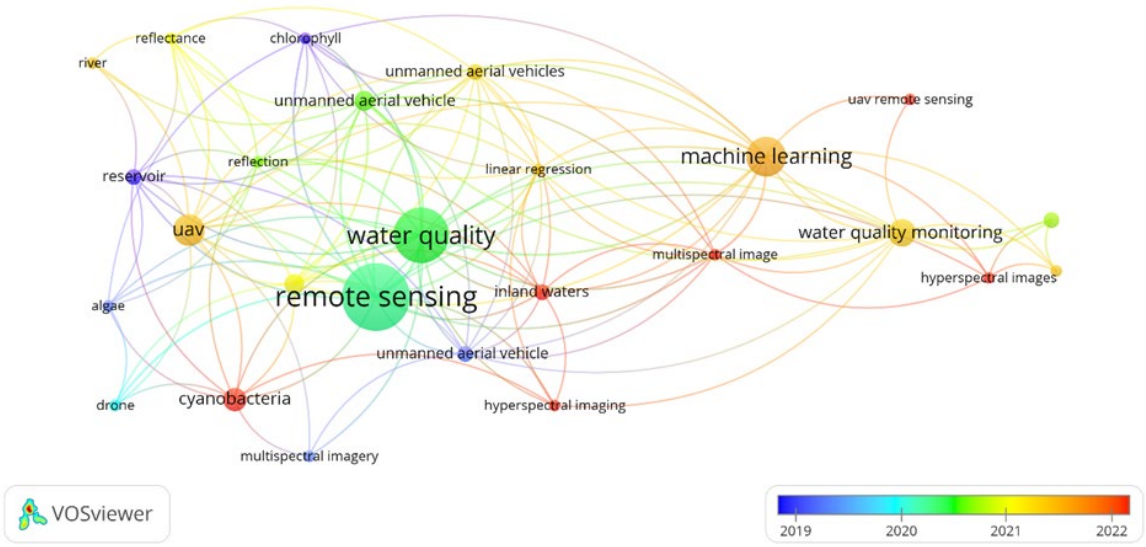

Figure 2-2 Evolution and direction of topical concepts on chl-a monitoring in small water bodies using UAV remote sensing, derived from abstracts, titles, and keywords of the selected literature

2.7.3 Spatio-temporal distribution of publications using UAVs for monitoring Chl-a in small water bodies

Figure 2-3 shows that from 2019 to 2023, using UAVs for chl-a monitoring became increasingly popular. The first study was conducted by Su (2015) in 2015, using multispectral sensors to map chl-a in the Tain-Pu reservoir in Kinmen, Taiwan. A notable surge in research activity was then observed in 2021 and 2023, accounting for 21% and 25% of the studies, respectively, focusing primarily on rivers, lakes, and reservoirs (Ahn 2021; Lu 2021; Hong 2022; Xiao 2022a; Cai 2023). A slight decline (22%) in research articles was observed between 2015 and 2019 (Jang 2016; Guimarães 2017; Choo 2018; Arango 2019; Pyo 2022).

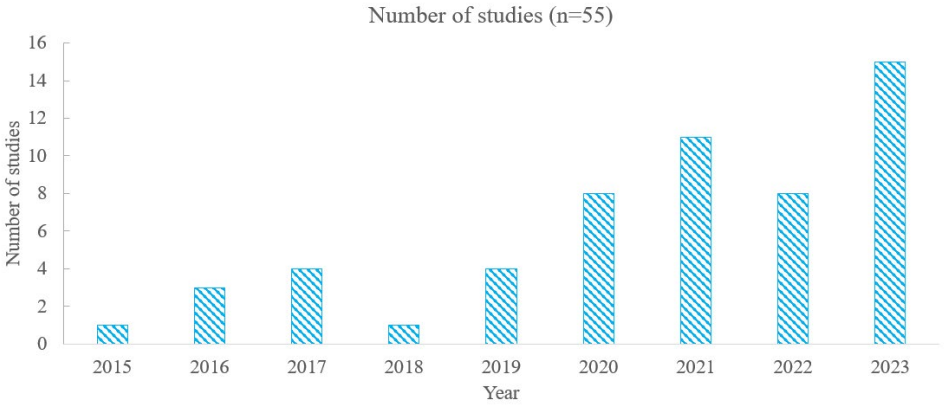

Figure 2-3 Annual frequency of UAV-based studies monitored chl-a in inland water bodies.

Figure 2-4 shows that the studies were spatially distributed in thirteen different countries, with 66% in Asia, 19% in North America, 9% in Europe and 6% in South America. In Asia, most of the studies were conducted in China (42%), followed by South Korea (23%), and 12% were done in North America, mainly in the United States of America (USA). The high volume of studies in China can be attributed to several factors. China has extensive and diverse water bodies, providing ample opportunities for water quality monitoring research using UAV technology. Additionally, China has invested heavily in UAV technology and remote sensing research, leading to more studies.

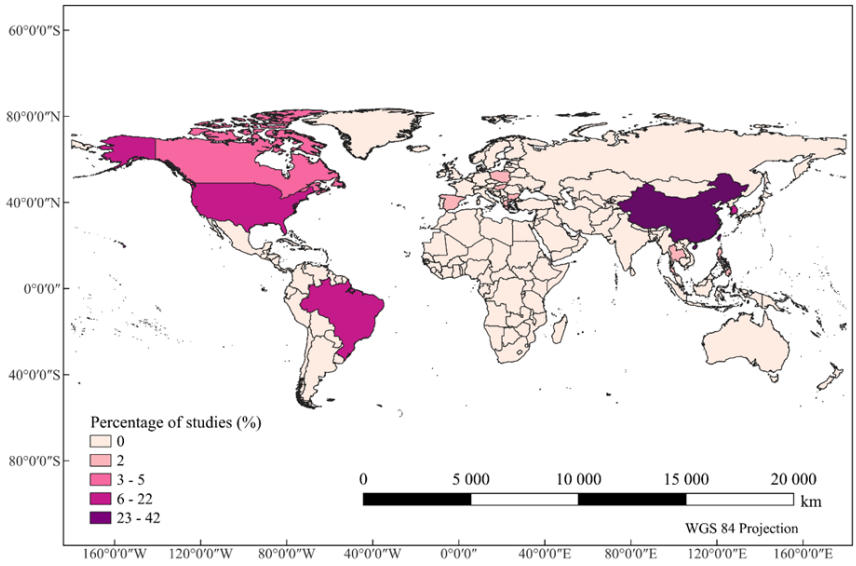

Figure 2-4 Spatial distribution of studies that utilised UAVs for chl-a monitoring in inland water bodies

2.7.4 Types of inland water bodies where the studies were done

Figure 2-5a shows that studies have used UAVs to monitor chl-a in solo or included other parameters. Approximately 60% of the articles exclusively focused on the chl-a, underscoring its importance as a key indicator of algal biomass. In comparison, 20% examined both chl-a and nutrients such as total nitrogen (TN) and total phosphorus (TP). These nutrients are primary drivers of eutrophication, which leads to increased algal growth and potential HABs. Additionally, 9% of the articles explored the relationship between chl-a and dissolved oxygen (DO). This relationship is important because excessive algal growth, indicated by high chl-a levels, can lead to oxygen depletion.

Regarding the type of water bodies, 39% of the retrieved studies were conducted in rivers, 25% in lakes and 14% in reservoirs. Interestingly, 2% of the studies focused on a dam, highlighting a significant gap in the literature. Based on the findings (Figure 2-5b), approximately 26% of the studies focused on water bodies for potable water supply, 15% on multi-purpose use (industrial, agricultural, living and drinking purposes), and 11% directed their focus towards water bodies designated for multi-

purpose and or irrigation purposes. This gives an understanding of the practical applications and relevance of the research findings.

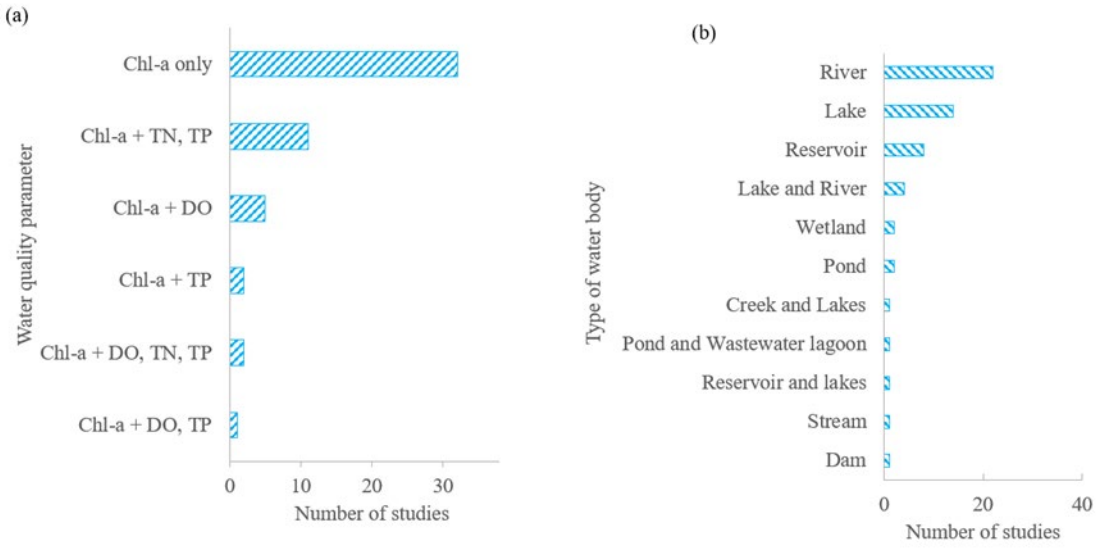

Figure 2-5 Water quality parameters, particularly those related to eutrophication, monitored with chl-a (a) types of inland water bodies studied for chl-a monitoring and their study frequency (b)

2.7.5 Characteristics of UAV platforms and sensors for mapping chl-a in inland water bodies

This review identified fixed-wing and multicopter as the primary UAV platform types used for chl-a monitoring. Multicopters dominate, with 75% of studies employing them, followed by fixed-wing drones (21%) and 4% unspecified. DJI platforms (60%) were the predominant choice among multicopter platforms, while SenseFly eBee (13%) platforms accounted for a significant share of fixed-wing vehicles. Fixed-wing UAVs offer aerodynamic benefits, enabling longer flight times, larger bloom surveillance, and multiple sensor deployment for enhanced chl-a concentration accuracy. They suit mapping broader spatial extents. Multicopters excel in closer proximity analysis due to their quick vertical take-off and landing (VTOL) capabilities. This capability makes them easily employed in environments different from fixed-wing platforms, which require substantially flat and dry areas to deploy and launch successfully near water bodies.

Thirteen multispectral and hyperspectral sensors with unique spectral bands were used in the reviewed studies. Approximately 55% of the studies utilised multispectral sensors, spanning the visible to near-infrared spectrum. These sensors predominantly utilised the near-infrared (NIR; 708nm - 842nm) and red (640nm - 668nm) bands as the optimal bands for detecting chl-a. Some studies also incorporated the green band (560nm) and blue band (475nm-497nm), and very few used the red-edge band (730nm - 740nm). The most commonly used multispectral sensor was the MicaSense Rededge, utilised by 18% of the studies.

On the other hand, 36% of the studies employed hyperspectral sensors, which captured data across a wavelength range of 350nm to 1700nm, with the 400nm-755nm band being the most utilised segment for chl-a detection. A significant number of the studies (16%) used the Nano-Hyperspec hyperspectral sensor, making it highly effective for detecting chl-a in various ecosystems. Notably, two studies (Wu 2023; Xiao 2023) employed a synergistic approach by concurrently utilising multispectral and hyperspectral sensors. This approach leveraged the strengths of both types of sensors: the broad spectral coverage and high spatial resolution of the multispectral sensors, detailed spectral information, and high precision offered by hyperspectral sensors. By combining these sensors, the studies enhanced the accuracy and reliability of chl-a monitoring and mapping.

2.7.6 Algorithms utilised for detecting chl-a concentrations in small water bodies

2.7.6.1 Spectral Indices and Band Combinations

Studies have used a variety of indices and band combinations for chl-a estimation in inland water bodies (Table 2-3) The studies have used the normalised difference vegetation index (NDVI) (Douglas Greene 2021), normalised difference red-edge index (NDRE) (Kim 2021), normalised difference chlorophyll index (NDCI) (Mishra & Mishra 2012; Pokrzywinski 2022) and surface algal bloom index (SABI) (Douglas Greene 2021) to estimate chl-a. Although each of these indices was tailored to the specific aquatic environment for which it was developed, the fluorescence line height blue (FLH B), three-band algorithms (3BDA), and the NDCI indices were observed to be more effective; each gave a coefficient of determination, R^2 value of greater than 0.7.

The most widely used spectral index (25%) was the NDVI index due to its utilisation of red and NIR bands, which are appropriate for determining chl-a. However, its R^2 values varied from 0.04 to 0.72. On the other hand, the accuracy of the NDCI index, which combines the red and Red-edge bands, was somewhat greater than that of the NDVI index. Different depths can alter the reflectance in the red and NIR bands, making NDVI less accurate and resulting in lower R^2 values. A solution is thus provided by alternative indices, such as the NDCI index (Mishra & Mishra 2012; Olivetti 2023), specifically for estimating the amount of chlorophyll in water. With higher R^2 values, the NDCI index's red and red edge bands show stronger and more consistent relationships. The NDCI's sensitivity to chlorophyll reduces the impact of confounding factors such as water turbidity and suspended particles (Chien et al. 2016), hence the higher accuracy.

The results showed that 34% of the studies utilised two-band algorithms (2BDA) while 15% utilised 3BDA. The literature revealed that 3BDA gave a higher precision than 2BDA and remarkably exhibited R^2 values, averaging at 0.77, compared to 2BDA, which yielded an average of 0.646 for R^2 values. This is because 3BDA leverages extra spectral information from the extra band, enhancing its ability to discern target parameter characteristics. Also, the interaction between different water components can be slightly eliminated using multiple bands (Gitelson 1992). Therefore, indices like the FLH B and INDEX demonstrate improved performance (Table 2-3) but only when hyperspectral sensors capture a wide range of the electromagnetic spectrum. Additionally, poor-performing indices (R^2: 0.0001 - 0.16) were computed from the green, red, and blue bands, for example, the visible atmospherically resistant index (VARIGREEN) and green–red ratio index (GRRI), while the moderate-performing indices (R^2: 0.4 - 0.6) computed from the red and NIR bands, vegetation indices such as NDVI, DVI and green NDVI.

Table 2-3 Accuracy measure for chl-a vegetation indices and band algorithms

Index name	Abbreviation	Formula	Metric (R^2)	References
Fluorescence line height blue	FLHB	$G-(R+(B-R))$	0.75 - 0.86, average 0.805	Pokrzywinski (2022); Olivetti (202
Normalised Difference Chlorophyll Index	NDCI	$\frac{708-665}{708+665}$	0.5 - 0.82, average 0.707	Pokrzywinski (2022); Olivetti (202 Xiao (2023)
	INDEX	$\frac{SR_{665}{}^{-1}-SR_{708}{}^{-1}}{[\![SR_{753}{}^{-1}+SR_{708}{}^{-1})}$	0.670	Olivetti (2023)
Ratio normalised difference vegetation index	RNDVI	$\left(\frac{NIR-R}{NIR+R}\right)\times\left(\frac{NIR}{R}\right)$	0.611	Zhao (2022b)
	NFH560	$\frac{700}{560\ or\ 675}$	0.610	Xiao (2023)
Excess green minus excess red	EXGR	$EXG-1.4*R-G$	0.580	Zhao (2022b)
Brute-Force Method		$\frac{684}{674}$	0.570	Logan (2023)
Brute-Force Method Normalised difference		$\frac{684-674}{684+674}$	0.570	
Fluorescence line height violet	FLH Violet	530 – (644 + [430 – 644] * SS (0.467))	0.550	Pokrzywinski (2022)
	Ocx	$\frac{443\ or\ 490\ or\ 510}{555}$	0.550	Xiao (2023)
Green Normalised Difference Vegetation Index	GNDVI	$\frac{NIR-G}{NIR+G}$	0.312 -0.74, average 0.519	Kim (2021); Zhao (2022b); Olivet (2023)
Ratio vegetation index	RVI	$\frac{NIR}{R}$	0.508	Zhao (2022b)
Two-band enhanced vegetation index	EVI2	$\frac{2.5*(NIR-R)}{NIR+2.4*R+1}$	0.440	Zhao (2022b)
Normalised difference vegetation index	NDVI	$\frac{(NIR-Red)}{(NIR+Red)}$	0.04 - 0.72, average 0.497	

B, blue; G, green; NIR, near-infrared; R, red; RE, red edge, SR – spectral reflectance, SS= Spectral Shape coefficient calculated as $(\lambda-\lambda\text{^}-)/(\lambda\text{^}+-\lambda\text{^}-)$

2.7.6.2 Machine Learning

The study revealed that linear regression (LR), followed by random forest (RF), extreme gradient boosting (XGBoost), and support vector machine (SVM), were the most widely used algorithms for the prediction of chl-a from UAV imagery. Linear regression was used in 40% of the studies due to its simplicity in computation. While 22% of the studies employed RF, which offers several significant advantages. It is quicker than bagging and highly accurate, effective in handling large data dimensionality and multicollinearity, making it suitable for complex datasets. As a non-parametric algorithm, RF does not assume a specific data distribution, adding to its versatility and ability to work with diverse sample types. Its built-in feature selection mechanism reduces overfitting, improving predictive performance. RF is also robust to outliers and noise, enhancing reliability, and can effectively handle imbalanced data. It is also easy to implement, can be parallelised, and significantly speeds up the training process (Breiman 2001; Pal 2005; Belgiu & Drăguţ 2016; Herrera et al. 2019).

Regarding the performance of these algorithms (Table 2-4), the Catboost, Adaboost regression, Artificial Neural Network (ANN), Deep Neural Network (DNN), and K-Nearest Neighbors (KNN) demonstrated high R^2 values over 0.8 and were used in more than three studies, establishing them as high-performing techniques. LR, RF, XGBoost, and Extreme Learning Machine (ELM) had average R^2 values greater than 0.7, positioning them as strong performers. Despite being used by numerous studies, multiple linear regression (MLR) yielded an average R^2 value of 0.62. This performance can be considered moderate compared to other high-performing algorithms and indicates limited performance in chl-a mapping. Conversely, Self-Adapting Selection of Multiple Neural Networks (SSNN), Ensemble-Based System (EBS), Hybrid Feedback Deep Factorisation Machine (HF-DFM), the Chen method (2023) and Gradient Boost Regression Tree (GBRT) achieved R^2 values exceeding 0.9, while Genetic Algorithm_AdaBoost Regression (GA_ABR), Ensemble Learning Regression (ELR), Genetic Algorithm_XGBoost, and Extremely Randomised Trees (ERT) surpassed 0.8. However, comparing these models is challenging due to their use in singular studies. Notably, Neural Networks (NN) emerged as a low-performing algorithm, with an accuracy of 0.093, rendering it challenging to assess its efficacy in chl-a estimation.

Table 2-4 Accuracy measure for chl-a machine learning and predictive modelling methods

Algorithm	Abbreviation	Metric (R^2)	References
Self-Adapting Selection of Multiple Neural Networks	SSNN	0.984	Zhang (2020)
Ensemble-Based System	EBS	0.940	El-Alem (2021)
Hybrid Feedback Deep Factorisation	HF-DFM	0.930	Zhang (2021)
Chen Method 2023		0.917	Chen (2023)
Gradient Boost Regression Tree	GBRT	0.900	(Lu 2021)
Catboost Regression	CBR	0.808 - 0.96, average 0.88	Chen (2021); Lu (2021); Fu (2023)
Extremely Randomised Trees	ERT	0.870	Lu (2021)
Genetic Algorithm_XGBoost	GA _XGBoost	0.855	Chen (2023)
Genetic Algorithm_AdaBoost Regression	GA_ABR	0.826	
AdaBoost Regression	ABR	0.784 - 0.89, average 0.819	Chen (2021); Lu (2021); Chen (2023)
Artificial Neural Network	ANN	0.73 - 0.9014, average 0.816	Silveira Kupssinskü (2020); Wu (2023)
Adaptive Ensemble Learning Regression	AELR	0.814	Fu (2023)
Deep Neural Network	DNN	0.805 - 0.817, average 0.811	Chen (2021); Chen (2023)
K-Nearest Neighbors	KNN	0.703 - 0.8964, average 0.8	Silveira Kupssinskü (2020); Chen (2021)
Particle Swarm Optimisation Algorithm	PSO–LSSVM	0.778	Liu (2021)
Regression trees	RT	0.77	Morgan (2020)
Partial Least Squares Algorithm	PLS	0.764	Liu (2021)
Extreme Learning Machine	ELM	0.7299 - 0.7609, average 0.745	Zhao (2022b; 2022a)
Extreme Gradient Boosting	XGBoost	0.415 - 0.92, average 0.737	Chen (2021); Lu (2021); Xiao (2022a); Chen (2023)
Genetic Algorithm Partial Least Squares	GA-PLS	0.730	Zhang (2021)
Random Forest	RF	0.317 - 0.874, average 0.705	Chen (2021); Xiao (2022a); Fu (2023); Yang (2023)
Linear regression	LR	0.203 - 0.980, average 0.7	Su (2017); Silveira Kupssinskü (2020); Yi (2023)
1D- Convolutional Neural Network	1D-CNN	0.1932 - 0.91, average 0.691	Hong (2022); Pyo (2022); Zhao (2022a); Lo (2023b)
Mixture Density Network	MDN	0.650	
Support Vector Machine	SVM	0.4813 - 0.759, average 0.623	Silveira Kupssinskü (2020); Lu (2021); Zhao (2022a)
Multi-Layer Perceptron Regression	MLPR	0.620	Lu (2021)
Integrated Data Fusion and Mining	IDFM	0.620	Zhang (2021)

2.8. Limitations of the Study

Research on mapping chl-a in small water bodies using UAVs has gained momentum in recent years, driven by advancements in UAV sensor technologies. This study extensively reviewed existing literature and identified several key gaps, challenges, and opportunities for using UAVs for chl-a mapping in small water bodies. Previous studies of chl-a estimation using UAV-remotely sensed have not done any work in Africa. This may have been impeded by the high costs of UAVs and piloting licenses, as well as legal restrictions on UAV usage in many African countries (Rhee et al. 2018; Wang et al. 2020; Sibanda et al. 2021). Most affordable UAVs are also designed for recreational use rather than research (Sibanda et al. 2021). Although several studies have successfully used UAVs to monitor chl-a in small water bodies, there is a lack of robust models that can be trusted across multiple studies. While several models (EBS, Chen method, PSO-LSSVM, GA_ABR, GA_XGB, AELR, GBRT, ERT, GA_PLS, and SSNN) have shown strong predictive power (R^2 >0.7), each has only been evaluated in a single study, raising concerns about their reliability and generalisability. Furthermore, the limited number of comparative studies makes it difficult to determine the best-performing algorithm.

The use of thirteen different cameras, ten different UAV platforms, several different algorithms, and an overall methodology study highlights UAVs' flexibility and customised application in estimating chl-a for different geographical settings. While this is a merit, it also reveals a lack of standardisation in the processes involved in UAV-based remote sensing of chl-a. A solution to this will be to provide a standardised framework and simplified inversion models (Shen et al. 2012) for different case scenarios (based on the type of water body and size of the water body). This will assist in reducing the time spent testing and evaluating multiple UAVs, sensors, and algorithms.

3. ASSESSING DRONE-BASED REMOTE SENSING FOR MONITORING WATER TEMPERATURE, SUSPENDED SOLIDS AND CDOM IN INLAND WATERS.

3.1. Introduction

Different remote sensing sensors onboard UAVs measure the radiation at various wavelengths reflected from the water surface. These reflections can be used directly or indirectly to detect optically active parameters, including Total Suspended Solids (TSS), Chromophoric Dissolved Organic Matter (CDOM), temperature and chlorophyll-a, which can be directly derived from remote sensing reflection (Adjovu 2023; Lo 2023a). Conversely, non-optically active substances such as chemical oxygen demand, total nitrogen, electrical conductivity, pH, metals, and Escherichia coli (E. coli), which have no direct optical properties, can be derived using proxies or artificial intelligence (Sun et al. 2014; El Din et al. 2017). The principle behind water quality remote-sensing inversion is first to build a model using empirical data from water quality monitoring and corresponding data from remote sensing images (forward modelling), then use the model to obtain the temporal and spatial distribution of water quality parameters (Chen 2021; Hou 2023). Although positive outcomes have been achieved in estimating optically active parameters in small water bodies using Landsat (Ciancia 2020), MODIS (Hamidi 2017), MERIS (Campbell 2011) and Sentinel satellites (Rahul 2023), limitations still arise. Coarse spatial resolutions hinder the monitoring of small-scale water bodies, atmospheric interferences such as the presence of clouds, long revisit times, and data accessibility limitations, which have been mentioned in the literature as some of the challenges (Cillero Castro et al. 2020; Omondi 2023).

Unmanned Aerial Vehicles (UAVs) or drones have recently emerged as a viable solution, providing ultra-high spatial resolution data suitable for capturing detailed information on water quality parameters in small inland water bodies (Xiao 2022b; Mishra 2023; Bangira 2024). UAVs offer an advanced, practical and near-real-time method for monitoring water quality parameters (Nhamo et al. 2018; Koutalakis et al. 2019; Xiao 2022b). Since drone technology is fairly recent, studies such as Cillero Castro et al. (2020) have utilised satellite data as a primary source of information and drone-based data as a form of validation when monitoring water quality in a reservoir

in Spain. The performance of both platforms was evaluated, and there was an agreement when comparing the water quality parameter results from both platforms.

While agriculture is the major use of water stored in small water bodies (Bangira et al. 2019). This review focuses on three major water quality indicators for water suitable for irrigation, considering that they can be measured using remote sensing techniques. This study focuses on surface water temperature, Total Suspended Solids (TSS) and Chromophoric Dissolved Organic Matter (CDOM). Water temperature is the measure of the kinetic energy of water, expressed as degrees Celsius (°C). Changes in water temperature stem from changing climates, diurnal temperature changes, seasonal changes, precipitation and evaporation (Woolway et al. 2020; Adjovu 2023). In agriculture, varying water temperatures from irrigated water sources lead to decreased crop yields since changing water temperatures directly impact soil temperatures, specifically for sensitive crops during growing stages (Wierenga & Hagan 1996). Meanwhile, Total Suspended Solids (TSS) are fine particles suspended in water, including bacteria, algae, mineral particles, and organic debris (Al-Abed 2009; Khouni et al. 2021). An increase in the TSS in reservoirs stems from increased soil erosion and runoff containing organic and inorganic pollutants flowing into the reservoir (Al-Abed 2009).

Consequently, significant amounts of suspended sediments can affect drip, centre pivot and ditch irrigation methods (El Bilali & Taleb 2020). Chromophoric Dissolved Organic Matter (CDOM) is a fundamental subsection of Dissolved Organic Matter (DOM). It comprises a combination of compounds, dissolved organic matter and nutrients stemming from polluted residential, agricultural and industrial runoff (Zheng et al. 2023). Zheng et al. (2023) further explain that CDOM reduces light penetration and limits the production of beneficial nutrients needed for crop growth. These parameters are crucial for assessing physical, chemical, and microbial degradation of water quality, especially for agricultural use.

Furthermore, given the prevalent challenges of water scarcity in southern Africa, farmers require timely information on water quality to sustain agricultural production and avert hunger and poverty. This emphasises that the suitability of water needs to be monitored regularly to meet irrigation and environmental standards as well as

human and animal consumption standards (Nhamo et al. 2018). Subsequently, by utilising drone-derived high spatial resolution information, farmers can make educated decisions about their everyday activities and early warning systems for timely intervention, leading to resilience building and enhancing productivity and economic benefits (Nhamo et al. 2018; Bangira 2024).

3.2. Literature search

The initial step of the literature search was to identify keywords, terms and phrases about the scope of the intended study (Sibanda et al. 2021; Bangira et al. 2023). These keywords and phrases, along with Boolean operators such as "AND", “OR”, and “NOT” to form search strings which retrieved relevant publications were put into five search engines, namely, SCOPUS, Web of Science, Google Scholar, IEEE Xplore and Science Direct, and filtered to ensure relevant literature about the mapping and monitoring of water quality in inland water bodies was retained (Bangira et al. 2023). The Boolean operators aided in determining inclusive/exclusive criteria for each search string, which were restricted to keywords, titles, and abstracts of relevant literature. The search covered the period from 1980-2023, and 702 articles were retained from the five search engines (Table 3-1).

Table 3-1 Search strings, keywords and Boolean operators used in the review

Search engine	Search criterion	Total number of articles
Web of Science	TS=(“unmanned aerial vehicles” OR “drones” OR “UAVs” OR “remote sensing”) AND (“water quality monitoring” OR “inland water quality”) AND (“water bodies” OR “dams” OR “rivers” OR “reservoirs”) AND (“TSS” OR “suspended sediment” OR “temperature” OR “CDOM”) NOT (“sea water” OR “coastal water”)	328
Google Scholar	(“unmanned aerial vehicles” OR “drones” OR “UAVs” OR “UAS”) AND (“water quality monitoring” OR “water quality assessment” OR “inland water quality”) AND (“dams” OR “reservoirs”) AND (“remote sensing”) AND (“TSS” OR “CDOM” OR “temperature” OR “Chromophoric dissolved organic matter” OR “suspended sediments”) AND (“machine learning algorithms” OR “regression algorithms”) NOT (“coastal waters” OR “ocean water”)	165
Scopus	(TITLE-ABS-KEY(“Unmanned aerial vehicles” OR “drones” OR “UAVs” OR “UAS”) AND (“water quality monitoring” OR “water quality assessment” OR “inland water quality”) AND (“water bodies” OR “dams” OR “reservoirs” OR “rivers”) AND (“TSS” OR “suspended sediment” OR “CDOM” OR “Chromophoric dissolved organic matter” OR “temperature”) AND NOT (“coastal waters” OR “groundwater”)	136

Science Direct	((“unmanned aerial vehicles” OR “drones” OR ‘UAVs”) AND (“water quality imaging” OR “monitoring”) AND (“TSS” OR “CDOM” OR “temperature”) NOT (“seawater”))	57
IEEE Xplore	(“All Metadata “unmanned aerial vehicles OR “All Metadata “drones OR “All Metadata “UAVs) AND (“All Metadata “water quality monitoring OR “All Metadata “inland water quality) AND (“All Metadata “TSS OR “All Metadata “CDOM OR “All Metadata “temperature) AND (“All Metadata “remote sensing) NOT (“All Metadata”: ocean water)	16
	Total number of Articles retained	**702**

All retrieved literature was exported into Endnote for further screening processes. The screening process was done in five stages. Firstly, 68 duplicates were removed since similar search terms can result in the same papers appearing across multiple search engines. The second step involved excluding 12 papers not written in English and 43 papers not identified as journal articles (such as conference proceedings). Thirdly, the abstracts of the remaining articles were read. A total of 282 papers which conducted predictive modelling, observed coastal regions and those which did not fit the scope of the study were excluded. Finally, 297 full-length articles were downloaded and exported into an Excel spreadsheet for further screening. Upon the last stage of screening, the inclusion criteria focused on selecting articles which:

- Monitored any of the three specific parameters of TSS, CDOM or temperature
- Involved utilisation of unmanned aerial vehicles as a platform to aid remote sensing techniques

This resulted in 247 articles being excluded since they focused solely on satellite-based remote sensing, focused exclusively on monitoring other water quality parameters outside of the specified parameters, utilised UAVs for groundwater monitoring and since numerous articles utilised UAVs to collect water samples rather than a platform for remote sensing sensors. After that, the final 50 articles were thoroughly read, and valuable characteristics were extracted and recorded.

3.3. Spatio-temporal distribution of UAV-based literature for water quality monitoring

Figure 3-1(a) shows the spatial distribution of the studies that have used UAVs to map CDOM, TSS and surface water temperature in small water bodies. More research has

been conducted in the USA, Latin America, Europe and South-East Asia compared to Africa and Southern Africa. The USA and China had the highest number of 12 UAV-based articles monitoring TSS, Temperature and CDOM. This was followed by Brazil having four articles, Spain having three, India and South Korea having two. Southern Africa only accounted for 6.3% of the selected literature compared to South Asia, which accounted for 50%, and North and South America, which accounted for 25% and 10.4%, respectively.

Figure 3-1(b) illustrates that there has been much focus on the mapping and modelling water quality using both remotely sensed satellite and UAV data, with the number of studies steadily increasing. Although remote sensing techniques have been popular since the 20th century and the selected range for this literature search was from 1980-2023, it is evident that there had only been a steep increase in published literature utilising UAV data since 2012. Before this, remote sensing was primarily conducted via satellites. Landsat 8 OLI has appeared more frequently within the selected studies and accounted for 13% of the total selected studies since UAV data was used for validation Figure 3-1(b). For instance, a study by Xiao (2023) to monitor TSS across a lake utilised UAV-based data to calibrate satellite-based models directly. The results of this study exclaimed that the UAV-based data improved the satellite-based models due to the advances in spatial resolutions.

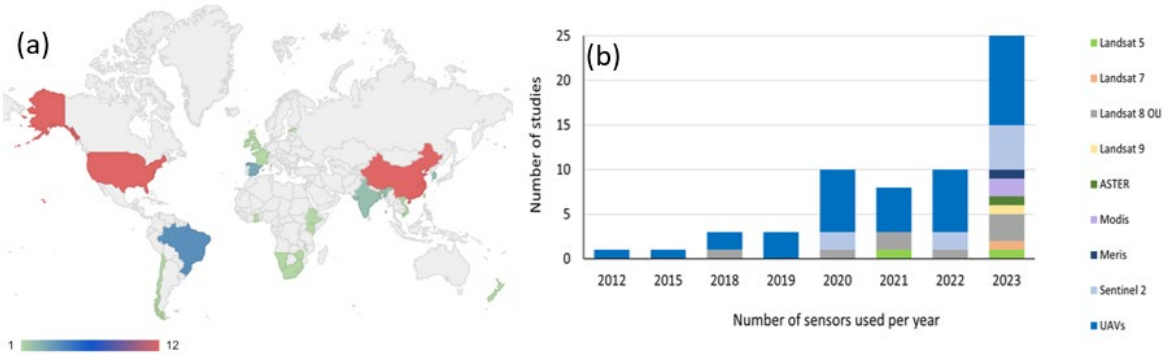

Figure 3-1 Spatial (a) and temporal (b) distribution of studies that have used UAVs in mapping CDOM, TSS and Temperature in small water bodies

3.4. Characteristics of UAV platforms and sensors for mapping TSS, CDOM and water temperature

Various UAV platforms have been utilised throughout the years, including the DJI, the Octocopter, and the Sense fly eBee. The multicopter DJI UAV platform was dominantly used and accounted for 76% of the selected studies. It has been a popular choice of platform since 2020. The reason for the dominance of the DJI platform is that it is more compatible with many types of sensors and is better suited to surface water resource mapping, according to Brito (2019). The DJI platforms are also more cost-effective, and their taking-off and landing systems are advantageous. Conversely, the MD4-1000, Sense fly eBee, Hexacopter, Octocopter and 3DRSolo accounted for 4.8% individually.

Additionally, 2021 and 2023 accounted for the remaining studies using UAV and satellite-based sensors such as Landsat 5, 7 and 9, ASTER, MODIS, MERIS and Sentinel 2. Alternately, Figure 3-1(b) highlights the significant increase in studies that ventured solely into using UAV-based data for mapping and monitoring water quality parameters. From 2020-2023, it is evident that there has been a significant increase in UAV-based studies, with 47% of the selected studies being found in this period. Additionally, the average number of UAV-based articles for these four years was eight articles per year.

Regarding sensor types, it is apparent that multispectral sensors appeared more frequently than thermal or hyperspectral sensors when characterizing surface water temperature, TSS and CDOM (Figure 3-2). The multispectral sensor is cost-effective compared to the hyperspectral sensor and observes more multiple spectral bands than the thermal sensor. The multispectral sensor captures imagery within the visible spectrum, at red, green and blue bands and outside of the visible spectrum at the near-infrared, red-edge and thermal infrared portions of the electromagnetic spectrum. While water temperature can be monitored using thermal infrared bands, CDOM uses blue and green bands, while TSS uses red and near-infrared bands (Figure 3-2).

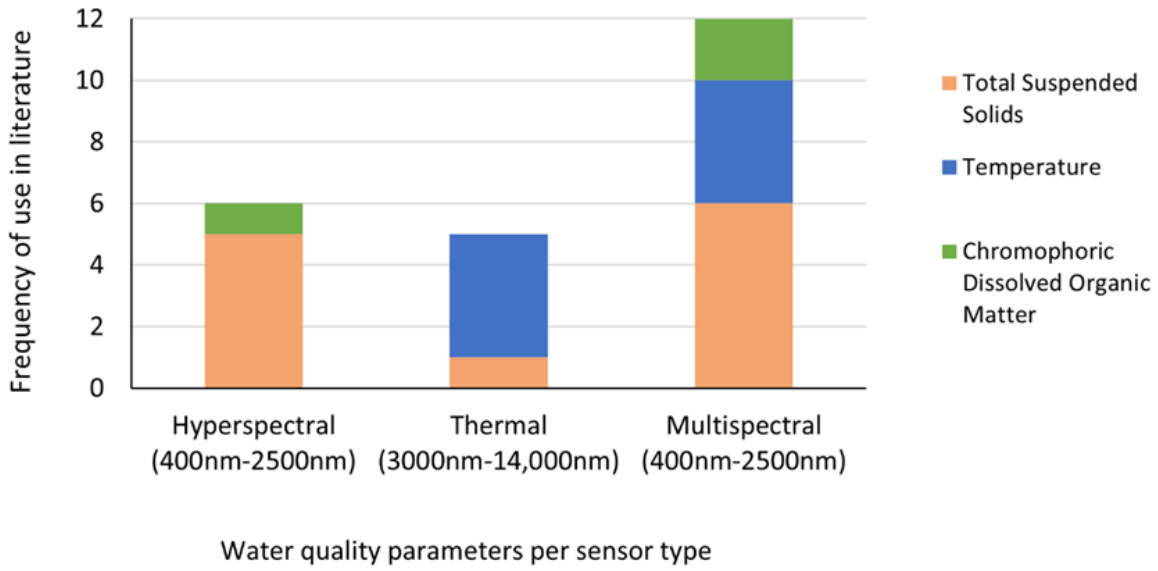

Figure 3-2 Sensor types used onboard drone platforms for detecting water temperature, TSS and CDOM.

Multispectral sensors were used to detect all three water quality parameters; however, thermal sensors were used mainly to detect water temperature and TSS. Multispectral and hyperspectral sensors were used for CDOM since they fall within the blue and green bands of the electromagnetic spectrum, and for TSS, they fall within the red and near-infrared bands.

3.5. Spectral indices used for estimating surface water temperature, TSS and CDOM in inland water bodies using sensors onboard UAVs

Studies have derived spectral indices algorithms using individual bands or multiple bands to predict the concentration of TSS, CDOM and water temperature in inland water bodies. The combination of spectral indices and machine learning algorithms has significantly improved estimation and prediction models in estimating surface water temperature, TSS and CDOM in small water bodies (Sagan et al. 2020a). Table 3-2 presents indices for detecting TSS and CDOM in inland water bodies. Spectral indices for TSS are typically derived from red and near-infrared wavelengths. In contrast, spectral indices for CDOM are derived from wavelengths in the visible and ultraviolet portions of the electromagnetic spectrum. Veronez et al. (2018) proved that combining spectral indices and machine learning algorithms can improve the R^2 and RMSE when estimating TSS and CDOM in an artificial lake.

Table 3-2 Spectral indices utilised in literature to characterize TSS and CDOM

Water Quality parameter	Formula	R^2	Characteristics of the study area	Author and year
TSS	$\mathrm{TSS} = 45.4 \times \mathrm{NDVI}^2 + 43.1 \times \mathrm{NDVI} + 20.9$	0.65	Small artificial lake in the South of Brazil	Veronez et al. (2018)
	$\mathrm{TSS} = 68.7 \times \mathrm{NDWI}^2 - 111.2 \times \mathrm{NDWI} + 56.1$	0.76		
	$\mathrm{TSS} = 151.2 + (384 \times (\mathrm{RE})) + (173.9 \times (\frac{\mathrm{G}}{\mathrm{R}}))$ Where G is the green band (480-520nm) and R is the red band (640-680nm)	0.60	Stream is located in Alabama, USA	Larson (2018) Prior (2021)
	$\mathrm{TSS} = 142.7 - (53.8 \times (\frac{\mathrm{R}}{\mathrm{RE}}))$ Where R is the red band (640-680nm) and RE is the red-edge band (730-740nm)	0.60		
	$\mathrm{TSS} = 8133.15 - 11002.9 \times \frac{\mathrm{B7}}{(\mathrm{B6} + \mathrm{B8A})}$ Where B7 is 783 nm, B6 is 740 nm and B8A is 865 nm	0.73	Lake situated in Tamil Nadu, India	Rahul (2023)
CDOM	$\mathrm{CDOM} = 244.9 \times \mathrm{NDVI}^3 + 186.2 \times \mathrm{NDVI}^2 + 7 \times \mathrm{NDVI} + 21.8$	0.54	Small artificial lake in the South of Brazil	Veronez et al. (2018)
	$\mathrm{CDOM} = 2119.5 \times \mathrm{NDWI}^3 + 4559.1 \times \mathrm{NDWI}^2 - 2760.4 \times \mathrm{NDWI} + 603.6$	0.59		
	$\mathrm{aCDOM}\,(420) = 5.20\mathrm{x}^{-2.76}$ Where aCDOM (420) is the absorption of CDOM at 420 nm	0.84	Lake located in Finland	Kutser et al. (2005)
	$\mathrm{CDOM} = 0.89 \times \frac{\rho 700\ \mathrm{nm}}{\rho 450\ \mathrm{nm}} - 0.15$ Where ρ is the spectral reflectance at wavelengths 700nm and 450 nm	0.83	River, located in the USA	Fan (2014)

Finally, when looking at temperature, 50% of the studies took place in China and utilised in-situ thermometers and multiprobes. Additionally, most studies utilised linear regression, obtaining an R^2 value higher than 0.90. This is due to linear regression being easier to understand and implement.

3.6. Machine learning algorithms for estimating TSS, CDOM and surface water temperature

Table 3-3 shows the most popular machine learning algorithms (only studies with R2 greater than 70% are presented) for estimating TSS, CDOM and surface water temperature using remotely sensed data acquired by UAVs. Linear regression (LR), empirical methods, random forest classification (RF), support vector machines (SVM), artificial neural networks (ANN), XGBoost, deep neural networks (DNN) and gradient boost decision trees (GBDT) were the most used algorithms. Linear regression appeared more frequently than other statistical methods in 27.5% of the articles. The random forest and empirical methods appeared in 12.5% of the articles. SVM and ANN appeared in 11.25% and 10%, respectively, and each of the remaining algorithms, such as IMP-MPP, LSTM, Semi-empirical, Semi-analytical, LASSO, GBDT, DNN and XG Boost, appeared in less than 7% of the total number of articles.

The parameter also influences the algorithm selection. In contrast to surface water temperature monitoring, the examined studies demonstrated that machine learning methods were applied for TSS and CDOM monitoring. This is mainly due to the fact that most of the sensors have a single thermal band.

Table 3-3 Case studies used to emphasise the statistical methods for estimating temperature, TSS and CDOM from drone-derived data and their error assessment (R^2).

Title	Location of the study	Parameter	In-situ data collection technique	Statistical Technique	Metric error (R^2)	Author (year)
Evaluation of surface water quality of Ukkadam Lake in Coimbatore using UAV and Sentinel-2 multispectral data	India	TSS	Colorimeter	Linear regression	0.86	Rahul (2023)
Evaluation of water quality based on UAV images and the IMP-MPP algorithm	China	TSS		IMP-MPP algorithm	0.83	Ying (2021)
Low-Cost Unmanned Aerial Multispectral Imagery for Siltation Monitoring in Reservoirs	Brazil	TSS	TriOS RAMSES spectroradiometer	Empirical and semi-empirical models	0.94	Olivetti (2020)
A method for chlorophyll-a and suspended solids prediction through remote sensing and machine learning	Brazil	TSS	APHA standard weighing method	RF	0.81	Silveira-Kupssinskü (2020)
Machine learning models applied to TSS estimation in a reservoir using a multispectral sensor onboard to RPA	Brazil	TSS	APHA standard weighing method	SVM	0.87	Dias (2021)
Proposal of a method to determine the correlation between total suspended solids and dissolved organic matter in water bodies from spectral imaging and artificial neural networks	Brazil	TSS	APHA standard weighing method	ANN	0.77	Vernonez (2019)
Local algorithm for monitoring total suspended sediments in micro-watersheds using drone and remote sensing applications. Case study: Teusaca River, La Calera, Columbia	Columbia	TSS	Sampling and lab analysis	Linear regression	0.89	Saenz et al. (2015)

Inland waters suspended solids concentration retrieval based on PSO-LSSVM for UAV-borne hyperspectral remote sensing imagery	China	TSS	Sampling and lab analysis	SVM	0.96	Wei et al. (2019)
Drone with a thermal infrared camera provides high-resolution georeferenced imagery of the Waikite geothermal area, New Zealand	New Zealand	Temp		Linear regression	0.98	Harvey et al. (2016)
Medium-Sized Lake Water Quality Parameters Retrieval Using Multispectral UAV Image and Machine Learning Algorithms: A Case Study of the Yuandang Lake, China	China	Temp	Multiprobe	Gradient boosting	0.75	Lo (2023a)
Urban Land Surface Temperature Monitoring and Surface Thermal Runoff Pollution Evaluation Using UAV Thermal Remote Sensing Technology	China	Temp	Thermometer	Linear regression	0.83	Xu (2021)
UAV Multispectral Image-Based Urban River Water Quality Monitoring Using Stacked Ensemble Machine Learning Algorithms—A Case Study of the Zhanghe River, China	China	CDOM	In-situ sensor	XGBoost	0.92	Xiao (2022b)
Remote sensing Estimation of CDOM and DOC with the Environmental implications for Lake Khanka	China	CDOM	Spectrophotometer	GBDT	0.95	Qiang et al. (2023)
Estimation of the Biogeochemical and Physical Properties of Lakes Based on Remote Sensing and Artificial Intelligence Applications	Estonia	CDOM		XGBoost	0.92	Toming et al. (2024)
Estimation of Water Quality Parameters in Oligotrophic Coastal Waters Using Uncrewed-Aerial-Vehicle-Obtained Hyperspectral Data	Croatia	CDOM	Fluorometer	Linear regression	0.92	Divi´c et al. (2023)
Autonomous learning of new environments with a robotic team employing Hyperspectral Remote sensing, Comprehensive in-situ sensing and machine learning	USA	CDOM	In-situ sensor	Linear regression	0.97	Lary et al. (2021)

3.7. Limitations of utilising drone technologies in monitoring TSS, CDOM and water temperature in small water bodies

Although drone technologies have been proven beneficial for monitoring water temperature, CDOM, and TSS, there are many limitations, specifically in southern Africa. One of the limitations is the cost of equipment. Although this technique is low-cost, acquiring a license, a suitable UAV platform, and various sensors can become costly, specifically when limited funding is available (Adjovu 2023). Furthermore, these costs raise concerns about security, theft, and damage to equipment, which leads to the limited use of drone technology. Additionally, since the use of drone technology is still a novel approach for water quality monitoring in Southern Africa, there is a lack of skilled and trained technicians who can operate the drones over water bodies, as well as a lack of trained professionals who can interpret the collected data (Adjovu 2023).

Further challenges include connectivity issues since many parts of southern Africa lack network coverage. Technical challenges include limited battery efficiency, flight ranges, and limited altitudes of drones. Environmental challenges, such as the interference of drone technology on wildlife and challenges due to weather sensitivity, such as heavy rainfall periods experienced in Southern Africa during summer months, hinder drone flights. Furthermore, aviation restrictions and privacy concerns limit where drones can be flown.

4. METHODS AND MATERIALS FOR MONITORING WATER QUALITY AND LEVELS USING UAVs

After the literature reviews, this project was done in two parallel stages as follows:

i. Mapping of water quality parameters
ii. Mapping of water level and extent of water bodies using drone imagery

Figure 4-1 shows an overview of the project phases and the various activities within each phase. The next subsections detail the techniques utilised to finish these tasks.

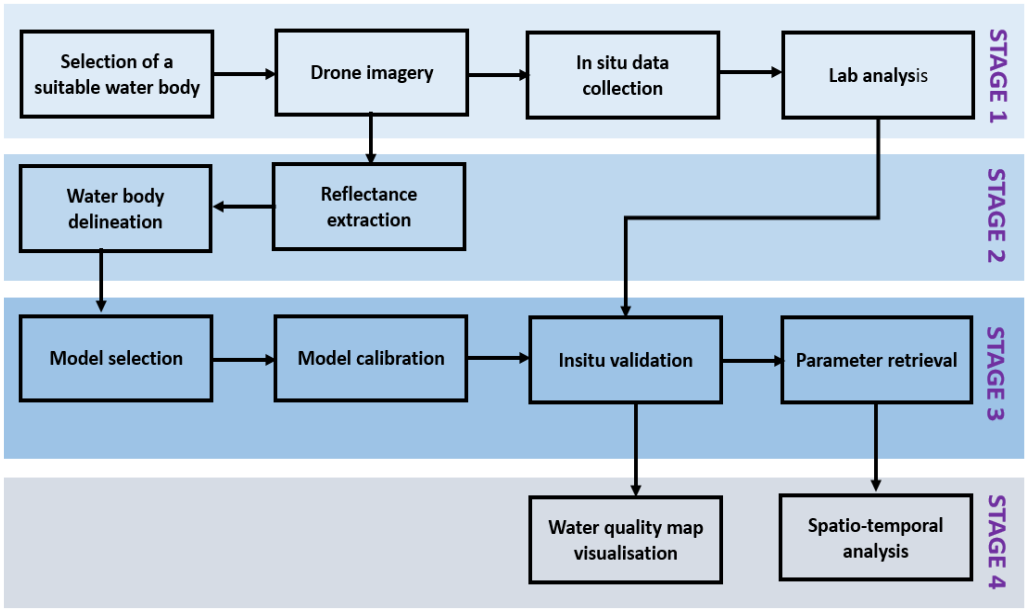

Figure 4-1 Project stages from case study selection to water quality and quantity maps

4.1. Selection of the case study

The first activity of Stage 1 was to select the most suitable water body for mapping changes in water quality and quantity. The selected High Flight farm dam is the upper Midmar Dam sub-catchment of the Umgeni catchment, KwaZulu-Natal, South Africa (-29.454537°, 29.902512°) (Figure 4-2a-c). This catchment receives 400 – 1000mm of precipitation annually, primarily during the summer (October to April), with occasional winter rains. The average annual temperature ranges from 12°C to 14°C, with cooler conditions in June and July and warmer temperatures from December to February. Potential evaporation, recorded at the A-pan, averages 1600–1800 mm yearly (UmgeniWater 2016). The reservoir, covering 20 hectares, replenishes through

rainfall and natural springs and serves as a critical water source for irrigating crops such as potatoes, maize, sugar, eggplant, beans, and fruits like pears, apples, and lemons. Livestock, including goats, sheep, cows, and horses, also rely on this reservoir. Agricultural practices within the Midmar sub-catchment involve fertilisers containing nitrogen and phosphorus, which contribute nutrients to nearby rivers, potentially causing eutrophication. For this study area, nutrient loading is reflected in hyacinth growth in parts of the dam Figure 4-2(a). Primary irrigation methods include canal systems and some centre-pivot systems, which farmers maintain regularly to prevent clogging, cleaning at least four times a year. These factors make the dam a good example of a system that needs preventive and periodic monitoring to ensure sustained water quality and system functionality.

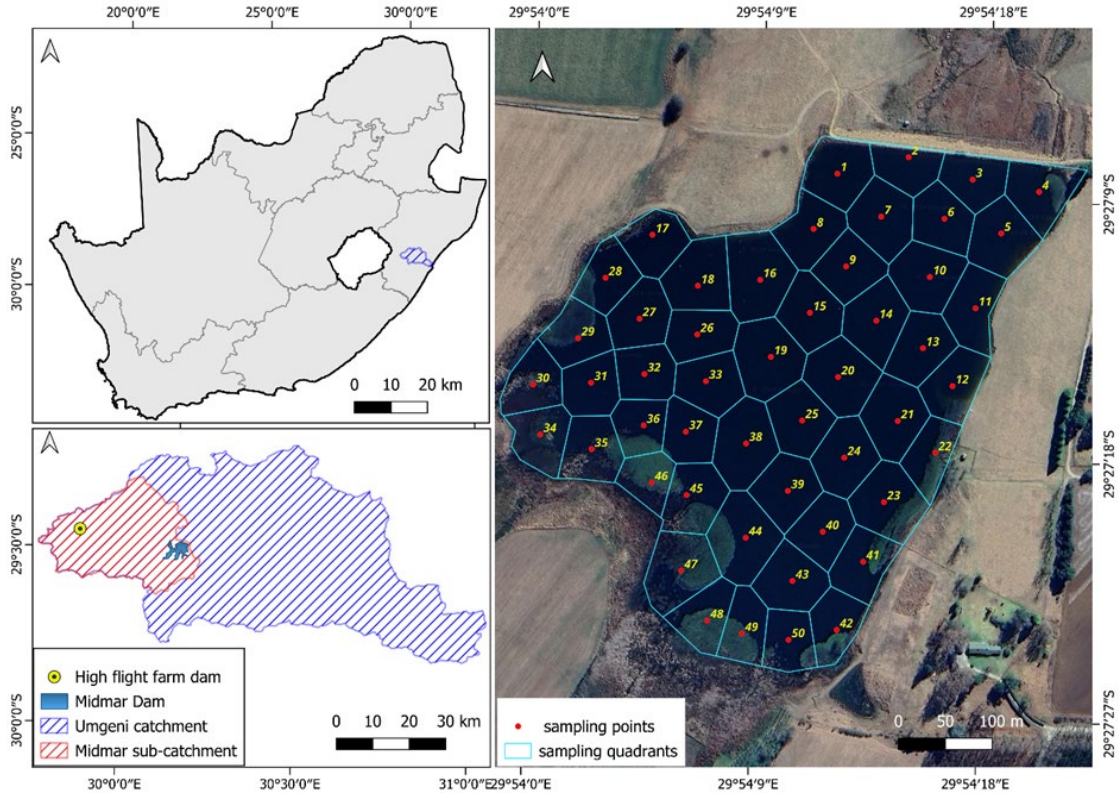

Figure 4-2 Study area location: South Africa(a), Umgeni and Midmar catchments with High Flight Farm Dam (b), and High Flight Farm Dam divided into 50 sampling quadrants (c), with red dots as sampling points.

4.2. Data collection and processing

UAV images and water samples were collected concurrently during three field campaigns: once in autumn and twice in winter, under clear skies and calm wind conditions. Flights occurred between 10 a.m. and 12 p.m. to ensure optimal solar irradiance. Notably, rainfall occurred between the April and June campaigns, potentially influencing water quality and quantity results.

4.2.1 Water quality sample collection

Figure 4-3 shows how the in situ and drone image data were collected in the field. A total of 50, 50, 41, and 47 water samples were taken on April 15, May 20, June 5, and July 16, 2024. The dam was divided into 50 quadrants using the k-means clustering tool in QGIS (Figure 4-2c), and sampling stations were identified at the centroid of each quadrant. Using a boat and GPS, we navigated to these stations, where a Hanna multiparameter probe measured DO, temperature, pH, turbidity, and electrical conductivity. Water samples were taken 0.5 m below the surface using 500ml amber bottles, then immediately transported to the laboratory in ice-filled cooler boxes with ice for analysis chl-a, TN, and TP analysis. Samples were stored at -20°C, with chl-a analysis conducted within 24 hours of collection.

Figure 4-3 (a) Field observation of the dam showing water hyacinth presence, (b) UAV deployed for high-resolution multispectral imaging over the dam, (c) Field team navigating to sampling points within the dam by boat, (d) Laboratory analysis of water samples collected from the field

4.2.2 UAV data collection

Field campaigns were conducted exclusively on the April, June, and July dates. The UAV utilized in this study was a DJI Matrice 300, equipped with a multispectral MicaSense Altum camera and a Downwelling Light Sensor 2 (DLS-2). Table 4-1 shows the camera`s five spectral bands: blue, green, red, red-edge, and near-infrared. It has an 8 mm focal length and a field of view (FOV) of 48° × 37°. The UAV was flown at an altitude of 100 meters, with a ground sample distance (GSD) of 5.2 cm per pixel.

An image-side overlap of 80% was maintained to assist with post-processing challenges from flying over water. A digitized shapefile of the dam was imported into the DJI M-300 smart console to create a flight plan that covered the entire dam surface. This enabled the UAV to complete the flight mission autonomously. Before the flight, the MicaSense Altum was calibrated using a reflectance panel, and an image was captured directly over the panel to assess the lighting conditions specific to the flight's time, date, and location. The total UAV flight duration was approximately 90 minutes.

Table 4-1 The wavelengths and bandwidths captured by the MicaSense sensor

Band	Centre	Band Width	Range
Blue	475 nm	32 nm	443 – 507 nm
Green	560 nm	27 nm	533 – 587 nm
Red	668 nm	16 nm	652 – 684 nm
Red Edge	717 nm	12 nm	705 – 729 nm
Near Infrared (NIR)	842 nm	57 nm	785 – 899 nm

4.2.3 Data processing for chlorophyll-a monitoring

In-situ and UAV data were processed according to the framework shown in Figure 4-4.

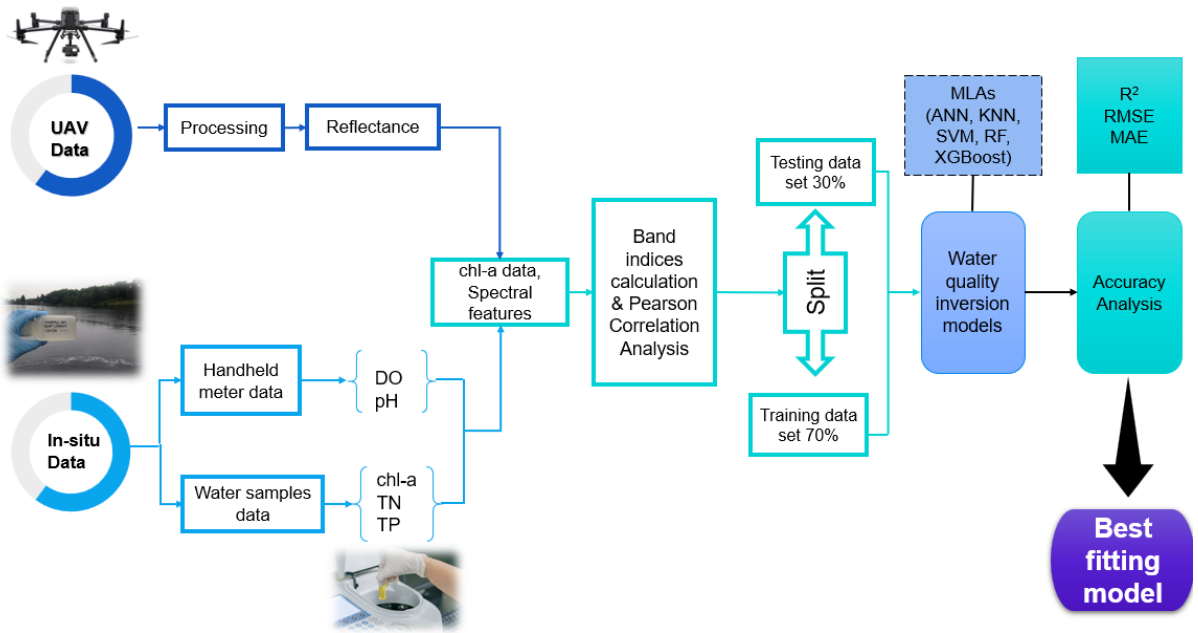

Figure 4-4 Methodological framework for chl-a estimation using UAV-derived data

4.2.3.1 Image pre-processing for chlorophyll-a monitoring

The image processing step aimed to extract spectral values from each band at each sampling station as captured by the multispectral sensor. First, the images captured by the sensor were uploaded into Pix4DFields software and stitched together to create a single mosaic image. This mosaic was then imported into QGIS software, where the spectral values for each band were extracted at each sampling point. The original spectra were pre-processed using the band ratio method to mitigate background noise and reduce interference from rough water surfaces (Huang et al. 2016). Based on the extracted spectral values, a total of 60 band combinations were generated in a GIS environment, including band ratios (10), band differences (20), band sums (10), band products (10), and normalised differences (10). The resulting band combinations were exported to Microsoft Excel for correlation analysis with chl-a data. The coefficient of determination (R^2) was then calculated to determine the key wavelengths for accurately estimating water quality parameter concentrations. The band combination showing the highest correlation with in situ data was selected for model construction.

4.2.3.2 In situ data processing

Chl-a was derived in the laboratory using the acetone extraction method under subdued light, as explained by Arar (1997). The following steps were followed: i) samples were stored in the dark at -20ºC, ii) 400ml of the sample was filtered using 0.45µm GF/F 151 microfiber glass filters within 24 hours of sampling time, iii) 10ml of 90% acetone was added to filtered samples in 15ml centrifuge tubes, iv) the filtered paper was then mechanically ground by hand using a pestle for 10 to 15 seconds, v) the ground filter paper was allowed to extract for 2 to 24 hrs, vi) followed by 15 minutes of centrifuging at 600G to separate the materials, and vii) finally analysis using a spectrophotometer at the 750nm, 665nm, 664nm, 647nm, and 630nm (Shimadzu UV-1800, Spectrophotometer). Chl-a concentration was computed using equation [1].

$$\mathrm{Chl_a uncorrected}\left(\frac{\mathrm{ug}}{\mathrm{L}}\right) = \frac{[11.85(664_B) - 1.54(647_B) - 0.8(630_B)] \times V_1}{V_2 \times L} \qquad [1]$$

Where 664_B = Subtract 750 nm value (turbidity correction) from the absorbance at 664 nm before acidification, 647_B = turbidity corrected absorbance at 647 nm before

acidification, 630_B = turbidity corrected absorbance at 630 nm before acidification, V_1 = volume of extract (mL), V_2 = volume of sample filtered (L), L = path length (cm).

Total nitrogen (TN) was measured based on the reaction of the nitrate ion with brucine sulfate in a 13N sulfuric acid solution at 100°C, as done by Jenkins and Medsker (1964). The resulting solution was measured at 410 nm using a spectrophotometer (EPA 1971). On the other hand, total phosphorus (TP) was determined by reacting ammonium molybdate and antimony potassium tartrate in an acidic medium with diluted phosphorus solutions to form an antimony-phospho-molybdate compound. When treated with ascorbic acid, the complex turned a deep blue colour and was subsequently analysed for absorbance at 660 nm and 880 nm using a UV spectrophotometer (Eleuterio & Neethling 2010).

4.2.3.3 Image pre-processing

The image processing step aimed to extract spectral values from each band at each sampling station as captured by the multispectral sensor. First, the images captured by the sensor were uploaded into Pix4DFields software and stitched together to create a single mosaic image. This mosaicked was then imported into QGIS software, where the spectral values for each band were extracted at each sampling point. The original spectra were pre-processed using the band ratio method to mitigate background noise and reduce interference from rough water surfaces (Huang et al. 2016). Based on the extracted spectral values, a total of 60 band combinations were generated in a GIS environment, including band ratios (10), band differences (20), band sums (10), band products (10), and normalised band differences (10). The resulting band combinations were exported to Microsoft Excel for correlation analysis with chl-a data. The coefficient of determination (R^2) was then calculated to determine the key wavelengths for accurately estimating water quality parameter concentrations. The band combination showing the highest correlation with in situ data was selected for model construction.

4.2.3.4 *Machine learning algorithm implementation*

This study utilized artificial neural networks (ANN), extreme gradient boosting (XGBoost), K-nearest neighbours (KNN), random forest (RF), and support vector machine (SVM) to develop models for estimating chl-a. In model development, in situ

data was divided into 70% for training and 30% for testing, with data from each field campaign processed separately.

RF is an ensemble machine learning approach that combines predictions from many decision trees to produce a final result (Breiman 2001). It uses the bootstrap aggregation (bagging) technique to generate multiple decision trees, each constructed from a random sample of the original dataset. For each tree, only a subset of the available features is randomly selected at each node split to avoid overfitting and to ensure diversity among trees. The attribute that provides the highest information gain is chosen for the split. This study used the optimal band combination to train the RF model, generating classification and regression trees (CART) based on the number of samples. The final prediction was obtained by averaging the outputs from all trees. RF was well-suited for this study because of its robustness to noise and its ability to handle small datasets without compromising predictive performance (Ali et al. 2012).

SVM is a supervised machine learning algorithm designed for classification and regression tasks. It works by finding the optimal hyperplane that maximises the margin between different classes or fitting the best line to predict continuous values. SVM can accommodate linear and non-linear relationships using kernel functions, such as radial basis function (RBF) and polynomial kernels (Ghosh et al. 2019). One advantage of SVM is its effectiveness with small datasets, making it an ideal choice for water quality assessments where sample collection is limited (Deka 2014). The present study applied SVM to predict chl-a concentrations, leveraging its ability to perform well with limited data points.

ANN is a computer model made up of layers of interconnected nodes (neurons) inspired by the human brain's composition and operation. (Maier et al. 2010). We used the ANN algorithm for chl-a estimation, leveraging its ability to model intricate, non-linear relationships between input features and output variables (Zhao et al. 2019). The network consisted of an input layer with nodes corresponding to the selected band combination, one or more hidden layers to capture underlying patterns, and an output layer predicting chl-a concentration. ANN models were trained using backpropagation, an algorithm that adjusts the connection weights to minimise the error between predicted and actual values.

KNN is a simple, non-parametric machine learning algorithm that predicts a target value by averaging the outcomes of the k-nearest neighbours in the feature space. The algorithm measures the Euclidean distance between a given sample and other points in the dataset (Modaresi & Araghinejad 2014). The k closest neighbours were found, and their mean values were used to make chl-a predictions.

XGBoost is a high-performance, tree-based ensemble algorithm that constructs models sequentially, where each new tree aims to correct the errors of the preceding trees. It uses gradient boosting, where residuals from earlier predictions are minimised to improve the model's performance iteratively. XGBoost is known for its speed and ability to prevent overfitting through regularisation techniques, making it suitable for small datasets (Nasir et al. 2022). This research used XGBoost to predict chl-a concentrations, benefiting from its flexibility in handling complex feature interactions and its efficiency in working with limited samples.

4.2.4 Data processing for TSS, CDOM and surface water monitoring

In the laboratory, the APHA standard method for measuring TSS was followed, whereby 200ml of the sample water from each sample point was measured in a beaker (APHA 2005). The samples were filtered through 0.45µm pore-sized glass fibre filtration paper inside a vacuum filtration unit. Thereafter, the filter paper and its remaining residue were put into metal dishes (Figure 4-5) and dried in an oven at 104°C for 24 hours.

(a) (b)

Figure 4-5 (a) Vacuum filtration unit containing a glass fibre filtration paper, (b) filter paper along with the filtered residue

The filter paper was then weighed to calculate the weight of the residue (suspended solids), which was then used to calculate the concentration of TSS using equation [2.

$$\boldsymbol{TSS\ (mg.L)} = \frac{(\boldsymbol{Weight\ of\ filter} + \boldsymbol{dried\ residue}) - (\boldsymbol{Weight\ of\ filter}) \times \mathbf{1000}}{\mathbf{200}} \quad [2]$$

The remaining filtrate, which passed through the glass fibre filtration unit, was placed in 50ml glass amber bottles to minimise light exposure (Figure 4-5(a)) and refrigerated for further analysis of CDOM concentration using a spectrophotometer to measure the absorption of light at specific wavelengths (Green & Blough 1994). The first step in determining CDOM absorption was to calibrate the spectrophotometer with quinine sulfate as a standard method for creating a calibration curve to quantify CDOM concentrations (Coble 1996). Quinine sulfate, a widely used fluorescing compound, was used to investigate the best wavelength for fluorescence excitation. Approximately 100mg of quinine sulphate was dissolved in 100 ml of a 0.1 N sulfuric acid solution to prepare a stock solution and working standards. A series of quinine sulfate solutions with concentrations of 0.5, 1.0, 1.5, 2.0, and 2.5 µg/mL were prepared by serial diluting the stock solution to produce the calibration curve. The fluorescence intensity of each standard was measured using a spectrophotometer at an excitation wavelength range of 200nm to 800nm (Figure 4-6b).

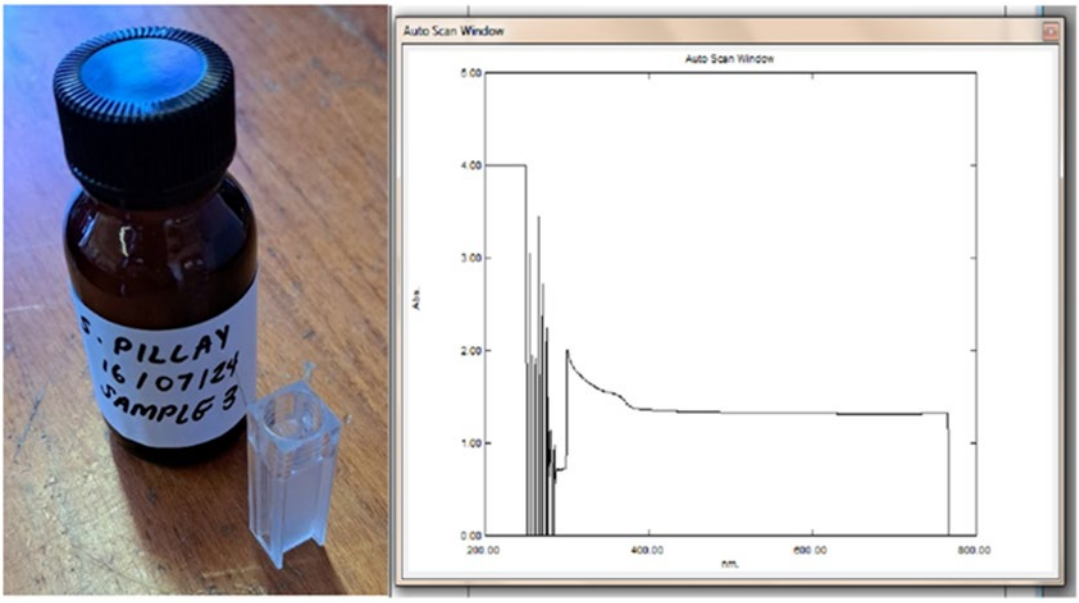

(a) (b)

Figure 4-6 Glass amber bottles (4-750 ml) containing filtrate (a) and wavelength range from 200nm to 800nm indicating fluorescence excitation (b).

The measured fluorescence values were plotted against the known concentrations of quinine sulphate to produce a linear calibration curve (Figure 4-7) expressed as y=mx+b, where y represents the absorbance or fluorescence intensity, x is the concentration, m is the slope, and b is the intercept. Once the calibration curve was established, the filtered water samples were prepared in individual 1ml cuvettes, and the absorbance of each sample was measured under the same conditions as the standards. Finally, the samples' absorbance values were interpolated using the calibration curve equation to determine their CDOM concentrations expressed in mg/L.

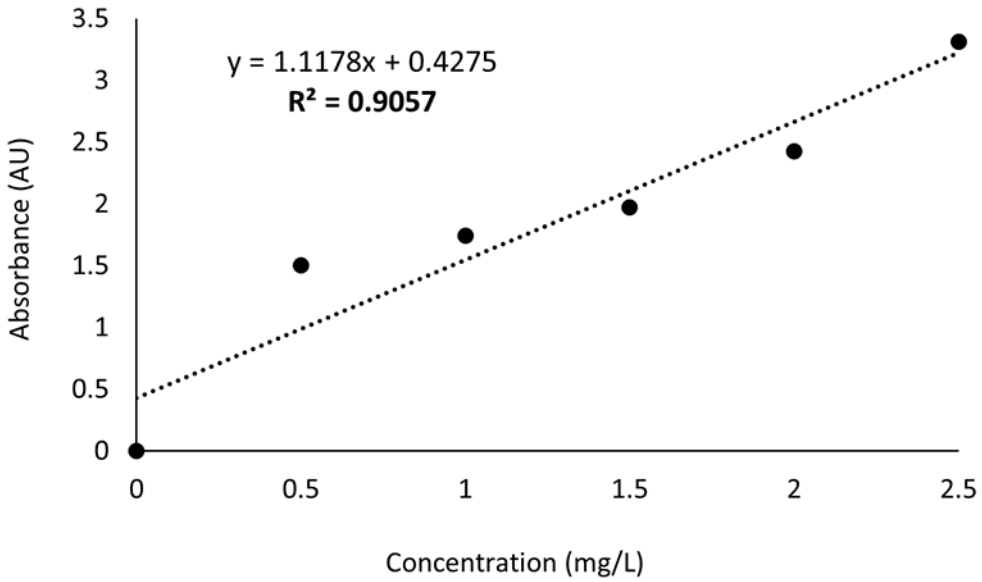

Figure 4-7 Calibration curve of a quinine sulphate standard stock solution

Equation [3] converted the thermal infrared band to absolute temperature values.

$$\boldsymbol{Temperature}\ (°\boldsymbol{C}) = \frac{\boldsymbol{Thermal\ infrared\ (Band\ 6)}}{\boldsymbol{100}} - \boldsymbol{273.15} \quad [3]$$

4.2.4.1 Models for estimating and predicting TSS and CDOM

Figure 4-8 shows the stages followed for estimating and predicting TSS and CDOM concentrations using in situ and remotely sensed data captured by a multispectral sensor onboard a UAV.

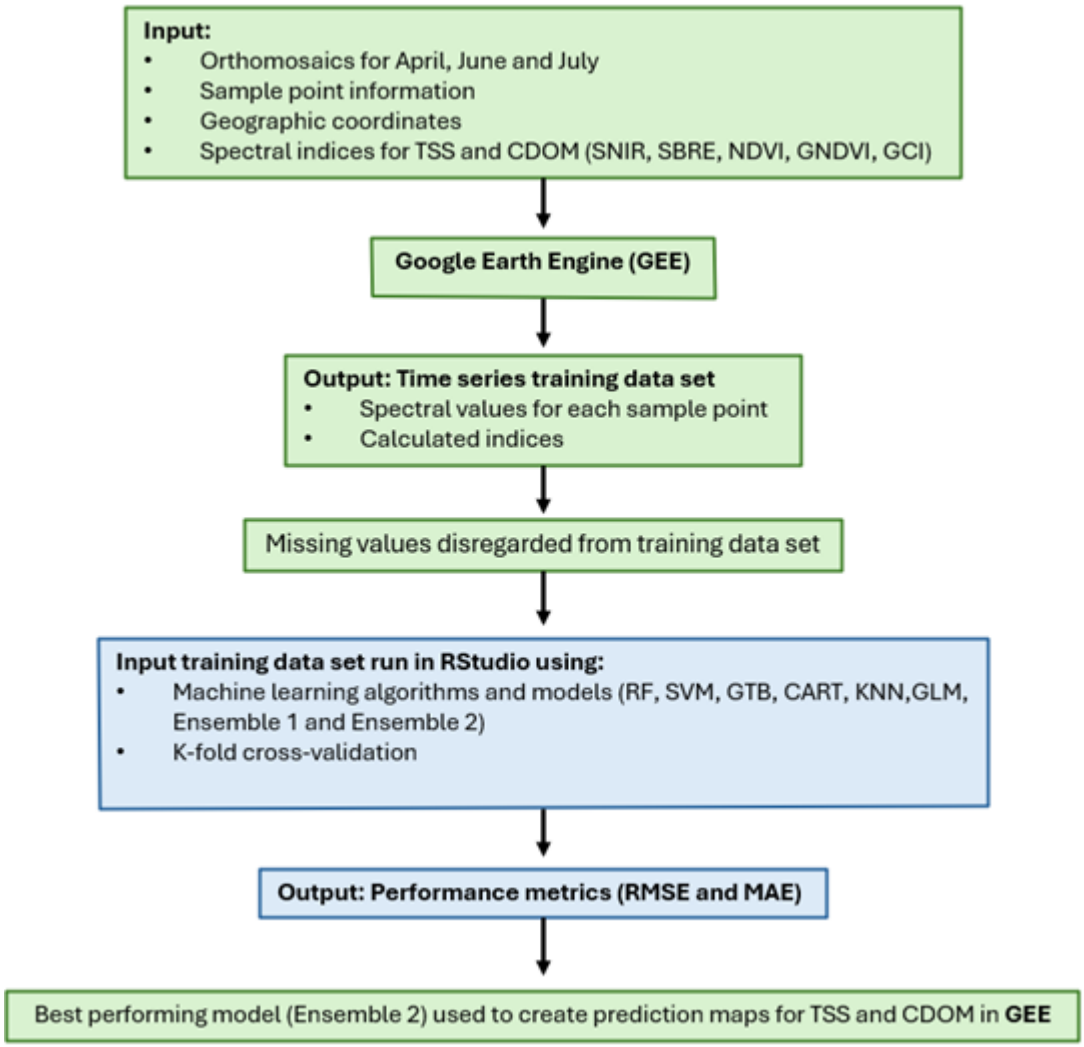

Figure 4-8 Methodology used in estimating and predicting TSS and CDOM concentrations.

The first step involves the generation of orthomosaics, which were then exported to Google Earth Engine for further analysis. It is important to understand that the reflection of the atmosphere influences the total reflectance recorded by the sensor, the water body surface, the water body's volume, and the background reflectance (Dias et al. 2021). The drone's proximity to the body of water, however, limited the impact of the atmosphere. The reflectance source pertinent to our investigation is the volumetric reflectance, which contains data about the TSS in the water. In addition to the individual bands, several band ratios and spectral indices were generated using the five bands for all sample sizes extracted. Thus, 55 variables were generated each day to generate a high correlation with the in situ TSS and CDOM.

The in-situ data was split randomly into two datasets, 75% and 25% of the data for training and validation, respectively. Six machine learning algorithms, namely Random Forest (RF), Support Vector Machines (SVM), Gradient Boosting (GTB), Classification and Regression Trees (CART), k-Nearest Neighbours (KNN), and Generalised Linear Models (GLM), were chosen to estimate the TSS and CDOM. These models, which include rule-based, decision tree-based, linear, and non-linear methods, were chosen to represent a range of regressors. The way the models handle the data in their training set is the primary distinction between them. As a result, a significant variable for one model might not be typical of another. TSS and CDOM estimation is carried out using six distinct sets of factors. The performance and results of each model were recorded to assess their predictive accuracy.

4.2.4.2 Evaluation of spectral indices and machine learning algorithms

Accuracy assessments were conducted to assess the model's performance for the predicted chl-a, TSS and CDOM. The accuracy metrics used were the coefficient of determination (R^2), the root-mean-squared error (RMSE) and the Mean absolute error (MAE). R^2 measures how well the independent variable's variance accounts for the dependent variable's variation. Squaring the difference between the estimated and observed data yields the RMSE, a measure of model accuracy, whereas the MAE provides an average value of absolute errors. Additionally, higher errors are given more weight by the RMSE; hence, it should be more helpful when large errors are especially undesired.

$$R^2 = 1 - \frac{\sum_{i=1}^{n}(y_{i-} \widehat{y_i})^2}{\sum_{i=1}^{n}(y_i - \bar{y})^2} \quad [4]$$

$$RMSE = \sqrt{\frac{1}{n}\sum_{i=1}^{n}(\widehat{y_i} - y_i)^2} \quad [5]$$

$$MAE = \frac{1}{n}\sum_{i=1}^{n}|\widehat{y_i} - y_i| \quad [6]$$

Where *n* is the ample size, $\widehat{y_i}$ represent predicted values of the water quality parameter and y_i represents the response of measured water quality parameter.

5. ASSESSING WATER QUALITY IN A SMALL RESERVOIR USING UNMANNED AERIAL VEHICLE SYSTEMS (UAVS)

The concentration of chl-a, TSS, CDOM, nutrients and surface water temperature in small water bodies has a high spatial and temporal variability. The seasons, land use, and land cover affect the water quality. The section below describes the feasibility of using multispectral sensors onboard UAVs to monitor water quality parameters in small water bodies.

5.1 Temporal and spatial variation of chl-a in High Flight Dam

Periodic monitoring revealed significant differences in water quality across different months. Chl-a levels were highest in April, with a mean value of 24.947 µg/L, suggesting a potential algal bloom. The concentrations decreased steadily over the study period, reaching the lowest mean value of 1.956 µg/L in July. Spatial variability was most pronounced in April, as indicated by the 12.2–34.25 µg/L range, whereas July showed the most uniform conditions with a range of 0.392–6.328 µg/L. TN concentrations were highest in April (0.191 mg/L) and July (0.150 mg/L), while June recorded the lowest concentration at 0.00010 mg/L. The widest variability in TN was observed in April, with values ranging from 0.0632 to 0.315 mg/L, indicating spatial heterogeneity in nitrogen availability across the sampling sites. TP concentrations displayed notable variability, with the highest mean value of 0.644 mg/L in July and the lowest of 0.02419 mg/L in June. These results highlight temporal differences in phosphorus dynamics during the study period. DO concentrations peaked in May with a mean value of 1.595 mg/L, while the lowest mean concentration of 1.345 mg/L was recorded in April. The range of DO values was greater in May (0.19–3.87 mg/L) than in April (0.11–2.36 mg/L), reflecting higher spatial or temporal heterogeneity in May. Then, in early winter (June), reduced chl-a, TN, and TP concentrations suggest decreased nutrient availability and lower algal productivity. Mid-winter (July) results showed the lowest mean for chl-a, likely due to colder temperatures and lower nutrient inputs. Also, the dam's condition changed significantly due to lower water levels. This variability in space and time highlights the dynamic nature of the irrigation dam, underscoring the importance of continuous monitoring. Detailed statistics of the in situ water quality data are provided in Table 5-1.

Table 5-1 Summary of in situ water quality results collected in April, June, and July 2024

		15 April 2024	20 May 2024	5 June 2024	16 July 2024
	Sample size	**50**	**50**	**41**	**47**
Chl-a (µg/L)	Mean	24.947	4.503	8.218	1.956
	Min	12.2	2,020	0.504	0.392
	Max	34.25	9,790	13.23	6.328
TN (mg/L)	Mean	0.191	0.0635	0.00010	0.150
	Min	0.0632	0.0249	0.00001	0.054
	Max	0.315	0.165	0.00024	0.356
TP (mg/L)	Mean	0.056	0.298	0.02419	0.644
	Min	0.014	0.095	0.00138	0.011
	Max	0.099	0.852	0.05512	1.644
DO (mg/L)	Mean	1.345	1.595		
	Min	0.110	0.19		
	Max	2.36	3.87		

The temporal analysis of chl-a levels based on UAV-derived reflectance data demonstrates notable variability across different water body sections over three months. In April, reflectance values were highest in the inlet and periphery sections, particularly in the NIR and Red edge bands, with NIR reflectance exceeding 0.3 sr^{-1}. These elevated values suggest significant chl-a presence, indicative of potential algal blooms. The shallow, deep, and outlet sections exhibited lower reflectance, with values below 0.1 sr^{-1} in most bands. By June, reflectance values decreased across all sections, with the inlet still showing relatively higher reflectance, particularly in the NIR and Red edge bands. The decline continued into July, where reflectance values were uniformly low across all sections, suggesting minimal chl-a concentrations due to low temperatures that lower phytoplankton growth. The deep and outlet sections consistently exhibited the lowest reflectance throughout the period, while the inlet and periphery demonstrated greater variability and higher overall reflectance levels. Figure 5-1 shows the results of the spatio-temporal profile of chl-a in High Flight Dam.

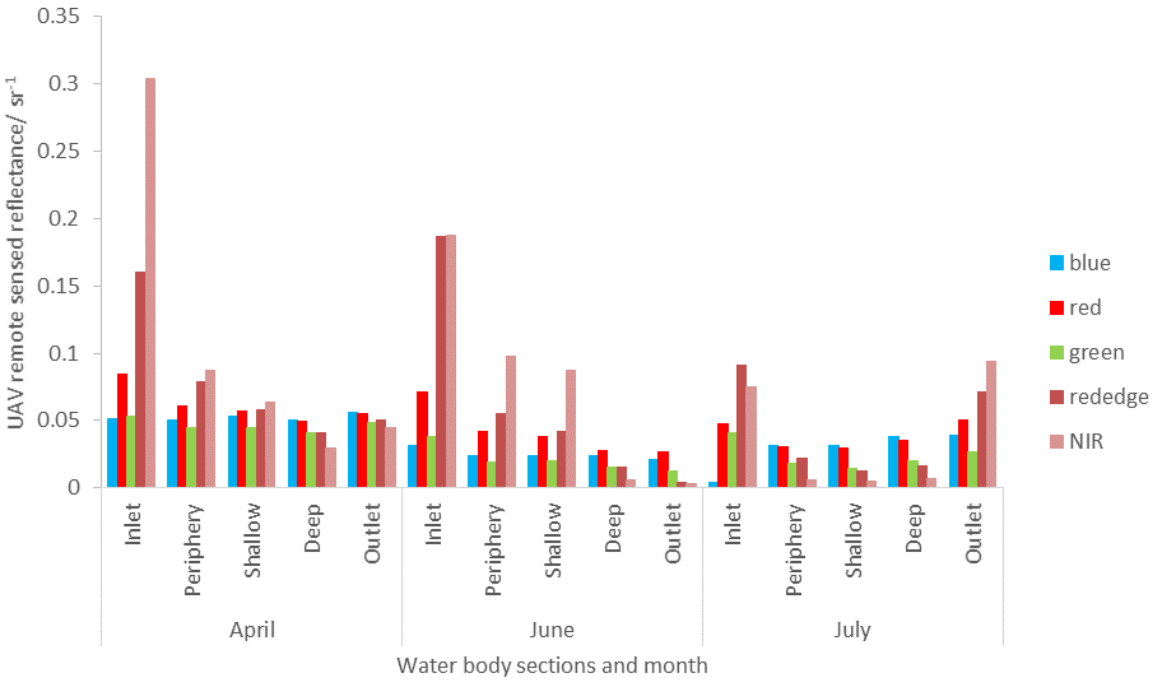

Figure 5-1 Spatio-temporal profile of chl-a across different positions of the dam, showing April, May, June, and July 2024 data

5.2 Correlation between in situ Chl-a and TP, TN, and DO

Figure 5-2 shows the scatter plots for the in situ chl-a measurements against DO, TN and TP for April. There is a positive correlation between the concentration of chl-a and TN ($R^2 = 0.73$), TP ($R^2 = 0.77$) and DO ($R^2 = 0.68$). The presence of nutrients increases algal blooms. The presence of cyanobacteria increases the concentration of dissolved oxygen in water because it performs photosynthesis, releasing oxygen as a by-product. However, large cyanobacteria blooms can eventually lead to decreased oxygen levels due to the decomposition of dead cyanobacteria cells by other organisms in the water, which may reflect the influence of algal photosynthesis on DO levels through oxygen production.

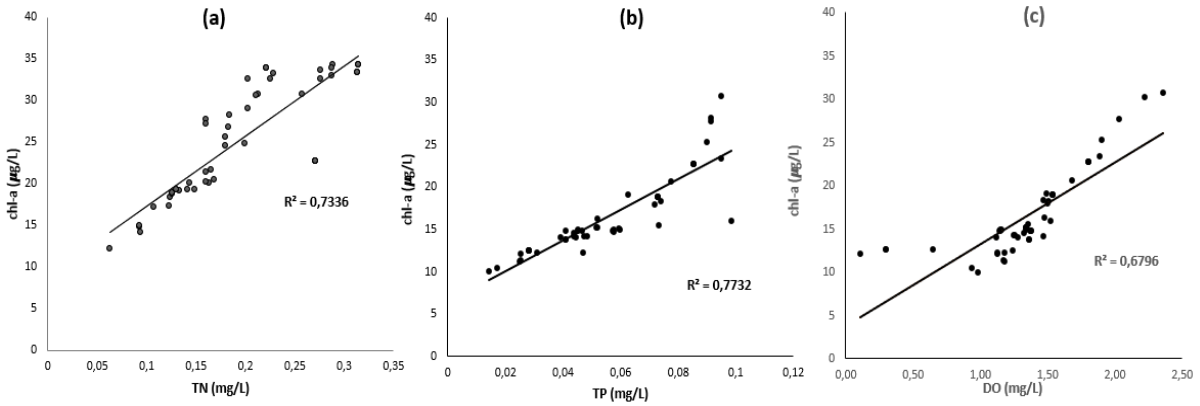

Figure 5-2 Relationships between chl-a concentrations and key water quality parameters: (a) TN, (b) TP, and (c) DO based on April field data

5.3 Spectral reflectance profile of the water body

Chl-a exhibits a distinct spectral signature, marked by high absorption in the blue (443 nm) and red (around 675 nm) wavelengths, alongside high reflectance in the green (550–555 nm) and red-edge (685–710 nm) regions (Beck et al. 2016; Buma & Lee 2020; He et al. 2020). The spectral reflectance of the water body under study was quantitatively analysed across five different wavelengths (475 nm, 560 nm, 668 nm, 717 nm, and 842 nm). The spectral curves for the sampled data from the pre-processed UAV-borne multispectral imagery are presented in Figure 5-3. Reflection peaks were observed at 560 nm and 717nm, while an absorption peak was formed at 668nm. These results showed a high reflection peak at 717 nm for all three datasets (Song et al. 2013). Regarding different locations in the water body, we observed that the inlet had higher reflection peaks than other sections. This may be due to the high amount of nutrient loading in the dam's inlet. Lower reflectance was observed in July (Figure 5-3c), showing the dam's reduced water levels.

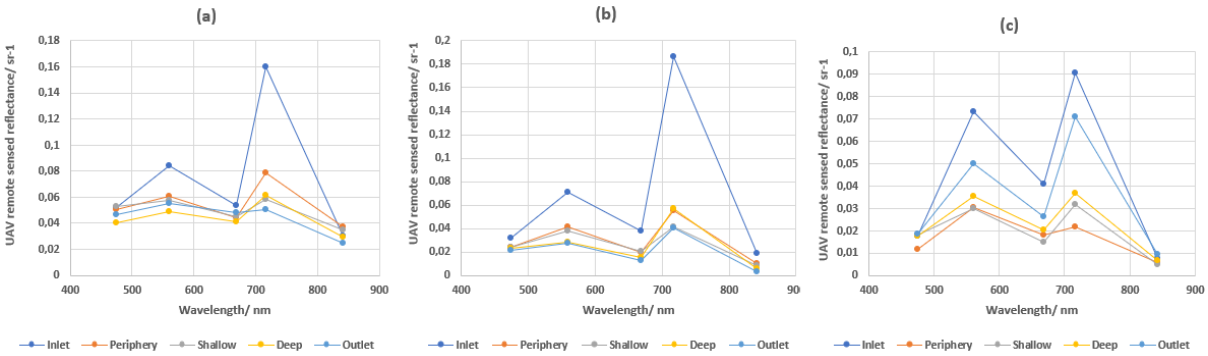

Figure 5-3 Spectral profile for the study water body across different sections of the water body a) April, b) June, and c) July 2024 data

5.4 Spatial distribution of chl-a

The spectral analysis from UAV images revealed that certain specific band combinations performed better for chl-a estimation. In April, June and July, the ratio of green to red-edge bands (G/RE), the ratio of red and green bands (G/R) and the difference between the red and green band combination (R-G) bands produced the highest performance. These findings suggest that the green, red, and red-edge bands are the most effective for chl-a retrieval using the MicaSense multispectral sensor for this water body. Table 5-2 shows the performances of the machine learning algorithms.

Table 5-2 Evaluation metrics in the cross-validation phase. The highest values for R^2 are highlighted in bold

		Training			Testing		
	MLA	**R^2**	**RMSE**	**MAE**	**R^2**	**RSME**	**MAE**
15 April 2024	RF	0.970	1.175	0.354	0.826	7.784	2.919
	SVM	0.921	1.831	0.628	0.527	10.703	4.246
	XGBoost	0.994	0.663	0.190	0.859	6.776	2.449
	KNN	0.646	8.882	7.788	0.512	10.306	8.76
	ANN	0.999	0.020	0.013	**0.949**	3.882	1.082
	MLA						

05 June 2024	RF	0.991	0.222	0.121	0.860	1.785	0.796
	SVM	0.989	0.343	0.240	0.300	3.198	1.430
	XGBoost	0.999	0.002	0.001	0.896	1.513	0.742
	KNN	0.829	9.280	7.672	0.857	10.614	9.628
	ANN	0.999	0.009	0.007	**0.991**	0.590	0.235
16 July 2024	MLA						
	RF	0.904	1.835	1.461	0.697	3.028	2.446
	SVM	0.760	2.846	2.127	0.638	3.357	2.585
	XGBoost	0.975	0.987	0.772	0.703	3.315	2.653
	KNN	0.667	13.084	11.656	0.124	15.489	13.087
	ANN	0.815	2.488	1.940	**0.734**	3.044	2.456

The ANN model was applied to retrieve chl-a concentration for the study area (Figure 5-4). White patches in the images are attributed to factors such as sun glint caused by the reflection of sunlight on the water surface and GPS inaccuracies during the UAV flight, which may have led to gaps in the captured imagery. Figure 5-4a shows that chl-a concentrations ranged between 2.054 and 2.271 µg/L in April, a rainy period. Figure 5-4b shows that chl-a was strongly concentrated on the periphery of the dam in June (17.651 µg/L). June marks the onset of winter, with cooler temperatures and changes in hydrological conditions. The chl-a distribution map for this period shows significantly higher concentrations than in April. This increase may be attributed to nutrient accumulation during the rainy season, followed by more stable conditions as the rains tapered off and water movement slowed. Despite cooler winter temperatures in June, which generally suppress algal activity, the nutrient-enriched environment might have supported localised algal blooms, especially on the periphery of the dam.

Figure 5-4c illustrates the chl-a distribution during mid-winter, with high concentrations of chl-a (18.289 µg/L) observed at the periphery, inlet, and shallow areas of the water body. In comparison, lower concentrations (1.644 µg/L) were found in the deep and outlet sections. Similar to June, the overall chl-a concentrations remain relatively low, reflecting the continued influence of winter conditions, such as reduced temperatures and diminished biological activity. However, the wide range in chl-a concentrations observed in July suggests localised factors, such as nutrient retention in shallow areas

or reduced water flow, creating favourable conditions for algal growth even during winter. These localised dynamics highlight the complexity of environmental interactions influencing chl-a levels.

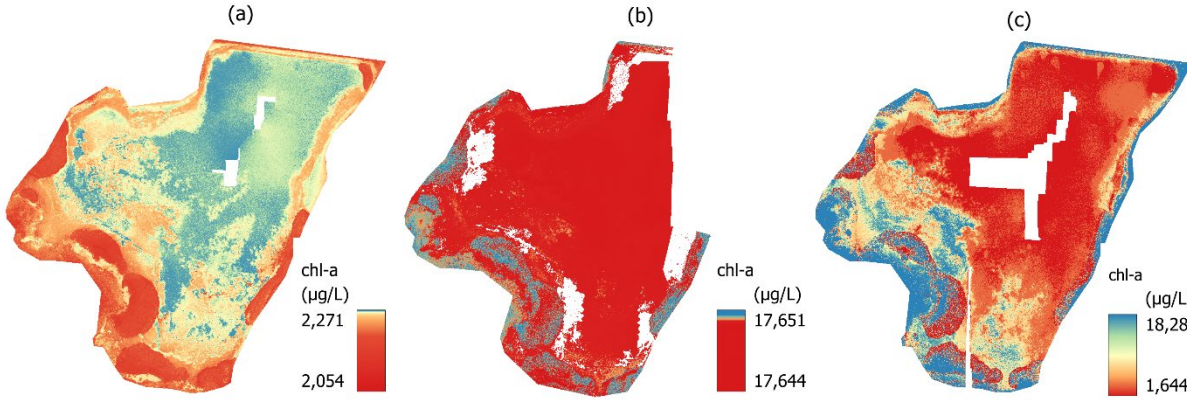

Figure 5-4 Spatial distribution of chl-a concentration for (a) 15 April (b) 5 June and (c) 16 July 2024 based on the ANN model

5.5 Spatio-temporal variability of surface water temperature

Figure 5-5 below shows the spatio-temporal variability of surface water temperature in the High Flight Dam as depicted by the thermal sensor on the UAV and the multi-probe. In April, the UAV recorded higher temperature values from 15-21°C, while the multi-probe recorded values from 17-19°C. When looking at seasonal variation, it is evident that water temperatures decrease from April to July, signifying seasonal change from Autumn to Winter.

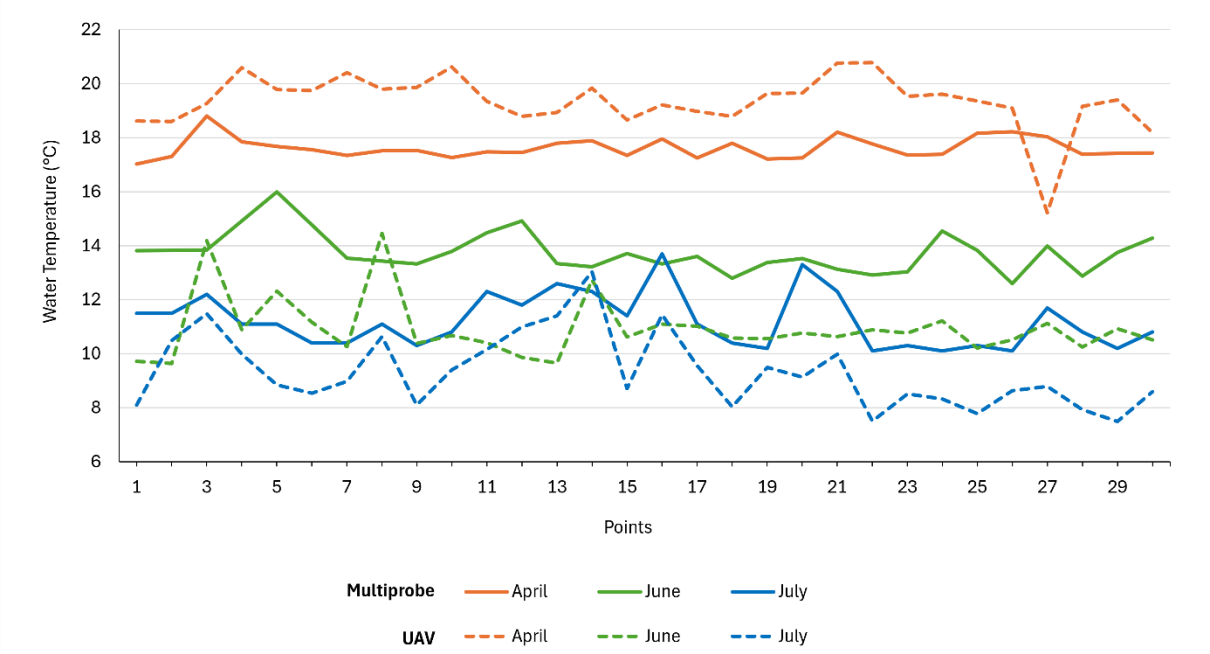

Figure 5-5 Water temperature measured by a multiprobe and UAV

Furthermore, the thermal maps in Figure 5-6 depict UAV-derived water temperature data across the dam, starting at the inlet and moving to the outlet during April, June, and July. These maps emphasised the spatial and temporal variations. In April, higher temperatures (up to 22 °C) are observed near the inlet (Points 1-8), with a gradual decrease toward the outlet (Points 26-30). By June, water temperatures drop significantly across the reservoir, ranging from 10 °C to 16 °C, indicating seasonal change. At the inlet and specifically around aquatic vegetation, temperatures are predominantly higher. However, the spatial gradient across the rest of the dam is less distinct, with cooler temperatures observed more uniformly across the area. In July, the water temperature decreases further, especially around the aquatic vegetation, ranging from 15 °C to 17°C. Warmer zones are still concentrated near the inlet, while the outlet region shows the coolest temperatures, suggesting reduced thermal inputs and increased mixing across the dam during the cooler months. This seasonal trend highlights the influence of inflow dynamics and environmental cooling on water temperature distribution within the dam.

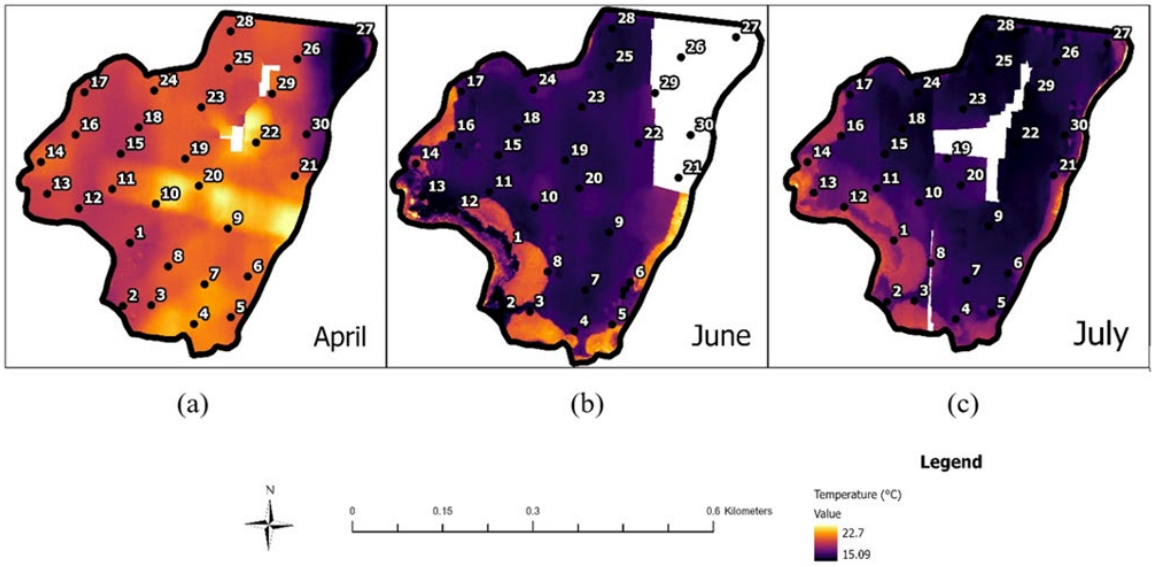

Figure 5-6 Spatial and temporal variations of surface water temperature for (a) April, (b) June and (c) July

5.6 Spatio-temporal distribution of Total Suspended Solids (TSS)

Figure 5-7 illustrates the TSS concentrations from in situ measurements in April, June and July. In all months, TSS concentrations are highest at the inlet, where levels peak at approximately 250 mg/L. This indicates substantial sediment and organic matter upstream, mainly due to the surrounding aquatic vegetation in the dam. As the water flows toward the outlet, TSS concentrations decrease sharply, stabilising below 100 mg/L. TSS levels follow a similar pattern in June, with concentrations peaking around 200 mg/L at the inlet and decreasing more gradually compared to April. Notable fluctuations are observed between Points 7 and 25. By July, TSS levels at the inlet will be comparatively lower and exhibit less variation throughout the reservoir. At the outlet (Point 30), TSS concentrations remain consistently low (<50 mg/L) across all months, highlighting effective sediment deposition within the reservoir. Overall, seasonal trends indicate higher sediment loads in April, likely linked to increased runoff with a progressive decline in sediment distribution by July.

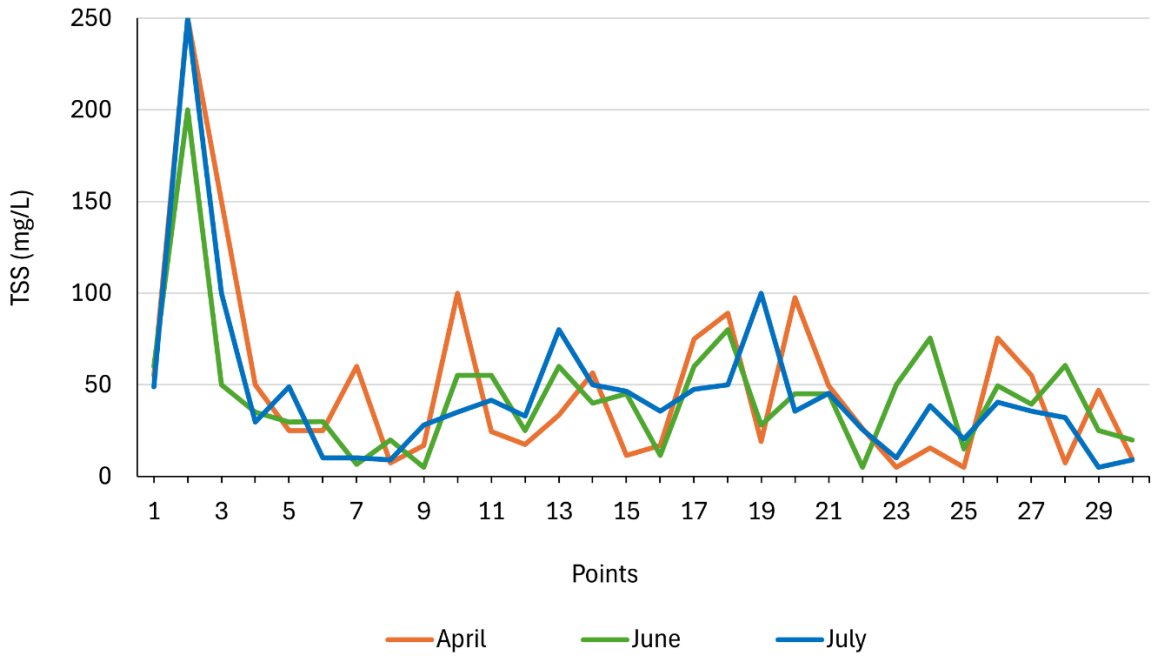

Figure 5-7 TSS concentrations measured using the collected water samples in April, June and July

Individual models such as the Generalized Linear Model (GLM), k-Nearest Neighbors (kNN), Classification and Regression Trees (CART), Random Forest (RF), Gradient Tree Boosting (GTB) and Support Vector Machine (SVM) showed RMSE values ranging from 47.70 to 51.20 mg/L. These models also showed MAE values ranging from 34.00 to 38.40 mg/L. The SVM model exhibited the lowest RMSE of 45.20 mg/L and the lowest MAE of 30.90 mg/L among the individual models. Ensemble models outperformed individual algorithms, demonstrating the advantage of combining multiple approaches. Ensemble 2 achieved the lowest RMSE of 30.50 mg/L and MAE of 19.20 mg/L.

Figure 5-8 shows the predicted spatial distribution of TSS concentrations for April, June and July, created using model ensemble 2, which achieved the lowest RMSE value of 30.50 mg/L and MAE value of 19.20 mg/L. This indicates lower errors between the observed and predicted TSS than other models, suggesting that the ensemble effectively captured the spatial and temporal variations.

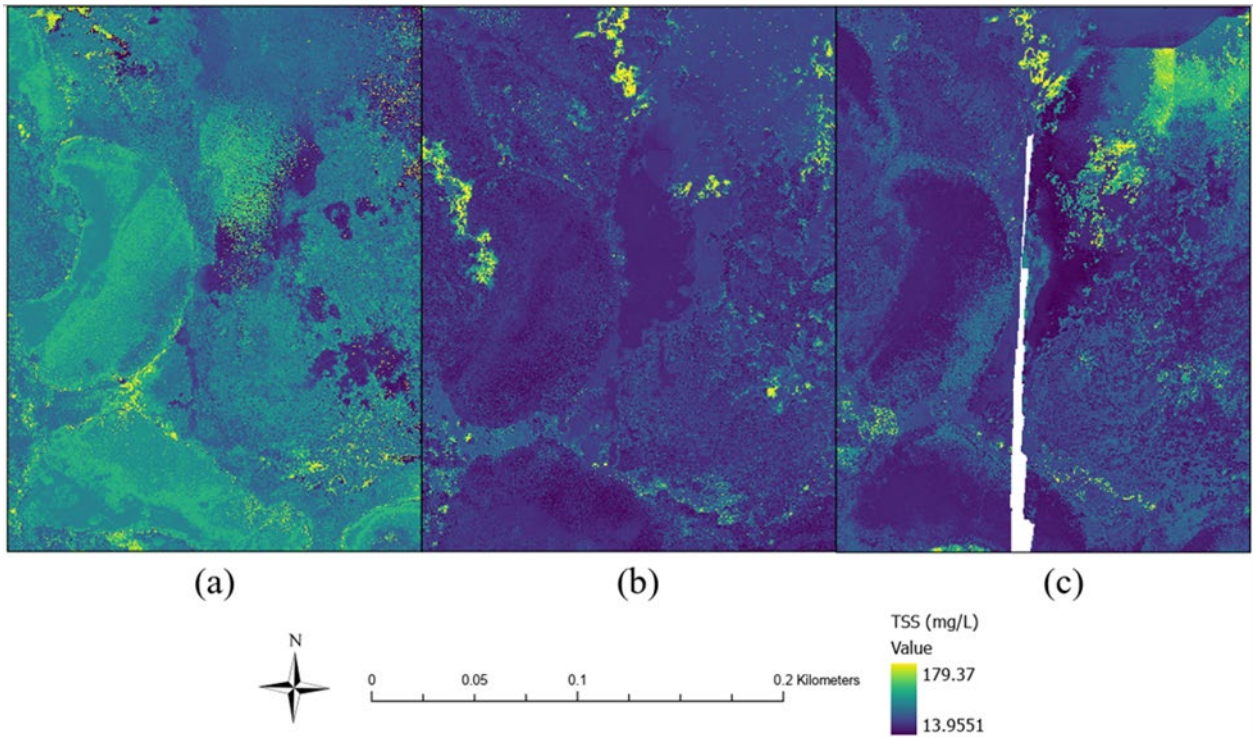

Figure 5-8 Predicted maps showing the spatial variability of TSS concentrations for (a) April, (b) June and (c) July

5.7 Spatiotemporal distribution of Chromophoric Dissolved Organic Matter (CDOM)

Figure 5-9 illustrates the concentrations of CDOM across 30 points, ranging from the inlet at point 1 to the outlet at point 30 during April, June and July. A distinct seasonal variation in CDOM levels is evident, with April exhibiting the highest concentrations overall. A general decline in CDOM is observed across all months from the inlet to the outlet. However, the decline is not uniform and pronounced fluctuations are evident. April shows the greatest variability with peaks near points 9, 15, 22 and 26, reflecting influences such as tributary inflow or variations in organic matter input.

In contrast, June and July show lower concentrations and less pronounced peaks. Notably, July exhibits more stable trends, except for a peak at point 9. Closer to the outlet (point 27-30), CDOM concentrations decrease below 1 mg/L for all months. The results highlight spatial and seasonal variations, with higher CDOM concentrations in April potentially linked to runoff or increased organic matter.

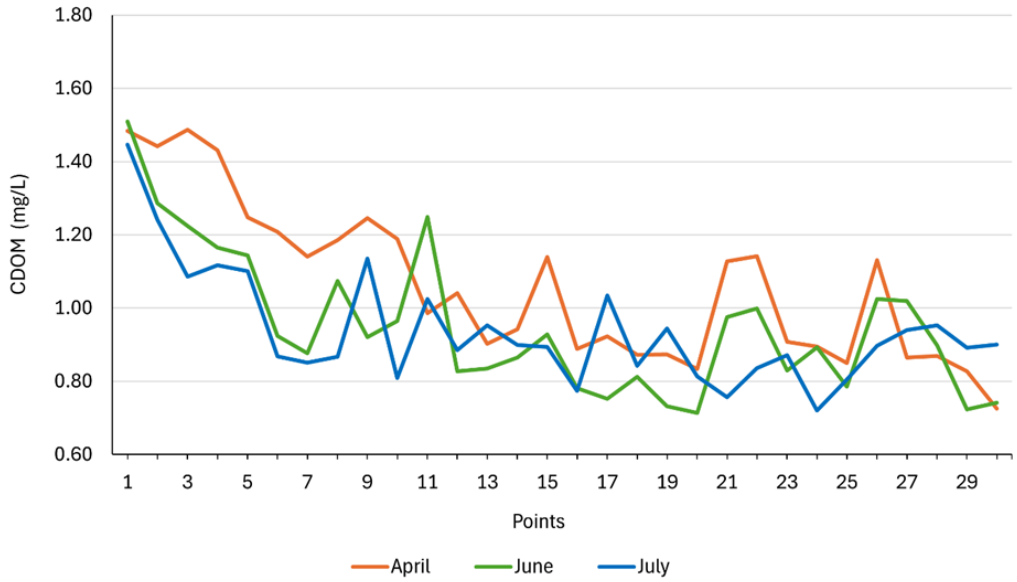

Figure 5-9 In-situ CDOM concentrations in April, June and July

Table 5-3 summarises the performance of various machine learning models in predicting CDOM concentrations evaluated using RMSE and MAE. Individual models such as the Generalized Linear Model (GLM), k-Nearest Neighbours (kNN), Classification and Regression Trees (CART), Random Forest (RF), Gradient Tree Boosting (GTB) and Support Vector Machine (SVM) showed RMSE values ranging from 0.26 to 0.28 mg/L. These models also showed MAE values ranging from 0.21 to 0.23 mg/L. Support Vector Machines (SVM) achieved the best performance among the machine learning algorithms, with the lowest RMSE of 0.25 mg/L and the lowest MAE of 0.20 mg/L.

Table 5-3 Performance metrics for individual algorithms and model ensembles for predicting CDOM concentrations

Model	**RMSE (mg/L)**	**MAE (mg/L)**
GLM	0.28	0.23
kNN	0.26	0.21
CART	0.27	0.21
RF	0.26	0.21
GTB	0.26	0.21
SVM	0.25	0.20
Ensemble 1	0.25	0.20
Ensemble 2	0.17	0.12

Figure 5-10 shows the predicted spatial distribution of CDOM concentrations for April, June and July, based on model Ensemble 2 with an RMSE and MAE of 0.17 and 0.12 mg/L, respectively. In April, the predicted map shows higher CDOM concentrations within vegetative areas, consistent with the observed data during this period Figure 5-10(a). In June, the predicted CDOM values show increased concentrations across the water with decreased vegetative areas. By July, the predicted CDOM values decreased both across the water and within the vegetative areas. While the model adequately predicted CDOM concentrations with low errors, inconsistencies in finer details may still exist due to data not fully captured by the model. Machine learning models, such as the ensemble model used in this study, predict values based on input variables like spectral indices, which may not capture fine spatial details. The fuzziness arises due to the model's generalised patterns from the training data, smoothing and oversimplifying spatial variations in TSS.

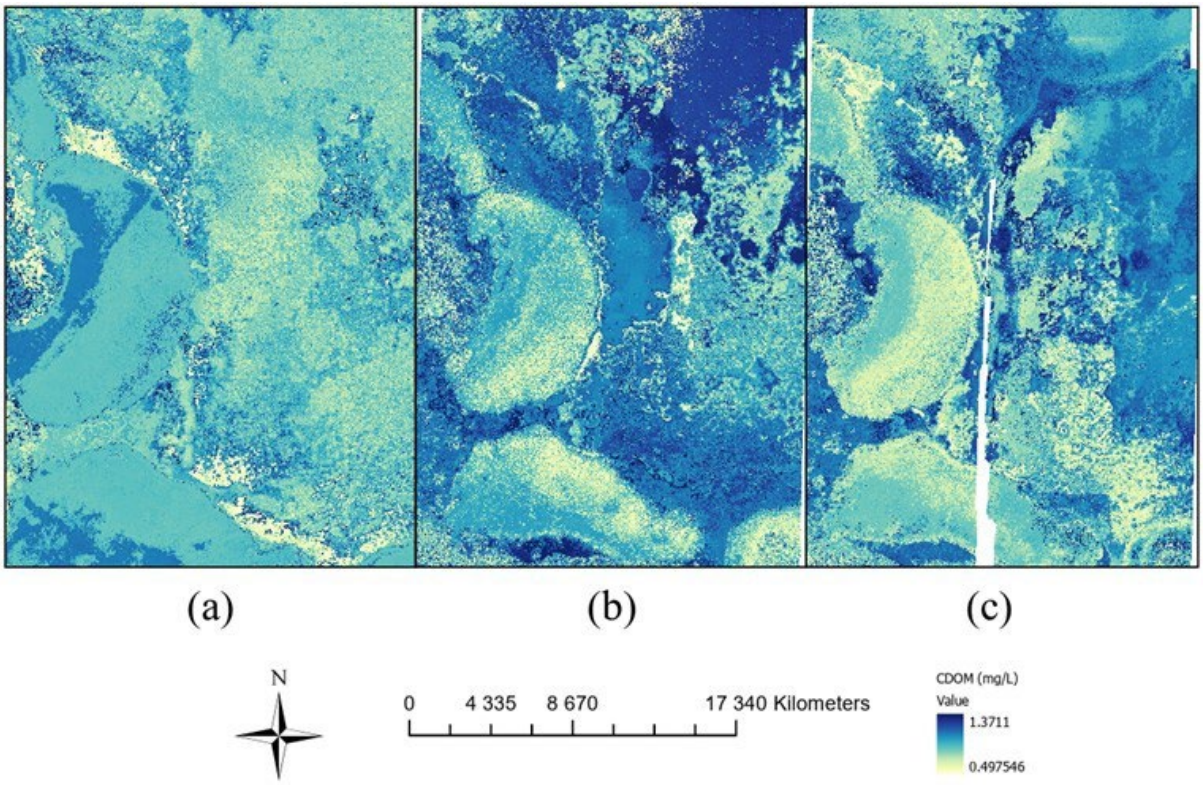

Figure 5-10 Maps showing the spatial variability of CDOM concentrations for (a) April, (b) June and (c) July based on the Ensemble 2 model

6. ASSESSMENT OF THE FEASIBILITY OF USING DRONES IN DETECTING AND MAPPING WATER LEVELS IN INLAND SMALL WATER BODIES

6.1. Introduction

In the global south, particularly in Southern Africa, water resources are unevenly distributed, compounded by climate variability (i.e., an unpredictable seasonality of precipitation) (Masocha et al. 2018; Dube, Nhamo & Chikodzi 2022). One of the leading indicators of climate change has been identified as changes in the water extent of small water bodies (Ruwanza et al. 2022). Small water bodies experience flooding as a natural result of large rainstorms that quickly drain into reservoirs. Although the risk of flooding varies across South Africa, most low-lying areas are susceptible to floods, even in dry and mountainous regions. The size, or magnitude, of flood events is influenced by how much and how quickly water enters the waterway upstream at a certain area (Masocha et al. 2018). Flood frequency of small water bodies largely depends on the size of the water body, rainfall intensity and duration, drainage characteristics, land use and land cover in the area. Large flood events can damage homes, roads, bridges, and other infrastructure, wipe out farmers' crops, and harm or displace people. Although regular flooding helps to maintain the nutrient balance of soils in the floodplain, larger or more frequent floods could disrupt ecosystems by displacing aquatic life, impairing water quality, and increasing soil erosion (Singh et al. 2022). By inundating water treatment systems with sediment and contaminants and promoting the growth of harmful microbes, floods can directly affect the water supplies that communities depend on.

Conversely, droughts can occur when the water levels fall below the average threshold, causing a lack of water in rivers, lakes, reservoirs, and aquifers (Masocha et al. 2018; Singh et al. 2022). Dry season often sees a decline in water levels in reservoirs (Figure 6-1). Low water levels can be caused by the absence of rainfall for prolonged periods. This can be further exacerbated by factors like increased water usage by humans or animals and changes in land use that impact water runoff patterns. In 1964, 1986, 1988, 1990, 1995, 2002 – 2004, 2015 – 2019, and 2022 – 2023, South Africa had periods of extreme drought and flooding (Bangira et al. 2019; Bhaga et al. 2023). Water scarcity can be exacerbated by poor surface water

management and low precipitation rates, which increase susceptibility to droughts, climate change, and variability. It is necessary to continuously monitor minor water bodies to assess water availability, identify the onset of drought conditions, and guarantee sustainable use. Knowledge of water level provides information about the variability of water bodies and thus plays a key role in monitoring and managing water resources. To develop skillful flood and hydrological forecasting systems and estimate future changes in water resources, there is a need to monitor the spatio-temporal extent of the small water bodies.

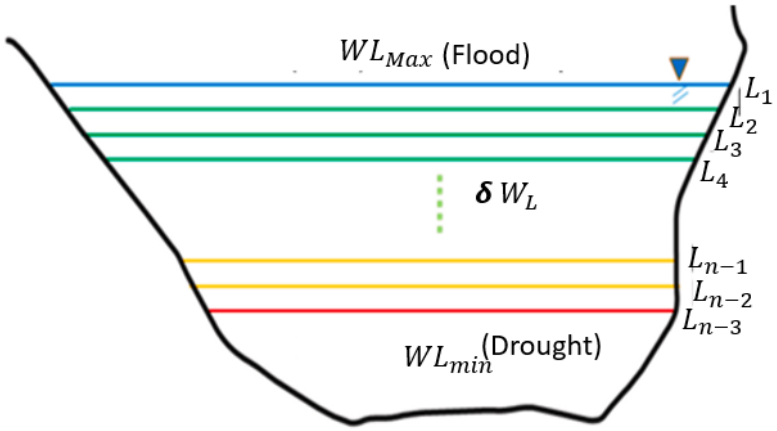

Figure 6-1 Changes of water level in a small water body

Conventional drought monitoring methods include palaeoclimatology and climatological data, e.g., rainfall, river flow, soil moisture, and evapotranspiration rates (Bhaga et al. 2023). Paleoclimatology uses previous climate data to predict future climates and comprehend past climates. In-situ measurements physically measure water levels using gauges, floats, loggers, buoy systems, pressure-based equipment, and ultrasonic and radar techniques are the mainstay of conventional surface waterbody monitoring approaches (Zhang et al. 2011). Nevertheless, these methods are expensive, time-consuming, vulnerable to theft and destruction, and challenging to implement, especially in isolated or mountainous regions. High-frequency and reproducible observations are thus made possible by the use of remotely sensed datasets for drought and surface water body monitoring (Bangira et al. 2019).

The utilisation of remotely sensed data acquired by sensors onboard satellites has been popularly used to monitor changes in water resources (Haas et al. 2009; Isikdogan et al. 2017; Huang et al. 2018; Bangira et al. 2019). While many studies have explored satellite remote sensing data for surface water body monitoring, most have focused on large water bodies. A satellite with high spatial resolution will have a lower temporal resolution, while a satellite with high temporal resolution might have lower spatial detail. Satellite sensors with coarse (approximately 1 km) spatial resolution but higher (daily) temporal resolution, such as the Moderate Resolution Imaging Spectroradiometer (MODIS) (Chen et al. 2013; Khandelwal et al. 2017), and the Advanced Very High Resolution Radiometer (AVHRR) (Barton & Bathols 1989; Li et al. 2024) may not be suitable for inland surface water monitoring due to their inability to detect small waterbodies. Although satellites with fine (less than 30 km) spatial resolution, such as Sentinel-2 and Landsat family, have successfully monitored changes in surface water, they take longer to revisit (5 to 15 days) the same area (Bioresita et al. 2019; Yang et al. 2020; Cai et al. 2024).

The spreading use of unmanned aerial vehicles (UAVs) has paved the way for the integration of drone technology and optical sensing aimed at quantitatively estimating hydraulic data such as inundated areas (Feng et al. 2015) and water level estimations (Bandini et al. 2017). Drones equipped with multispectral sensors can map small bodies of water in near real-time at high spatial resolution. Drones may be flown at low altitudes, even in cloudy conditions, and are simple to operate and deploy(Ridolfi & Manciola 2018). This allows observing small-scale changes in nearshore and shoreline zones where adjacency effects and mixed pixels hamper satellites. Since 2013, interest has steadily increased in employing drone data for optical small water body extent monitoring.

6.2. Surface water mapping using remotely sensed data

The surface water extraction algorithms for optical images can be mainly classified into image classification and spectral analysis (Dong et al. 2022). Supervised image classification with machine learning algorithms is an effective and direct way to extract surface water using optical image surface water (Munawar et al. 2021; Dong et al. 2022), such as support vector machines (Avand & Moradi 2021), random forest

(Goudarzi et al. 2021) and deep learning (Munawar et al. 2021). These supervised classification methods depend on the quality and amount of the training samples and can achieve satisfying water extraction results under the premise of sufficient representative samples. Contrary to this image classification approach, the method based on spectral analysis does not rely on training samples. It is realised by thresholding the water index image, which is established to enhance the contrast between water bodies and other land covers (Dong et al. 2022).

6.2.1 Spectral indices derived from drones for mapping surface water bodies

Utilising remotely sensed data, particularly multispectral indices and machine learning algorithms, presents a valuable opportunity to develop spatially explicit methods for monitoring surface waterbodies and assessing drought and flood impacts on these resources; different surface water body monitoring techniques are not universal. The technique's success is based on its potential to enhance the contrast between water bodies and other thematic classes eventually present in the image (Bie et al. 2020; Dong et al. 2022).

Several indices have been derived from remotely sensed data collected by sensors onboard UAVs. For instance, Tymków et al. (2019) presented a UAV-based framework for estimating water body extent using high-resolution spectral indices derived from the RGB (Red, Green, Blue) images. In a similar study, Cermakova et al. (2019) used spectral wetness indices to detect water bodies in UAV data remotely. Imam et al. (2020) derived wetness indices from remotely sensed data acquired from UAV images to quantify a flood event's spatial and temporal dynamics. Bandini et al. (2017) used the time series of UAV RGB images through spectral indices to classify water area and vegetation in a river floodplain. The potential of spectral indices in water body mapping was also highlighted in the work of (Lewicka et al. 2022). These studies have used multispectral water indices due to their high detection accuracy, cost-effectiveness, and ease of use (Bie et al. 2020).

Several water indices have been developed using remotely sensed data. This study utilises several wetness indices based on their performance in previous studies (Table 6-1). These include the Normalised Difference Water Index (NDWI) (Gao 1996), Modified Normalised Difference Water Index (MNDWI) (Xu 2006), Land Surface Water

Index (LSWI+5) (Du et al. 2014), Normalised Difference Vegetation Index (NDVI) (Rouse et al. 1974), Vegetation Condition Index (VCI) (Quiring & Ganesh 2010), and Water Requirement Satisfaction Index (WRSI) (Masupha & Moeletsi 2020).

Table 6-1 Spectral indices utilised in this study

Index	Equation	Source
Normalized difference water index (NDWI)	$\frac{\mathrm{GREEN}-\mathrm{NIR}}{\mathrm{GREEN}+\mathrm{NIR}}$	McFeeters (1996)
modified NDWI (mNDWI)	$\frac{\mathrm{GREEN}-\mathrm{SWIR}}{\mathrm{GREEN}+\mathrm{SWIR}}$	Xu (2006)
Automated water extraction index (AWEI)	4×(GREEN−SWIR) −(0.25×NIR +2.75×SWIR)	Feyisa et al. (2014)
Normalised difference vegetation index (NDVI)	$\frac{NIR-Red}{NIR+Red}$	Rouse et al. (1974)
Water index (WI)	$\frac{x+a}{(GREEN)+y(RED)-b(NIR)-c\times SWIR1-d(SWIR2)}$ $x, y, b, c\ and\ d\ are$ constants	Fisher et al. (2016)

The water index approaches by spectral analysis mainly rely on selecting appropriate thresholds to classify water and non-water features. However, the variability of spectral information challenges setting appropriate transferable thresholds, as settings are often specific to each case study. Specifically, some low-albedo objects (such as shadows) and high-albedo targets (e.g. built-up areas) often have a water index value similar to or higher than the water body, which may create several false positives (incorrect extractions), especially in complex urban scenes. To reduce false positives, the threshold to segment the water index map may need to be set relatively higher (closer to value 1). On the other hand, small water bodies tend to have relatively small water index values compared to pure water bodies due to the influence of the surrounding environment and mixed pixels. To completely extract small surface water bodies, it is best to lower the corresponding threshold value (closer to −1). This dilemma of reducing false positives and increasing the extraction integrity of small water bodies by adjusting the threshold is the major challenge when using spectral indices.

The threshold can be set empirically (e.g. 0) or automatically. The currently widely used automatic threshold determination, Otsu's (1975) method, maximises the variance between water bodies and other land covers. It is thus challenging to adjust the threshold to reduce incorrect water extractions and increase the precision of detected water bodies simultaneously. In addition, determining the optimal threshold for time-series analysis of water bodies is especially important and difficult.

6.3 Mapping small water bodies using spectral indices

The performance of the spectral indices on drone-derived images covering High Flight Dam in April, June and July were tested. Generally, all the spectral indices applied for water extraction have achieved acceptable performances, with OA and F1 accuracy indicators greater than 86% and 0.75, respectively (Table 6-2). However, these algorithms have shown different results for balancing between reducing incorrect water extractions and increasing the integrity of water extraction. The UA values of MNDWI, NDWI, and WI spectral indices are 97.5%, 93.6%, and 93.1%, respectively, while the corresponding PA values are 76.9%, 92.5% and 86.8%. This is mainly because extracting shallow small-scale water bodies for these water surface methods is challenging, considering the effects of adjacency pixels. Compared with these commonly applied wetness indices, the proposed NDWI and MNDWI algorithms can extract small water bodies more effectively to reduce the omission error. Among all these methods applied for water extraction, the NDWI achieves the highest OA and F1 accuracy.

Table 6-2 Average overall accuracies for water extent in April, June and July

Spectral Index	OA (%)	PA (%)	UA (%)	F1
NDWI	**96.2**	**92.5**	93.6	**0.94**
MNDWI	91.4	76.9	**97.5**	0.87
AWEI	92.4	83.3	92.7	0.89
NDVI	91.3	82.0	91.7	0.88
WI	92.3	86.8	93.1	0.90

Surface water mapping using spectral indices remains an open research area, as no index or thresholding algorithm is suitable for all data sets and conditions. Most of the methods developed have been based on case studies of specific regions, and adapting these methods globally was not advisable. This study is ongoing. The next stages involve applying machine learning algorithms in surface water mapping.

7. DISCUSSION, CONCLUSION AND RECOMMENDATIONS

Few studies have typically focused on water quality and quantity monitoring of small water bodies using remotely sensed data acquired by UAVs in the global South. This study aimed to improve our understanding of how the water quality parameters and changes in water extent can be monitored using drone images acquired by multispectral sensors onboard UAVs. The first specific aim was to review the literature on the available models for remote sensing water quantity and quality using UAVS. In this study, five comprehensive literature reviews were done. The results from these reviews were used to determine the suitable methods and techniques for retrieving water quality parameters and delineating wet and dry pixels in small water bodies. The second aim was to assess the feasibility of drones detecting and mapping flooding or leaks along irrigation canals and dams. It was challenging to achieve this aim, as there were no functional nearby irrigation canals.

Nevertheless, the study mapped changes in the water extent of small water bodies in flood and drought prediction. The fourth and final aim was to assess drones' spatial and temporal resolution capabilities in detecting and mapping water levels and quality in irrigation canals and dams. Analyses were conducted to monitor the spatio-temporal variability of different water quality parameters. The methods and results of these experiments are detailed in Sections 5 and 6. Some of the main findings are summarised in the next subsection. The section concludes with proposals for future research and several recommendations.

7.1. Main findings

Machine learning methods were used to extract the spatiotemporal concentration of water quality measures, specifically chl-a, TSS, surface temperature, and CDOM, and the results showed good agreement with in situ observations. For example, high concentrations of chl-a (18.289 µg/L) were observed at the periphery, inlet, and shallow areas of the water body. In comparison, lower concentrations (1.644 µg/L) were found in the deep and outlet sections. The overall chl-a concentrations remain relatively low in June, reflecting the continued influence of winter conditions, such as reduced temperatures and diminished biological activity. However, the wide range in chl-a concentrations observed in July suggests localised factors, such as nutrient

retention in shallow areas or reduced water flow, creating favourable conditions for algal growth even during winter. These localised dynamics highlight the complexity of environmental interactions influencing chl-a levels.

Furthermore, the strong correlations between temperature, TSS and CDOM signify the importance of understanding thermal dynamics in aquatic systems. For instance, higher temperatures accelerate the breakdown of aquatic vegetation, contributing to increased CDOM while simultaneously reducing TSS levels by promoting sediment settling. Conversely, TSS levels are greatly influenced by runoff events, soil erosion and human activities such as agricultural practices. Rainfall in warmer months significantly contributes to increased TSS due to sediment transport from catchment areas, whereas reduced runoff in drier months results in lower TSS levels. CDOM concentrations, on the other hand, are linked to organic matter decomposition influenced by vegetation cover, land use and river inflows. When looking at the High Flight farm dam, aquatic vegetation played a dual role since it contributed to increased CDOM concentrations through decomposition and influenced light attenuation, affecting CDOM concentrations' detectability. The use of spectral indices in delineating water bodies is not universal.

7.2. Innovations and new knowledge creation

This work made a substantial contribution to the body of knowledge. In particular, tracking the quantity and quality of water in tiny bodies of water using remotely sensed data collected by multispectral sensors aboard UAVs. To the best of our knowledge, the use of remote sensing to estimate water quality indicators in the Umgeni catchment's small bodies of water is new. Furthermore, extracting water quality metrics from very high resolution (5 cm) colour drone photos is novel using machine learning techniques. These innovative methods, which were created and assessed by the three master's students involved in the research, show the substantial human capacity built into this project.

7.3. Recommendations

This study's findings may be valuable to the ongoing discussions on water resources management for food security. The water quality of small water bodies is crucial as

they serve as vital sources for irrigation, livestock watering and domestic use, particularly in rural and agricultural areas. Poor water quality can lead to reduced crop yields, clogged irrigation systems and increased maintenance costs due to sedimentation or algal growth. Contaminants such as excess nutrients, pesticides or pathogens can also affect water safety for agricultural and human use, potentially impacting food security and public health. Additionally, small water bodies often support local biodiversity and serve as habitats for aquatic organisms essential to maintaining ecological balance. Ensuring good water quality is fundamental for sustaining the productivity of these systems, promoting sustainable water management and supporting the livelihoods of communities that rely on them.

Ideally, this study's water quality parameter estimations should be compared to other water bodies to assess the relationship between land use and water pollution. Unfortunately, we did not estimate the water quality of multiple water bodies. More work is advised to reach a definitive judgement about using remotely sensed data in water quality monitoring in the Umgeni basin. High spatial resolution remotely sensed data were used in this work to monitor the quantity and quality of water across small bodies of water. This research project was costly, even though it significantly advanced our understanding. In situ sample analysis reagents are expensive. Future research is advised to test water quality parameters in situ using probes. This should be combined with installing water quality sensors in key areas around South Africa.

Furthermore, a key limitation is the high cost of UAV platforms, sensors and necessary licensing. This financial barrier is particularly significant in regions like southern Africa, where funding for advanced technologies is limited. Furthermore, the operational costs are exacerbated by concerns over equipment security, theft, and damage. Additionally, challenges lay in the technical expertise required for UAV operation and data analysis. The lack of trained professionals to handle these systems reduces their accessibility and usability for many stakeholders, including smallholder farmers and local governments. Lastly, UAVs face technical constraints such as limited battery life, flight ranges and sensitivity to adverse weather conditions, which can impede data collection during critical periods, such as heavy rainfall seasons. Additionally, connectivity issues, particularly in rural regions, further complicate the ability to transmit or analyse data efficiently.

These barriers highlight the need for more robust and adaptable UAV systems tailored to southern Africa's unique socio-economic and environmental contexts and similar regions. Future research should consider integrating UAV data with in-situ measurements, which can offer a comprehensive, multiscale approach to water quality monitoring. Such hybrid methods can improve accuracy, scalability and cost efficiency. Moreover, integrating advanced sensors, such as LiDAR and hyperspectral sensors, and increasing sample sizes can provide a more comprehensive understanding of complex aquatic ecosystems. Additionally, capacity building and training programs should be implemented to develop a skilled workforce capable of operating UAV systems and interpreting the collected data. Collaborative research efforts involving government bodies, academic institutions and local communities can provide interdisciplinary applications and ensure that UAV-based technologies are accessible and beneficial to a broader audience. Expanding the scope of research to include underrepresented regions and parameters is also essential. Most studies have focused on large lakes, rivers and coastal areas, leaving smaller inland water bodies like farm reservoirs underexplored. Given their socio-economic importance, particularly for agriculture and rural development, these water bodies should be a primary focus of future research. Finally, future efforts should emphasize the socio-economic benefits of UAV-based monitoring. By demonstrating its value in improving water resource management, agricultural productivity, and environmental sustainability, researchers can build a stronger case for investment and adoption.

References

Adjovu GE, Stephen H, James D & Ahmad S 2023. Overview of the Application of Remote Sensing in Effective Monitoring of Water Quality Parameters. *Remote Sensing* 15: 1938.

Adjovu GES, Haroon; James, David; Ahmad, Sajjad 2023. Overview of the Application of Remote Sensing in Effective Monitoring of Water Quality Parameters. *Remote Sensing* 15: 1938.

Ahn JMK, Byungik; Jong, Jaehun; Nam, Gibeom; Park, Lan Joo; Park, Sanghyun; Kang, Taegu; Lee, Jae-Kwan; Kim, Jungwook 2021. Predicting cyanobacterial blooms using hyperspectral images in a regulated river. *Sensors* 21: 530.

Al-Abed N, Abdulla, Fayez and Zahrawi, Raed 2009. Evaluation of irrigation water total suspended solids (TSS) on a farm scale'. *Archives of Agronomy and Soil Science* 53: 345-353.

Ali J, Khan R, Ahmad N & Maqsood I 2012. Random forests and decision trees. *International Journal of Computer Science Issues (IJCSI)* 9: 272.

Ali K, Abiye T & Adam E 2022. Integrating in Situ and Current Generation Satellite Data for Temporal and Spatial Analysis of Harmful Algal Blooms in the Hartbeespoort Dam, Crocodile River Basin, South Africa. *Remote Sensing* 14: 4277.

Anderson DM 2009. Approaches to monitoring, control and management of harmful algal blooms (HABs). *Ocean & coastal management* 52: 342-347.

Anderson K & Gaston KJ 2013. Lightweight unmanned aerial vehicles will revolutionize spatial ecology. *Frontiers in Ecology and the Environment* 11: 138-146.

APHA 2005. Standard Operating Procedure for: Total Suspended Solids 2540D. *Standard Methods for the Examination of Water and Waste Water.*

Arango JGN, Robert W 2019. Prediction of optical and non-optical water quality parameters in oligotrophic and eutrophic aquatic systems using a small unmanned aerial system. *Drones* 4: 1.

Arar EJ 1997. *Method 446.0, In vitro determination of chlorophylls a, b, c1, +c2 and pheopigments in marine and freshwater algae by visible spectrophotometry.* Washington, DC: U. S.: Environmental Protection Agency.

Avand M & Moradi H 2021. Using machine learning models, remote sensing, and GIS to investigate the effects of changing climates and land uses on flood probability. *Journal of Hydrology* 595: 125663.

Baiphethi MN & Jacobs PT 2009. The contribution of subsistence farming to food security in South Africa. *Agrekon* 48: 459-482.

Bandini F, Jakobsen J, Olesen D, Reyna-Gutierrez JA & Bauer-Gottwein P 2017. Measuring water level in rivers and lakes from lightweight Unmanned Aerial Vehicles. *Journal of Hydrology* 548: 237-250.

Banerjee A, Chakrabarty M, Rakshit N, Bhowmick AR & Ray S 2019. Environmental factors as indicators of dissolved oxygen concentration and zooplankton abundance: Deep learning versus traditional regression approach. *Ecological indicators* 100: 99-117.

Bangira T, Alfieri SM, Menenti M & Van Niekerk A 2019. Comparing thresholding with machine learning classifiers for mapping complex water. *Remote Sensing* 11: 1351.

Bangira T, Matongera TN, Mabhaudhi T & Mutanga O 2024. Remote sensing-based water quality monitoring in African reservoirs, potential and limitations of sensors and algorithms: A systematic review. *Physics and Chemistry of the Earth, Parts A/B/C* 134: 103536.

Bangira T, Mutanga O, Sibanda M, Dube T & Mabhaudhi T 2023. Remote sensing grassland productivity attributes: A systematic review. *Remote Sensing* 15.

Bangira TM, T. N.; Mabhaudhi, T.; Mutanga, O. 2024. Remote sensing-based water quality monitoring in African reservoirs, potential and limitations of sensors and algorithms: A systematic review. *Physics and Chemistry of the Earth* 134.

Banna MH, Syed I, Alex F, Homayoun N, Rehan S, Manuel R & and Hoorfar M 2014. Online Drinking Water Quality Monitoring: Review on Available and Emerging Technologies. *Critical Reviews in Environmental Science and Technology* 44: 1370-1421.

Barton IJ & Bathols JM 1989. Monitoring floods with AVHRR. *Remote sensing of Environment* 30: 89-94.

Beck R, Zhan S, Liu H, Tong S, Yang B, Xu M, Ye Z, Huang Y, Shu S & Wu Q 2016. Comparison of satellite reflectance algorithms for estimating chlorophyll-a in a temperate reservoir using coincident hyperspectral aircraft imagery and dense coincident surface observations. *Remote Sensing of Environment* 178: 15-30.

Belgiu M & Drăguţ L 2016. Random forest in remote sensing: A review of applications and future directions. *ISPRS Journal of Photogrammetry and Remote Sensing* 114: 24-31.

Bhaga TD, Dube T, Shekede MD & Shoko C 2023. Investigating the effectiveness of Landsat-8 OLI and Sentinel-2 MSI satellite data in monitoring the effects of drought on surface water resources in the Western Cape Province, South Africa. *Remote Sensing Applications: Society and Environment* 32: 101037.

Bie W, Fei T, Liu X, Liu H & Wu G 2020. Small water bodies mapped from Sentinel-2 MSI (MultiSpectral Imager) imagery with higher accuracy. *International Journal of Remote Sensing* 41: 7912-7930.

Bioresita F, Puissant A, Stumpf A & Malet J-P 2019. Fusion of Sentinel-1 and Sentinel-2 image time series for permanent and temporary surface water mapping. *International Journal of Remote Sensing* 40: 9026-9049.

Brando VE & Dekker AG 2003. Satellite hyperspectral remote sensing for estimating estuarine and coastal water quality. *IEEE transactions on geoscience and remote sensing* 41: 1378-1387.

Breiman L 2001. Random forests. *Machine learning* 45: 5-32.

Brito RCL, M.C.; Loureiro, J.F.; Favarim, F.; Todt, E. 2019. A comparative approach on the use of unmanned aerial vehicles kind of fixed-wing and rotative wing applied to the precision agriculture scenario. *Computer Software and Applications Conference (COMPSAC).* Milwaukee, USA.

Bronkhorst S, Pengelly C & Seyler H 2017. Water 2017 Market Intelligence Report. *City of Cape Town: GreenCape*.

Buma WG & Lee S-I 2020. Evaluation of sentinel-2 and landsat 8 images for estimating chlorophyll-a concentrations in Lake Chad, Africa. *Remote Sensing* 12: 2437.

Cai XW, Luyao; Li, Yunmei; Lei, Shaohua; Xu, Jie; Lyu, Heng; Li, Junda; Wang, Huaijing; Dong, Xianzhang; Zhu, Yuxing 2023. Remote sensing identification of urban water pollution source types using hyperspectral data. *Journal of Hazardous Materials* 459: 132080.

Cai Y, Shi Q & Liu X 2024. Spatiotemporal Mapping of Surface Water Using Landsat Images and Spectral Mixture Analysis on Google Earth Engine. *Journal of Remote Sensing* 4: 0117.

Campbell G, Phinn SR, Dekker AG & Brando VE 2011. Remote sensing of water quality in an Australian tropical freshwater impoundment using matrix inversion and MERIS images. *Remote Sensing of Environment* 115: 2402-2414.

Campbell GP, S. R.; Dekker, A. G.; Brando, V. E. 2011. Remote sensing of water quality in an Australian tropical freshwater impoundment using matrix inversion and MERIS images. *Remote Sensing of Environment* 115: 2402-2414.

Cao Q, Yu G & Qiao Z 2023. Application and recent progress of inland water monitoring using remote sensing techniques. *Environmental Monitoring and Assessment* 195: 125.

Cao Q, Yu G, Sun S, Dou Y, Li H & Qiao Z 2021. Monitoring water quality of the Haihe River based on ground-based hyperspectral remote sensing. *Water* 14: 22.

Carpenter D & Carpenter S 1983. Modeling inland water quality using Landsat data. *Remote Sensing of Environment* 13: 345-352.

Cermakova I, Komarkova J & Sedlak P 2019. Calculation of Visible Spectral Indices from UAV-Based Data: Small Water Bodies Monitoring. 2019 14th Iberian Conference on Information Systems and Technologies (CISTI).

Chebud Y, Naja GM, Rivero RG & Melesse AM 2012. Water quality monitoring using remote sensing and an artificial neural network. *Water, Air, & Soil Pollution* 223: 4875-4887.

Chen BM, Xi; Chen, Peng; Wang, Biao; Choi, Jaewan; Park, Honglyun; Xu, Sheng; Wu, Yanlan; Yang, Hui 2021. Machine learning-based inversion of water quality parameters in typical reach of the urban river by UAV multispectral data. *Ecological Indicators* 133: 108434.

Chen PW, Biao; Wu, Yanlan; Wang, Qijun; Huang, Zuoji; Wang, Chunlin 2023. Urban river water quality monitoring based on self-optimizing machine learning method using multi-source remote sensing data. *Ecological Indicators* 146: 109750.

Chen Y, Huang C, Ticehurst C, Merrin L & Thew P 2013. An evaluation of MODIS daily and 8-day composite products for floodplain and wetland inundation mapping. *Wetlands* 33: 823-835.

Chien W-H, Wang T-S, Yeh H-C & Hsieh T-K 2016. Study of NDVI application on turbidity in reservoirs. *Journal of the Indian Society of Remote Sensing* 44: 829-836.

Choo YK, G.; Kim, D.; Lee, S. 2018. A study on the evaluation of water-bloom using image processing. *Environmental Science and Pollution Research* 25: 36775-36780.

Chung W-Y & Yoo J-H 2015. Remote water quality monitoring in wide area. *Sensors and Actuators B: Chemical* 217: 51-57.

Ciancia EC, A.; Lacava, T.; Palombo, A.; Pascucci, S.; Pergola, N.; Pignatti, S.; Satriano, V.; Tramutoli, V. 2020. Modeling and Multi-Temporal Characterization of Total Suspended Matter by the Combined Use of Sentinel 2-MSI and Landsat 8-OLI Data: The Pertusillo Lake Case Study (Italy). *Remote Sensing* 12.

Cillero Castro C, Domínguez Gómez JA, Delgado Martín JHS, Boris Alejandro, Cereijo Arango JL, Cheda Tuya FA & Díaz-Varela R 2020. An UAV and Satellite Multispectral Data Approach to Monitor Water Quality in Small Reservoirs. *Remote Sensing* 12: 1514.

Coble PG 1996. Characterization of marine and terrestrial DOM in seawater using excitation-emission matrix fluorescence. *Marine Chemistry* 51: 325-346.

Congalton RG & Green K 2019. *Assessing the accuracy of remotely sensed data: principles and practices.* CRC press.

Davis KF, Rulli MC, Seveso A & D'Odorico P 2017. Increased food production and reduced water use through optimized crop distribution. *Nature Geoscience* 10: 919-924.

De Keukelaere L, Moelans R, Knaeps E, Sterckx S, Reusen I, De Munck D, Simis SG, Constantinescu AM, Scrieciu A & Katsouras G 2023. Airborne drones for water

quality mapping in inland, transitional and coastal waters—MapEO water data processing and validation. *Remote Sensing* 15: 1345.

Deka PC 2014. Support vector machine applications in the field of hydrology: a review. *Applied soft computing* 19: 372-386.

Dias RLS, da Silva DD, Fernandes-Filho EI, do Amaral CH, dos Santos EP, Marques JF & Veloso GV 2021. Machine learning models applied to TSS estimation in a reservoir using multispectral sensor onboard to RPA. *Ecological Informatics* 65: 101414.

Dias RLSdS, D. D.; Fernandes-Filho, E. I.; do Amaral, C. H.; dos Santos, E. P.; Marques, J. F.; Veloso, G. V. 2021. Machine learning models applied to TSS estimation in a reservoir using multispectral sensor onboard to RPA. *Ecological Informatics* 65.

Divi´c MGc, Ivankovi´c MKc, Divi´c V, Kiševi´c M, Pani´c M, Lugonja P, Crnojevi´c V & Andriˇcevi´c R 2023. Estimation of Water Quality Parameters in Oligotrophic Coastal Waters Using Uncrewed-Aerial-Vehicle-Obtained Hyperspectral Data. *Journal of Marine Science and Engineering* 11.

Dlamini S, Nhapi I, Gumindoga W, Nhiwatiwa T & Dube T 2016. Assessing the feasibility of integrating remote sensing and in-situ measurements in monitoring water quality status of Lake Chivero, Zimbabwe. *Physics and Chemistry of the Earth, Parts A/B/C* 93: 2-11.

Dong Y, Fan L, Zhao J, Huang S, Geiß C, Wang L & Taubenböck H 2022. Mapping of small water bodies with integrated spatial information for time series images of optical remote sensing. *Journal of Hydrology* 614: 128580.

Douglas Greene SBL, G. H.; Markfort, C. D. 2021. Improving the spatial and temporal monitoring of cyanotoxins in Iowa lakes using a multiscale and multi-modal monitoring approach. *Science of the Total Environment* 760.

Du Z, Li W, Zhou D, Tian L, Ling F, Wang H, Gui Y & Sun B 2014. Analysis of Landsat-8 OLI imagery for land surface water mapping. *Remote sensing letters* 5: 672-681.

Dube K, Nhamo G & Chikodzi D 2022. Flooding trends and their impacts on coastal communities of Western Cape Province, South Africa. *GeoJournal* 87: 453-468.

Dube T, Sibanda M & Shoko C 2016. Examining the variability of small-reservoir water levels in semi-arid environments for integrated water management purposes, using remote sensing. *Transactions of the Royal Society of South Africa* 71: 115-119.

DWAF 2004. National water resources strategy, Department of Water Affairs and Forestry. 1st edition ed. DWAF; Pretoria.

DWS 2022. National Eutrophication Monitoring Programme [online]. Department of Water and Sanitation, Republic of South Africa. Available from

http://www.dwa.gov.za/iwqs/eutrophication/NEMP/default.aspx. [Accessed 06 September 2023].

Dzurume T, Dube T & Shoko C 2022. Remotely sensed data for estimating chlorophyll-a concentration in wetlands located in the Limpopo Transboundary River Basin, South Africa. *Physics and Chemistry of the Earth, Parts A/B/C* 127: 103193.

El-Alem AC, K.; Venkatesan, A.; Rachid, L.; Agili, H.; Dedieu, J. P. 2021. How accurate is an unmanned aerial vehicle data-based model applied on satellite imagery for chlorophyll-a estimation in freshwater bodies? *Remote Sensing* 13.

El Bilali A & Taleb A 2020. Prediction of irrigation water quality parameters using machine learning models in a semi-arid environment. *Journal of the Saudi Society of Agricultural Sciences* 19: 439-451.

El Din ES, Zhang Y & Suliman A 2017. Mapping concentrations of surface water quality parameters using a novel remote sensing and artificial intelligence framework. *International Journal of Remote Sensing* 38: 1023–1042.

Eleuterio L & Neethling J 2010. Low Phosphorus Analytical Measurement Study. Proceedings of the 83rd Annual Water Environmental Federation Annual Conference and Exposition (WEFTEC). New Orleans, LA.

EPA U 1971. Method 352.1: Nitrogen, Nitrate (Colorimetric, Brucine) by Spectrophotometer. Environmental Protection Agency Washington, DC, USA.

Falconer I, Bartram J, Chorus I, Kuiper-Goodman T, Utkilen H, Burch M & Codd G 1999. Safe levels and safe practices. *Toxic cyanobacteria in water*: 155-178.

Fan C 2014. Spectral analysis of water reflectance for hyperspectral remote sensing of water quality in estuarine water. *Journal of Geoscience and Environmental Protection* 2: 19-27.

FAO 2022. World food and agriculture—Statistical pocketbook 2022.

Feng Q, Liu J & Gong J 2015. Urban flood mapping based on unmanned aerial vehicle remote sensing and random forest classifier—A case of Yuyao, China. *Water* 7: 1437-1455.

Fernandez-Figueroa EG, Wilson AE & Rogers SR 2022. Commercially available unoccupied aerial systems for monitoring harmful algal blooms: A comparative study. *Limnology and Oceanography: Methods* 20: 146-158.

Finley JW & Seiber JN 2014. The nexus of food, energy, and water. *Journal of agricultural and food chemistry* 62: 6255-6262.

Fischer G 2009. World food and agriculture to 2030/50. Technical paper from the Expert Meeting on How to Feed the World in.

Fisher A, Flood N & Danaher T 2016. Comparing Landsat water index methods for automated water classification in eastern Australia. *Remote Sensing of Environment* 175: 167-182.

Fu BL, Sunzhe; Lao, Zhinan; Yuan, Bingyan; Liang, Yiyin; He, Wen; Sun, Weiwei; He, Hongchang 2023. Multi-sensor and multi-platform retrieval of water chlorophyll a concentration in karst wetlands using transfer learning frameworks with ASD, UAV, and Planet CubeSate reflectance data. *Science of The Total Environment* 901: 165963.

Gao B-C 1996. NDWI—A normalized difference water index for remote sensing of vegetation liquid water from space. *Remote sensing of environment* 58: 257-266.

Gao Y, Gao J, Yin H, Liu C, Xia T, Wang J & Huang Q 2015. Remote sensing estimation of the total phosphorus concentration in a large lake using band combinations and regional multivariate statistical modeling techniques. *Journal of Environmental Management* 151: 33-43.

Gholizadeh MH, Melesse AM & Reddi L 2016. A Comprehensive Review on Water Quality Parameters Estimation Using Remote Sensing Techniques. *Sensors* 16: 1298.

Ghosh S, Dasgupta A & Swetapadma A 2019. A study on support vector machine based linear and non-linear pattern classification. 2019 International Conference on Intelligent Sustainable Systems (ICISS).

Gitelson A 1992. The peak near 700 nm on radiance spectra of algae and water: relationships of its magnitude and position with chlorophyll concentration. *International Journal of Remote Sensing* 13: 3367-3373.

Gohin F, Bryère P, Lefebvre A, Sauriau P-G, Savoye N, Vantrepotte V, Bozec Y, Cariou T, Conan P & Coudray S 2020. Satellite and in situ monitoring of chl-a, turbidity, and total suspended matter in coastal waters: Experience of the year 2017 along the French coasts. *Journal of Marine Science and Engineering* 8: 665.

Goudarzi S, Ahmad Soleymani S, Anisi MH, Ciuonzo D, Kama N, Abdullah S, Abdollahi Azgomi M, Chaczko Z & Azmi A 2021. Real-time and intelligent flood forecasting using UAV-assisted wireless sensor network. *Computers, Materials and Continua* 70: 715-738.

Green SA & Blough NV 1994. Optical absorption and fluorescence properties of chromophoric dissolved organic matter in natural waters. *Limnology and Oceanography* 39: 1903–1916.

Guimarães TTV, M. R.; Koste, E. C.; Gonzaga, L.; Bordin, F.; Inocencio, L. C.; Larocca, A. P. C.; de Oliveira, M. Z.; Vitti, D. C.; Mauad, F. F. 2017. An alternative method of spatial autocorrelation for chlorophyll detection in water bodies using remote sensing. *Sustainability (Switzerland)* 9.

Haas EM, Bartholomé E & Combal B 2009. Time series analysis of optical remote sensing data for the mapping of temporary surface water bodies in sub-Saharan western Africa. *Journal of Hydrology* 370: 52-63.

Hamidi SAH, H.; Ekhtari, N.; Khazaei, B. 2017. Using MODIS remote sensing data for mapping the spatio-temporal variability of water quality and river turbid plume. *Journal of Coastal Conservation* 21: 939-950.

Harding W 2015. Living with eutrophication in South Africa: a review of realities and challenges, Transactions of the Royal Society of South Africa 70 (2) 2015: pp. 155-171. *Transactions of the Royal Society of South Africa* 70: 299-303.

Harvey ET, Kratzer S & Philipson P 2015. Satellite-based water quality monitoring for improved spatial and temporal retrieval of chlorophyll-a in coastal waters. *Remote Sensing of Environment* 158: 417-430.

Harvey MC, Rowland JV & Luketina KM 2016. Drone with thermal infrared camera provides high resolution georeferenced imagery of the Waikite geothermal area, New Zealand. *Journal of Volcanology and Geothermal Research* 325: 61-69.

He J, Chen Y, Wu J, Stow DA & Christakos G 2020. Space-time chlorophyll-a retrieval in optically complex waters that accounts for remote sensing and modeling uncertainties and improves remote estimation accuracy. *Water Research* 171: 115403.

Herrera VM, Khoshgoftaar TM, Villanustre F & Furht B 2019. Random forest implementation and optimization for Big Data analytics on LexisNexis's high performance computing cluster platform. *Journal of Big Data* 6: 1-36.

Hong SMC, Kyung Hwa; Park, Sanghyun; Kang, Taegu; Kim, Moon Sung; Nam, Gibeom; Pyo, JongCheol 2022. Estimation of cyanobacteria pigments in the main rivers of South Korea using spatial attention convolutional neural network with hyperspectral imagery. *GIScience & Remote Sensing* 59: 547-567.

Hou YZ, Anbing; Lv, Rulan; Zhang, Yanping; Ma, Jie; Li, Ting 2023. Machine learning algorithm inversion experiment and pollution analysis of water quality parameters in urban small and medium-sized rivers based on UAV multispectral data. *Environmental Science and Pollution Research* 30: 78913-78932.

Huang C, Chen Y, Zhang S & Wu J 2018. Detecting, extracting, and monitoring surface water from space using optical sensors: A review. *Reviews of Geophysics* 56: 333-360.

Huang M, Kim MS, Delwiche SR, Chao K, Qin J, Mo C, Esquerre C & Zhu Q 2016. Quantitative analysis of melamine in milk powders using near-infrared hyperspectral imaging and band ratio. *Journal of Food Engineering* 181: 10-19.

Imam R, Pini M, Marucco G, Dominici F & Dovis F 2020. UAV-Based GNSS-R for Water Detection as a Support to Flood Monitoring Operations: A Feasibility Study. *Applied Sciences* 10: 210.

Isikdogan F, Bovik AC & Passalacqua P 2017. Surface water mapping by deep learning. *IEEE journal of selected topics in applied earth observations and remote sensing* 10: 4909-4918.

Ismail M 2012. Remote Sensing as a Tool in Assessing Water Quality. *Life Sci. J* 9: 246-252.

Jang SWY, Hong Joo; Kwak, Seok Nam; Sohn, Byeong Yong; Kim, Se Geun; Kim, Dae Hyun 2016. Algal bloom monitoring using UAVs imagery. *Adv. Sci. Technol. Lett* 138: 30-33.

Jenkins D & Medsker LL 1964. Brucine Method for the Determination of Nitrate in Ocean, Estuarine, and Fresh Waters. *Analytical Chemistry* 36: 610-612.

Joehnk KD, Huisman J, Sharples J, Sommeijer B, Visser PM & Stroom JM 2008. Summer heatwaves promote blooms of harmful cyanobacteria. *Global change biology* 14: 495-512.

Kabbara N, Benkhelil J, Awad M & Barale V 2008. Monitoring water quality in the coastal area of Tripoli (Lebanon) using high-resolution satellite data. *ISPRS Journal of Photogrammetry and Remote Sensing* 63: 488-495.

Khandelwal A, Karpatne A, Marlier ME, Kim J, Lettenmaier DP & Kumar V 2017. An approach for global monitoring of surface water extent variations in reservoirs using MODIS data. *Remote sensing of Environment* 202: 113-128.

Khouni I, Louhichi G & Ghrabi A 2021. Use of GIS based Inverse Distance Weighted interpolation to assess surface water quality: Case of Wadi El Bey, Tunisia. *Environmental Technology & Innovation* 24: 101892.

Kim EJN, S. H.; Koo, J. W.; Hwang, T. M. 2021. Hybrid Approach of Unmanned Aerial Vehicle and Unmanned Surface Vehicle for Assessment of Chlorophyll-a Imagery Using Spectral Indices in Stream, South Korea. *Water* 13.

Kim G, Baek I, Stocker MD, Smith JE, Van Tassell AL, Qin J, Chan DE, Pachepsky Y & Kim MS 2020. Hyperspectral Imaging from a Multipurpose Floating Platform to Estimate Chlorophyll-a Concentrations in Irrigation Pond Water. *Remote Sensing* 12: 2070.

Kim K-M & Ahn J-H 2022. Machine learning predictions of chlorophyll-a in the Han River basin, Korea. *Journal of Environmental Management* 318: 115636.

Kirk JT 1994. *Light and photosynthesis in aquatic ecosystems.* Cambridge University Press.

Koparan C, Koc AB, Privette CV, Sawyer CB & Sharp JL 2018. Evaluation of a UAV-assisted autonomous water sampling. *Water* 10: 655.

Koutalakis P, Tzoraki O & Zaimes G 2019. UAVs for Hydrologic Scopes: Application of a Low-Cost UAV to Estimate Surface Water Velocity by Using Three Different Image-Based Methods. *Drones* 3.

Kundzewicz ZW, Krysanova V, Benestad R, Hov Ø, Piniewski M & Otto IM 2018. Uncertainty in climate change impacts on water resources. *Environmental Science & Policy* 79: 1-8.

Kutser T, Metsamaa L, Strömbeck N & Vahtmäe E 2006. Monitoring cyanobacterial blooms by satellite remote sensing. *Estuarine, Coastal and Shelf Science* 67: 303-312.

Kutser T, Pierson D, Tranvik L, Reinart A, Sobek S & Kallio K 2005. Using Satellite Remote Sensing to Estimate the Colored Dissolved Organic Matter Absorption Coefficient in Lakes. *Ecosystems* 8: 709–720.

Lai Y, Zhang J, Song Y & Gong Z 2021. Retrieval and evaluation of chlorophyll-a concentration in reservoirs with main water supply function in Beijing, China, based on landsat satellite images. *International journal of environmental research and public health* 18: 4419.

Lally HT, O'Connor I, Jensen OP & Graham CT 2019. Can drones be used to conduct water sampling in aquatic environments? A review. *Science of The Total Environment* 670: 569-575.

Larson MDM, A. S.; Vincent, R. K.; Evans, J. E. 2018. Multi-depth suspended sediment estimation using high-resolution remote-sensing UAV in Maumee River, Ohio. *International Journal of Remote Sensing* 39: 5472-5489.

Lary DJ, Schaefer D, Waczak J, Aker A, Barbosa A, Wijeratne LOH, Talebi S, Fernando B, Sadler J, Lary T & Lary MD 2021. Autonomous learning of new environments with a robotic team employing Hyper-spectral Remote sensing, Comprehensive in-situ sensing and machine learning. *Sensors* 21.

Lewicka O, Specht M, Stateczny A, Specht C, Dardanelli G, Brčić D, Szostak B, Halicki A, Stateczny M & Widźgowski S 2022. Integration data model of the bathymetric monitoring system for shallow waterbodies using UAV and USV platforms. *Remote Sensing* 14: 4075.

Li H, Somogyi B & Tóth V 2024. Exploring spatiotemporal features of surface water temperature for Lake Balaton in the 21st century based on Google Earth Engine. *Journal of Hydrology* 640: 131672.

Li R & Li J 2004. Satellite remote sensing technology for lake water clarity monitoring: an overview. *Environmental Informatics Archives* 2: 893-901.

Lichtenthaler HK & Babani F 2000. Detection of photosynthetic activity and water stress by imaging the red chlorophyll fluorescence. *Plant Physiology and Biochemistry* 38: 889-895.

Lillesand T, Kiefer RW & Chipman J 2015. *Remote sensing and image interpretation.* John Wiley & Sons.

Lins RC, Martinez J-M, Motta Marques DD, Cirilo JA & Fragoso Jr CR 2017. Assessment of chlorophyll-a remote sensing algorithms in a productive tropical estuarine-lagoon system. *Remote Sensing* 9: 516.

Liu HY, Tao; Hu, Bingliang; Hou, Xingsong; Zhang, Zhoufeng; Liu, Xiao; Liu, Jiacheng; Wang, Xueji; Zhong, Jingjing; Tan, Zhengxuan 2021. Uav-borne hyperspectral imaging remote sensing system based on acousto-optic tunable filter for water quality monitoring. *Remote Sensing* 13: 4069.

Lo YF, L.; Lu, T. C.; Huang, H.; Kong, L. R.; Xu, Y. Q.; Zhang, C. 2023a. Medium-Sized Lake Water Quality Parameters Retrieval Using Multispectral UAV Image and Machine Learning Algorithms: A Case Study of the Yuandang Lake, China. *Drones* 7.

Lo YF, Lang; Lu, Tiancheng; Huang, Hong; Kong, Lingrong; Xu, Yunqing; Zhang, Cheng 2023b. Medium-Sized Lake Water Quality Parameters Retrieval Using Multispectral UAV Image and Machine Learning Algorithms: A Case Study of the Yuandang Lake, China. *Drones* 7: 244.

Logan RDT, Madison A; Feijó-Lima, Rafael; Colman, Benjamin P; Valett, H Maurice; Shaw, Joseph A 2023. UAV-Based Hyperspectral Imaging for River Algae Pigment Estimation. *Remote Sensing* 15: 3148.

Lu QS, Wei; Wei, Lifei; Li, Zhongqiang; Xia, Zhihong; Ye, Song; Xia, Yu 2021. Retrieval of water quality from UAV-borne hyperspectral imagery: A comparative study of machine learning algorithms. *Remote Sensing* 13: 3928.

Maier HR, Jain A, Dandy GC & Sudheer KP 2010. Methods used for the development of neural networks for the prediction of water resource variables in river systems: Current status and future directions. *Environmental modelling & software* 25: 891-909.

Malahlela OE, Oliphant T, Tsoeleng LT & Mhangara P 2018. Mapping chlorophyll-a concentrations in a cyanobacteria-and algae-impacted Vaal Dam using Landsat 8 OLI data. *South African Journal of Science* 114: 1-9.

Masocha M, Dube T, Makore M, Shekede MD & Funani J 2018. Surface water bodies mapping in Zimbabwe using Landsat 8 OLI multispectral imagery: A comparison of multiple water indices. *Physics and Chemistry of the Earth, Parts a/b/c* 106: 63-67.

Masupha TE & Moeletsi ME 2020. The use of Water Requirement Satisfaction Index for assessing agricultural drought on rain-fed maize, in the Luvuvhu River catchment, South Africa. *Agricultural Water Management* 237: 106142.

Matthews MW 2014. Eutrophication and cyanobacterial blooms in South African inland waters: 10 years of MERIS observations. *Remote Sensing of Environment* 155: 161-177.

Matthews MW & Bernard S 2015. Eutrophication and cyanobacteria in South Africa's standing water bodies: A view from space. *South African journal of science* 111: 1-8.

Matthews MW, Bernard S & Winter K 2010. Remote sensing of cyanobacteria-dominant algal blooms and water quality parameters in Zeekoevlei, a small hypertrophic lake, using MERIS. *Remote Sensing of Environment* 114: 2070-2087.

McEliece R, Hinz S, Guarini J-M & Coston-Guarini J 2020. Evaluation of nearshore and offshore water quality assessment using UAV multispectral imagery. *Remote Sensing* 12: 2258.

Mishra S & Mishra DR 2012. Normalized difference chlorophyll index: A novel model for remote estimation of chlorophyll-a concentration in turbid productive waters. *Remote Sensing of Environment* 117: 394-406.

Mishra VA, Ram; Prathiba, A. P.; Mishra, Prabuddh Kumar; Tiwari, Anuj; Sharma, Surendra Kumar; Singh, Chandra Has; Chandra Yadav, Bankim; Jain, Kamal 2023. Uncrewed Aerial Systems in Water Resource Management and Monitoring: A Review of Sensors, Applications, Software, and Issues. *Advances in Civil Engineering* 2023: 1-28.

Mobley C 1994. Light and Water: Radiative Transfer in Natural Waters' Academic Press. *San Diego, California*.

Modaresi F & Araghinejad S 2014. A comparative assessment of support vector machines, probabilistic neural networks, and K-nearest neighbor algorithms for water quality classification. *Water resources management* 28: 4095-4111.

Morgan BJS, M. D.; Valdes-Abellan, J.; Kim, M. S.; Pachepsky, Y. 2020. Drone-based imaging to assess the microbial water quality in an irrigation pond: A pilot study. *Science of The Total Environment* 716: 135757.

Munawar HS, Ullah F, Qayyum S & Heravi A 2021. Application of deep learning on UAV-based aerial images for flood detection. *Smart Cities* 4: 1220-1242.

Nasir N, Kansal A, Alshaltone O, Barneih F, Sameer M, Shanableh A & Al-Shamma'a A 2022. Water quality classification using machine learning algorithms. *Journal of Water Process Engineering* 48: 102920.

NEMP 2002. National Eutrophication Monitoring Programme Implementation Manual, Department of Water Affairs and Forestry. 1st Edition ed.

Nhamo L, Ndlela B, Nhemachena C, Mabhaudhi T, Mpandeli S & G M 2018. The Water-Energy-Food Nexus: Climate Risks and Opportunities in Southern Africa. *Water* 10.

Odume O, Griffin N, Mensah P, Forsyth D, Ncube L & van Niekerk H 2024. South African Water Quality Guidelines for Freshwater Ecosystems–Version 2.

Olivetti DC, Rejane; Martinez, Jean-Michel; Almeida, Tati; Casari, Raphael; Borges, Henrique; Roig, Henrique 2023. Comparing Unmanned Aerial Multispectral and Hyperspectral Imagery for Harmful Algal Bloom Monitoring in Artificial Ponds Used for Fish Farming. *Drones* 7: 410.

Olivetti DR, Henrique; Martinez, Jean-Michel; Borges, Henrique; Ferreira, Alexandre; Casari, Raphael; Salles, Leandro; Malta, Edio 2020. Low-Cost Unmanned Aerial Multispectral Imagery for Siltation Monitoring in Reservoirs. *Remote Sensing* 12: 1855.

Omer NH 2019. Water quality parameters. *Water quality-science, assessments and policy* 18: 1-34.

Omondi ANO, Y.; Kosgei, J. R.; Kongo, V.; Kemboi, E. J.; Njoroge, S. M.; Mecha, A. C.; Kipkorir, E. C. 2023. Estimation and mapping of water quality parameters using satellite images: a case study of Two Rivers Dam, Kenya. *Water Practice and Technology* 18: 428-443.

Otsu N 1975. A threshold selection method from gray-level histograms. *Automatica* 11: 23-27.

Ovakoglou G, Alexandridis TK, Crisman TL, Skoulikaris C & Vergos GS 2016. Use of MODIS satellite images for detailed lake morphometry: Application to basins with large water level fluctuations. *International journal of applied earth observation and geoinformation* 51: 37-46.

Paerl HW & Barnard MA 2020. Mitigating the global expansion of harmful cyanobacterial blooms: Moving targets in a human-and climatically-altered world. *Harmful Algae* 96: 101845.

Pal M 2005. Random forest classifier for remote sensing classification. *International journal of remote sensing* 26: 217-222.

Palmer SC, Kutser T & Hunter PD 2015. Remote sensing of inland waters: Challenges, progress and future directions. Elsevier.

Pokrzywinski KJ, Richard; Reif, Molly; Bourne, Scott; Hammond, Shea; Fernando, Brianna 2022. Remote sensing of the cyanobacteria life cycle: A mesocosm temporal assessment of a Microcystis sp. bloom using coincident unmanned aircraft system (UAS) hyperspectral imagery and ground sampling efforts. *Harmful Algae* 117: 102268.

Prior EMOD, F. C.; Brodbeck, C.; Runion, G. B.; Shepherd, S. L. 2021. Investigating small unoccupied aerial systems (sUAS) multispectral imagery for total suspended solids and turbidity monitoring in small streams. *International Journal of Remote Sensing* 42: 39-64.

Pugliesi D 2012. Absorbance spectra of free chlorophyll a (blue) and b (red) in a solvent. [online]. Available from https://commons.wikimedia.org/w/index.php?curid=20509583 [Accessed 1 November 2023].

Pulliainen J, Kallio K, Eloheimo K, Koponen S, Servomaa H, Hannonen T, Tauriainen S & Hallikainen M 2001. A semi-operative approach to lake water quality retrieval from remote sensing data. *Science of the Total Environment* 268: 79-93.

Pyo JH, S. M.; Jang, J.; Park, S.; Park, J.; Noh, J. H.; Cho, K. H. 2022. Drone-borne sensing of major and accessory pigments in algae using deep learning modeling. *GIScience and Remote Sensing* 59: 310-332.

Qiang S, Song K, Shang Y, Lai F, Wen Z, Liu G, Tao H & Lyu Y 2023. Remote sensing Estimation of CDOM and DOC with the Environmental implications for Lake Khanka. *Remote sensing* 15.

Quiring SM & Ganesh S 2010. Evaluating the utility of the Vegetation Condition Index (VCI) for monitoring meteorological drought in Texas. *Agricultural and forest meteorology* 150: 330-339.

Rahul TSB, J.; Wessley, G. Jims John 2023. Evaluation of surface water quality of Ukkadam Lake in Coimbatore using UAV and Sentinel-2 multispectral data. *International Journal of Environmental Science and Technology* 20: 3205-3220.

Ramnath A 2010. Umgeni Water infrastructure master plan, planning services, engineering and scientific service division. *Umgeni Water, Pietermaritzburg*.

Rankinen K, Bernal JEC, Holmberg M, Vuorio K & Granlund K 2019. Identifying multiple stressors that influence eutrophication in a Finnish agricultural river. *Science of the Total Environment* 658: 1278-1292.

Rhee DS, Kim YD, Kang B & Kim D 2018. Applications of unmanned aerial vehicles in fluvial remote sensing: An overview of recent achievements. *KSCE Journal of Civil Engineering* 22: 588-602.

Riches G 2018. *Food bank nations: Poverty, corporate charity and the right to food.* Routledge.

Ridolfi E & Manciola P 2018. Water Level Measurements from Drones: A Pilot Case Study at a Dam Site. *Water* 10: 297.

Rouse JW, Haas RH, Schell JA & Deering DW 1974. Monitoring vegetation systems in the Great Plains with ERTS. *NASA Spec. Publ* 351: 309.

Ruwanza S, Thondhlana G & Falayi M 2022. Research progress and conceptual insights on drought impacts and responses among smallholder farmers in South Africa: a review. *Land* 11: 159.

Saenz NA, Paez DE & Arango C 2015. Local algorithm for monitoring total suspended sediments in micro-watersheds using drone and remote sensing applications. Case study: Teusaca River, La Calera, Columbia. *The international Archives of the photogrammetry, Remote sensing and spatial information sciences* 19.

Sagan V, Peterson K, Maimaitjiang M, Sidike P, Sloan J, Greeling B, Maalouf S & Adams C 2020a. Monitoring inland water quality using remote sensing: Potential and limitations of spectral indices, bio-optical simulations, machine learning and cloud computing. *Earth Science Reviews* 205.

Sagan V, Peterson KT, Maimaitijiang M, Sidike P, Sloan J, Greeling BA, Maalouf S & Adams C 2020b. Monitoring inland water quality using remote sensing: Potential and limitations of spectral indices, bio-optical simulations, machine learning, and cloud computing. *Earth-Science Reviews* 205: 103187.

Sakuno Y, Yajima H, Yoshioka Y, Sugahara S, Abd Elbasit MA, Adam E & Chirima JG 2018. Evaluation of unified algorithms for remote sensing of chlorophyll-a and turbidity in Lake Shinji and Lake Nakaumi of Japan and the Vaal Dam Reservoir of South Africa under eutrophic and ultra-turbid conditions. *Water* 10: 618.

Sallam A, Bader Alharbi A, Usman AR, Hussain Q, Ok YS, Alshayaa M & Al-Wabel M 2018. Environmental consequences of dam construction: a case study from Saudi Arabia. *Arabian Journal of Geosciences* 11: 1-12.

Schaeffer BA, Schaeffer KG, Keith D, Lunetta RS, Conmy R & Gould RW 2013. Barriers to adopting satellite remote sensing for water quality management. *International Journal of Remote Sensing* 34: 7534-7544.

Serediak NA, Prepas EE & Putz GJ 2014. 11.8 - Eutrophication of Freshwater Systems. In Holland HD & Turekian KK (eds) *Treatise on Geochemistry (Second Edition)*, 305-323. Oxford: Elsevier.

Seyhan E & Dekker A 1986. Application of remote sensing techniques for water quality monitoring. *Hydrobiological Bulletin* 20: 41-50.

Shen L, Xu H & Guo X 2012. Satellite remote sensing of harmful algal blooms (HABs) and a potential synthesized framework. *Sensors* 12: 7778-7803.

Shi K, Zhang Y, Qin B & Zhou B 2019. Remote sensing of cyanobacterial blooms in inland waters: present knowledge and future challenges. *Science Bulletin* 64: 1540-1556.

Sibanda M, Mutanga O, Chimonyo VG, Clulow AD, Shoko C, Mazvimavi D, Dube T & Mabhaudhi T 2021. Application of drone technologies in surface water resources monitoring and assessment: A systematic review of progress, challenges, and opportunities in the global south. *Drones* 5: 84.

Silveira-Kupssinskü LTG, Tainá; Menezes de Souza, Eniuce; C. Zanotta, Daniel; Roberto Veronez, Mauricio; Gonzaga Jr, Luiz; Mauad, Frederico Fabio 2020. A method for chlorophyll-a and suspended solids prediction through remote sensing and machine learning. *Sensors* 20: 2125.

Silveira Kupssinskü LTG, Tainá; Menezes de Souza, Eniuce; C. Zanotta, Daniel; Roberto Veronez, Mauricio; Gonzaga Jr, Luiz; Mauad, Frederico Fabio 2020. A method for chlorophyll-a and suspended solids prediction through remote sensing and machine learning. *Sensors* 20: 2125.

Singh JA, Thalheimer L, van Aalst M, Li S, Sun J, Vecchi G, Yang W, Tradowsky J, Otto F & Dipura R 2022. Climate change exacerbated rainfall causing devastating flooding in Eastern South Africa. *World weather attribution KZN floods scientific report*.

Song K, Li L, Tedesco L, Li S, Duan H, Liu D, Hall B, Du J, Li Z & Shi K 2013. Remote estimation of chlorophyll-a in turbid inland waters: Three-band model versus GA-PLS model. *Remote Sensing of Environment* 136: 342-357.

Stephens GL, Slingo JM, Rignot E, Reager JT, Hakuba MZ, Durack PJ, Worden J & Rocca R 2020. Earth's water reservoirs in a changing climate. *Proceedings of the Royal Society A* 476: 20190458.

Stumpf RP, Davis TW, Wynne TT, Graham JL, Loftin KA, Johengen TH, Gossiaux D, Palladino D & Burtner A 2016. Challenges for mapping cyanotoxin patterns from remote sensing of cyanobacteria. *Harmful Algae* 54: 160-173.

Su T-C & Chou H-T 2015. Application of multispectral sensors carried on unmanned aerial vehicle (UAV) to trophic state mapping of small reservoirs: A case study of Tain-Pu reservoir in Kinmen, Taiwan. *Remote Sensing* 7: 10078-10097.

Su T-CC, Hung-Ta 2015. Application of multispectral sensors carried on unmanned aerial vehicle (UAV) to trophic state mapping of small reservoirs: A case study of Tain-Pu reservoir in Kinmen, Taiwan. *Remote Sensing* 7: 10078-10097.

Su TC 2017. A study of a matching pixel by pixel (MPP) algorithm to establish an empirical model of water quality mapping, as based on unmanned aerial vehicle (UAV) images. *International Journal of Applied Earth Observation and Geoinformation* 58: 213-224.

Sun D, Qiu Z, Li Y, Shi K & Gong S 2014. Detection of Total Phosphorus Concentrations of Turbid Inland Waters Using a Remote Sensing Method. *Water Air Soil Pollution* 225: 1-17.

Tebbs EJ, Avery ST & Chadwick MA 2020. Satellite remote sensing reveals impacts from dam-associated hydrological changes on chlorophyll-a in the world's largest desert lake. *River Research and Applications* 36: 211-222.

Tian S, Guo H, Xu W, Zhu X, Wang B, Zeng Q, Mai Y & Huang JJ 2023. Remote sensing retrieval of inland water quality parameters using Sentinel-2 and multiple machine learning algorithms. *Environmental Science and Pollution Research* 30: 18617-18630.

Toming K, Liu H, Soomets T, Uuemaa E, Nõges T & Kutser T 2024. Estimation of the Biogeochemical and Physical Properties of Lakes Based on Remote Sensing and Artificial Intelligence Applications. *Remote Sensing* 16.

Torbick N, Hession S, Hagen S, Wiangwang N, Becker B & Qi J 2013. Mapping inland lake water quality across the Lower Peninsula of Michigan using Landsat TM imagery. *International Journal of Remote Sensing* 34: 7607-7624.

Tymków P, Jóźków G, Walicka A, Karpina M & Borkowski A 2019. Identification of Water Body Extent Based on Remote Sensing Data Collected with Unmanned Aerial Vehicle. *Water* 11: 338.

UmgeniWater 2016. Umgeni Water Infrastructure Master Plan 2016, 2016/2017-2046/2047, vol.1, Umgeni Water, Pietermaritzburg, South Africa, 2016. Volume 1.

Urquhart EA, Schaeffer BA, Stumpf RP, Loftin KA & Werdell PJ 2017. A method for examining temporal changes in cyanobacterial harmful algal bloom spatial extent using satellite remote sensing. *Harmful algae* 67: 144-152.

Van Deventer R, Morris C, Hill T & Rivers-Moore N 2022. Use of biological and water quality indices to evaluate conditions of the Upper uMngeni Catchment, KwaZulu-Natal, South Africa. *African Journal of Aquatic Science* 47: 11-22.

Van Ginkel C 2011. Eutrophication: Present reality and future challenges for South Africa. *Water Sa* 37: 693-702.

Vernonez MR, Guimaraes, T. T, Koste, E. C, Souza, E. M, Brum, D, Gonzaga, L, Mauda, F. F 2019. Sustainability Article Evaluation of Regression Analysis and Neural Networks to Predict Total Suspended Solids in Water Bodies from Unmanned Aerial Vehicle Images.

Veronez MR, Kupssinskü LS, Guimarães TT, Koste EC, Da Silva JM, De Souza LV, Oliverio WFM, Jardim RS, Koch IÉ & De Souza JG 2018. Proposal of a method to determine the correlation between total suspended solids and dissolved organic matter in water bodies from spectral imaging and artificial neural networks. *Sensors* 18: 159.

Von Bormann T & Gulati M 2014. The food-energy-water nexus: Understanding South Africa's most urgent sustainability challenge. *WWF-SA, South Africa*: 1-35.

Wang L, Yue X, Wang H, Ling K, Liu Y, Wang J, Hong J, Pen W & Song H 2020. Dynamic inversion of inland aquaculture water quality based on UAVs-WSN spectral analysis. *Remote Sensing* 12: 402.

Wei L, Huang C, Zhong Y, Wang Z, Hu X & Lin L 2019. Inland waters suspended solids concentration retrieval based on PSO-LSSVM for UAV-borne hyperspectral remote sensing imagery. *Remote Sensing* 11.

Wierenga PJ & Hagan RM 1996. Effects Of Irrigation On Soil And Crop. Berkley, California: University of California, Division of Agricultural Science.

Woolway RI, Kraemer BM, Lenters JD, Merchant CJ, O'Reilly CM & Sharma S 2020. Global lake responses to climate change. *Nature Reviews Earth & Environment* 1: 388-403.

Wu DJ, Jie; Wang, Fangyi; Luo, Yunru; Lei, Xiangdong; Lai, Chengguang; Wu, Xushu; Xu, Menghua 2023. Retrieving Eutrophic Water in Highly Urbanized Area

Coupling UAV Multispectral Data and Machine Learning Algorithms. *Water* 15: 354.

Xiang T-Z, Xia G-S & Zhang L 2019. Mini-unmanned aerial vehicle-based remote sensing: Techniques, applications, and prospects. *IEEE geoscience and remote sensing magazine* 7: 29-63.

Xiao YC, Jiahao; Xu, Yue; Guo, Shihui; Nie, Xingyu; Guo, Yahui; Li, Xiran; Hao, Fanghua; Fu, Yongshuo H. 2023. Monitoring of chlorophyll-a and suspended sediment concentrations in optically complex inland rivers using multisource remote sensing measurements. *Ecological Indicators* 155: 111041.

Xiao YG, Y.; Yin, G.; Zhang, X.; Shi, Y.; Hao, F.; Fu, Y. 2022a. UAV Multispectral Image-Based Urban River Water Quality Monitoring Using Stacked Ensemble Machine Learning Algorithms—A Case Study of the Zhanghe River, China. *Remote Sensing* 14.

Xiao YG, Yahui; Yin, Guodong; Zhang, Xuan; Shi, Yu; Hao, Fanghua; Fu, Yongshuo 2022b. UAV Multispectral Image-Based Urban River Water Quality Monitoring Using Stacked Ensemble Machine Learning Algorithms—A Case Study of the Zhanghe River, China. *Remote Sensing* 14: 3272.

Xu H 2006. Modification of normalised difference water index (NDWI) to enhance open water features in remotely sensed imagery. *International Journal of Remote Sensing* 27: 3025-3033.

Xu JLX, Z.; Kuang, J. J.; Lin, C.; Xiao, L. H.; Huang, X. S.; Zhang, Y. F. 2021. An Alternative to Laboratory Testing: Random Forest-Based Water Quality Prediction Framework for Inland and Nearshore Water Bodies. *Water* 13.

Yang H, Kong J, Hu H, Du Y, Gao M & Chen F 2022. A Review of Remote Sensing for Water Quality Retrieval: Progress and Challenges. *Remote Sensing* 14: 1770.

Yang WF, Bolin; Li, Sunzhe; Lao, Zhinan; Deng, Tengfang; He, Wen; He, Hongchang; Chen, Zhikun 2023. Monitoring multi-water quality of internationally important karst wetland through deep learning, multi-sensor and multi-platform remote sensing images: A case study of Guilin, China. *Ecological Indicators* 154: 110755.

Yang X, Qin Q, Yésou H, Ledauphin T, Koehl M, Grussenmeyer P & Zhu Z 2020. Monthly estimation of the surface water extent in France at a 10-m resolution using Sentinel-2 data. *Remote Sensing of Environment* 244: 111803.

Yao H, Qin R & Chen X 2019. Unmanned aerial vehicle for remote sensing applications—A review. *Remote Sensing* 11: 1443.

Yi LZ, G.; Zhang, B. 2023. Application of UAV Push-Broom Hyperspectral Images in Water Quality Assessments for Inland Water Protection: A Case Study of Zhang Wei Xin River in Dezhou Distinct, China. *Remote Sensing* 15.

Ying HX, Kai; Huang, Xinxi; Feng, Hailin; Yang, Yinhui; Du, Xiaochen; Huang, Leijun 2021. Evaluation of water quality based on UAV images and the IMP-MPP algorithm. *Ecological Informatics* 61: 101239.

Zhang G, Xie H, Duan S, Tian M & Yi D 2011. Water level variation of Lake Qinghai from satellite and in situ measurements under climate change. *Journal of Applied Remote Sensing* 5: 053532-053532-15.

Zhang YW, Lun; Deng, Licui; Ouyang, Bin 2021. Retrieval of water quality parameters from hyperspectral images using a hybrid feedback deep factorization machine model. *Water Research* 204: 117618.

Zhang YW, Lun; Ren, Huazhong; Liu, Yu; Zheng, Yongqian; Liu, Yaowen; Dong, Jiaji 2020. Mapping water quality parameters in urban rivers from hyperspectral images using a new self-adapting selection of multiple artificial neural networks. *Remote Sensing* 12: 336.

Zhao N, Fan Z & Zhao M 2021. A new approach for estimating dissolved oxygen based on a high-accuracy surface modeling method. *Sensors* 21: 3954.

Zhao XL, Yanzhou; Chen, Yongli; Qiao, Xi 2022a. A Method of Cyanobacterial Concentrations Prediction Using Multispectral Images. *Sustainability* 14: 12784.

Zhao XL, Yanzhou; Chen, Yongli; Qiao, Xi; Qian, Wanqiang 2022b. Water Chlorophyll a Estimation Using UAV-Based Multispectral Data and Machine Learning. *Drones* 7: 2.

Zhao Y, Li T, Zhang X & Zhang C 2019. Artificial intelligence-based fault detection and diagnosis methods for building energy systems: Advantages, challenges and the future. *Renewable and Sustainable Energy Reviews* 109: 85-101.

Zheng K, Shao T, Ning J, Zhuang D, Liang X & Ding X 2023. Water quality, basin characteristics and discharge greatly affect CDOM in highly turbid rivers in the Yellow River basin, China. *Journal of Cleaner Production* 404.

Appendix A: List of graduated students

The project provided three MSc students: Ms Shannyn Pillay, Ms Nobubelo Ngwenya and Mr Elvis Mawodzeke. The first two students were registered in the Department of Hydrology and have submitted their thesis for examination. However, Mr Mawodzeke, who is registered in the Department of Geography, is still working on his thesis. Ms Pillay's research is on the use of remotely sensed data acquired by drones to estimate TSS, CDOM and surface water temperature, while Ms Ngwenya`s research is on the assessment of spatio-temporal variability of chl-a and nutrients in small water bodies using UAVs. Both studies made use of machine learning techniques. It is worth mentioning that each student has published a review paper. The following subsections provide brief overviews of the studies.

Nobubelo Ngwenya

Ms Ngwenya, supervised by Prof Tafadzwa Mabhaudhi and Dr Tsitsi Bangira, completed her thesis in January 2025. Below is a summary of the submitted thesis.

Monitoring water quality, particularly chlorophyll-a (chl-a) concentrations, is critical for managing irrigation water, as excessive chl-a can degrade aquatic ecosystems and reduce water availability. While multispectral satellite-based remote sensing is widely used, its spatial resolution is inadequate for small water bodies, which are crucial to smallholder farmers. Unmanned Aerial Vehicles (UAVs) offer high-resolution, near-real-time data, presenting a promising solution. This thesis investigates UAV-based multispectral imaging for chl-a estimation in small reservoirs, focusing on a systematic review and an empirical study in South Africa. The systematic review, following the Preferred Reporting Items for Systematic Reviews and Meta-Analysis (PRISMA) framework, evaluates progress, challenges, and best practices in UAV-based chl-a monitoring of small water bodies. Multispectral sensors, especially those on DJI platforms, dominate the literature due to their cost-efficiency, portability, and ability to capture key spectral bands (green, red, red-edge, and near-infrared) sensitive to chl-a. Machine learning models like Random Forest and Support Vector Machines are widely used for chl-a retrieval. However, a significant gap exists in Africa due to

financial, regulatory, and technical barriers. Standardised algorithms and validation protocols also remain a key research priority. The empirical study integrates UAV-based multispectral data from April, June, and July 2024 with in-situ measurements of chl-a, total nitrogen (TN), total phosphorus (TP), and dissolved oxygen (DO). Among machine learning models tested, Artificial Neural Networks (ANN), Random Forest (RF), Support Vector Machine (SVM), and Extreme Gradient Boost (XGBoost), K-Nearest Neighbours (KNN), ANN outperformed others, achieving R^2 values of 0.949, 0.991, and 0.734. The green, red, and red-edge bands were the most sensitive for chl-a estimation. Seasonal patterns emerged, with high chl-a concentrations in April and June, followed by a decline in July due to reduced water levels. In July, strong correlations were found between chl-a and nutrient parameters, particularly TP (R^2 = 0.87) and TN (R^2 = 0.71). This study highlights the potential of UAV-based remote sensing for high-resolution chl-a monitoring in small water bodies. The findings underscore the importance of continuous water quality monitoring to adapt to rapidly changing environmental conditions, offering a scalable solution for water resource management in smallholder agricultural systems worldwide.

Shannyn Pillay

Ms Pillay, supervised by Prof Tafadzwa Mabhaudhi and Dr Tsitsi Bangira, has submitted her thesis for examination. Her research uses machine learning and very high-resolution colour (RGB) imagery to estimate TSS, CDOM and surface water temperature. Some of the methods and findings were reported in Sections 2, 3 and 4 of this report. Below is a summary of the submitted thesis.

Over the past few decades, South Africa has faced severe water shortages, especially due to the declining quality of its natural water supplies. This decline has further strained on irrigation standards, directly impacting crop yields, livestock health and soil fertility. This has emphasised the need for advanced, near-real-time approaches to assess and monitor key water quality parameters affecting irrigation water quality, such as water temperature, total suspended solids (TSS), and Chromophoric dissolved organic matter (CDOM). This research explores the utility of UAV-based remote sensing for monitoring water quality parameters in small reservoirs to address the limitations of traditional remote sensing and ground-based methods, which are often labour-intensive, costly and lack sufficient spatial and temporal coverage.

Chapter 1 introduces the research problem, highlighting the increasing pressure on water resources in southern Africa's resources due to climate change, population growth and land-use changes. It outlines the study's objectives, which include developing a robust methodology for using UAV-derived data to monitor key water quality parameters and improving decision-making in water resource management at the farm scale. Chapter 2 presents a global systematic review of the literature for UAV-based remote sensing for water quality monitoring. It critically evaluates advancements in sensor technology, machine learning algorithms and statistical approaches, identifying key research gaps. The chapter emphasizes the potential of UAVs to provide high-resolution, real-time data but notes challenges such as cost, regulatory constraints and the lack of standardized validation protocols. Chapter 3 provides a case study of the High Flight Farm dam in the uMngeni catchment, illustrating the application approach of UAV-derived data in monitoring water temperature, TSS, and CDOM. The study demonstrates the integration of UAV-based observations with machine learning techniques and model development to produce high-accuracy predictive spatial maps that inform sustainable agricultural practices. Finally, Chapter 4 synthesises the findings, addressing limitations such as weather and operational constraints while offering recommendations for future research. These include expanding research on underrepresented water bodies and promoting interdisciplinary collaborations to enhance the accessibility and scalability of UAV technology in water quality monitoring.

Elvis Mawodzeke

Mr Mawodzeke, supervised by Prof Onisimo Mutanga and Dr Mbulisi Sibanda, is still busy with his thesis. Some of the methods and preliminary findings were overviewed in Section 6 of this report.

Appendix B: List of Publications

Four publications have been produced from this project at the time of writing. However, four articles are currently in preparation for submission to scientific journals.

1. Ngwenya, N*., Bangira, T., Sibanda, M., Gurmessa, S.K. and Mabhaudhi, T., 2025. *UAV-based remote sensing of chlorophyll-a concentrations in inland water bodies: A systematic review.* Geocarto International. https://doi.org/10.1080/10106049.2025.2452246
2. Pillay, S.J.; Bangira, T.; Sibanda, M.; Kebede Gurmessa, S.; Clulow, A.; Mabhaudhi, T. (2024) *Assessing Drone-Based Remote Sensing for Monitoring Water Temperature, Suspended Solids and CDOM in Inland Waters: A Global Systematic Review of Challenges and Opportunities.* Drones. 8, 733. https://doi.org/10.3390/drones8120733
3. Bangira T, Matongera TN, Mabhaudhi T, Mutanga O. *Remote sensing-based water quality monitoring in African reservoirs, potential and limitations of sensors and algorithms: A systematic review,* Physics and Chemistry of the Earth, Parts A/B/C, Volume 134,2024,103536, ISSN 1474-7065. https://doi.org/10.1016/j.pce.2023.103536
4. Sibanda, M.; Mutanga, O.; Chimonyo, V.G.P.; Clulow, A.D.; Shoko, C.; Mazvimavi, D.; Dube, T.; Mabhaudhi, T. *Application of Drone Technologies in Surface Water Resources Monitoring and Assessment: A Systematic Review of Progress, Challenges, and Opportunities in the Global South*. Drones 2021, 5, 84. https://doi.org/10.3390/drones5030084
5. Pillay, S.J.; Bangira, T.; Sibanda, M.; Kebede Gurmessa, S.; Clulow, A.; Mabhaudhi, T. (2025) *Assessing the Utility of Drone Technology in Estimating Surface Water Temperature, Total Suspended Solids and Chromophoric Dissolved Organic Matter in Reservoirs: A Case Study of the High Flight Farm Dam* (in preparation).
6. Ngwenya, N*, Bangira, T., Sibanda, M., Gurmessa, S.K., Gokool, S. and Mabhaudhi, T. (in press) Assessing cyanobacteria in a small reservoir using unmanned aerial vehicle systems (UAVs). (in press).

7. Bangira, T., Magidi, J., and Mabhaudhi, T. Remote sensing of cyanobacteria in small water bodies using optically active pigments, chlorophyll-a and phycocyanin (in preparation).